DISSERTATION ZUR ERLANGUNG DES DOKTORGRADES

DER FAKULTÄT FÜR BIOLOGIE

DER LUDWIG-MAXIMILIANS-UNIVERSITÄT MÜNCHEN

Cdk9 and Brd4 regulate

eukaryotic transcription

TIM-MICHAEL DECKER

April 2017

Completed at the Helmholtz Center Munich

German Research Center for Environment and Health (GmbH)

Institute of Functional Epigenetics

Department of Molecular Epigenetics

Eidesstattliche Erklärung

Ich versichere hiermit an Eides statt, dass die vorliegende Dissertation von mir selbstständig und ohne unerlaubte Hilfe angefertigt ist .

Erklärung

Hiermit erkläre ich, dass die Dissertation nicht ganz oder in wesentlichen Teilen einer anderen Prüfungskommission vorgelegt worden ist.

Ich erkläre weiter, dass ich mich anderweitig einer Doktorprüfung ohne Erfolg **nicht** unterzogen habe.

München, im April 2017

Tim-Michael Decker

I Summary

The bromodomain protein Brd4 is an epigenetic reader and binds to acetylated histone tails. Brd4 activates transcription by recruiting the positive elongation factor P-TEFb. Small molecule inhibitor JQ1 competitively binds the bromodomains of Brd4 and displaces the protein from acetylated histones. However, it remains unclear whether genes targeted by JQ1 are mainly regulated by Brd4 or by other bromodomain proteins such as Brd2 and Brd3. In this work, I describe anti-proliferative dominant-negative Brd4 mutants that compete with the function of distinct Brd4 domains. I used these Brd4 mutants to compare the Brd4-specific transcriptome with the transcriptome of JQ1-treated cells. I found that most JQ1-regulated genes are also regulated by dominant-negative Brd4 mutants, including the mutant that competes with the P-TEFb recruitment function of Brd4. My results suggest that Brd4 mediates most of the inhibitory effects of JQ1 and that the major function of Brd4 in this process is the recruitment of P-TEFb.

The kinase subunit of P-TEFb, Cdk9, is a well-known regulator of transcription elongation. Recruitment and activation of Cdk9 by Brd4 or other factors, is crucial for the release of promoter proximal paused RNA polymerase II. To characterize the role of Cdk9 in this process in more detail, I used a CRISPR/Cas9 engineered cell system for fast and efficient inhibition of Cdk9 kinase activity. Inhibition of this analog-sensitive Cdk9 decreased cell proliferation and reduced phosphorylation levels of RNA polymerase II C-terminal domain, in particular at Serine 2 residues. Nascent transcriptome analysis revealed that Cdk9 indeed facilitates efficient pause release. Strikingly, I further observed that pausing delimits the rate of transcription initiation, indicating that pause release activates genes by increasing the number of transcribing polymerases per time. Thus, Brd4 and Cdk9 together regulate transcription of RNA polymerase II by facilitating efficient pause release.

II Table of contents

1 Introduction

1.1 Chromatin

The deoxyribonucleic acid (DNA) of eukaryotes is not naked. Instead it is well organized in a higher order structure that heavily influences the activity of genes. Many components are involved in this structuring process. DNA, histones, and non-histone proteins contribute to build up the structure that allows a complex regulation of gene activity known as chromatin. There are two different ground states of chromatin: euchromatin and heterochromatin. Euchromatin is decondensed and typically comprises active genes. Heterochromating is condensed and genes located within heterochromatic chromatin are generally repressed. Chromatin states and thus gene activity is influenced by many factors, including DNA methylation and histone modifications. These are so-called epigenetic mechanisms that stabilize gene expression programs in addition to the DNA template (Allis & Jenuwein 2016).

1.1.1 Chromatin structure

The first step of chromatin assembly involves the incorporation of nucleosomes. Nucleosomes are the basic unit of eukaryotic chromatin structure and are built by histone proteins. Canonical histones are comprised of histone 2A, histone 2B, histone 3, histone 4 and the so-called linker histone 1 (H2A, H2B, H3, H4, H1). Two molecules of each H2A, H2B, H3 and H4 make up a core nucleosome, also called histone octamer. 147 base pairs (bp) of DNA is wound around the histone octamer and 'sealed' by H1 (Allis & Jenuwein 2016; Luger et al. 1997; Venkatesh & Workman 2015). Consecutive incorporation of nucleosomes leads to the 'beads-on-a-string' structure as it is seen for condensed chromatin in the electron microscope (Olins & Olins 1974). The DNA that connects nucleosomes is called 'linker DNA' and nucleosomes repeat at an interval of ~200 bp. Incorporation of histones is facilitated by designated remodeling enzymes.

Chromatin remodelers are also responsible for the correct spacing of the nucleosomes and contribute to the overall chromatin dynamics. Chromatin dynamics includes the dynamic addition, removal and exchange of nucleosomes or histones. Importantly, special histone variants are incorporated, e.g. at centromers or sites of DNA damage. Furthermore, structural analysis of histones revealed that the amino (N)-terminal tails of histones are not part of the histone fold but are protruding the core of the nucleosome. This makes the histone tails accessible for a multitude of binding and modifying factors (for review see Venkatesh & Workman, 2015).

1.1.2 Post-translational histone modifications

Similar to many other proteins, histones are post-translationally modified. Most modifications are described for the N-terminal histone tails, although histones can be modified in the histone fold as well (reviewed in Lawrence et al. 2017). Histone modifying enzymes ('writers') include acetyltransferases, methyltransferases, kinases, and ubiquitinases. Enzymes that remove such modifications ('erasers') include deacetylases, demethylases, phosphatases, and deubiquitinases (Marmorstein & Zhou 2014). A third group of proteins called 'readers' has become the focus of research only recently. Histone readers recognize and interpret specific histone modifications or their absence. Thereby they convey particular signals associated with those modifications to chromatin-related processes such as transcription or chromatin structure. The idea that histone modifications can arise in a particular pattern that triggers downstream events is also known as the 'histone code' (Strahl & Allis 2000). Overall the histone code defines not only the accessibility of chromatin but also the activity of associated genes (Figure 1-1).

Acetylation of histones has been extensively studied over the last two decades. After the first histone acetyltransferase (HAT) and histone deacetylase (HDAC) were identified in 1996 (Brownell et al. 1996; Taunton et al. 1996), over 20 HATs and HDACs have been studied in detail (Verdin & Ott 2015). Proteins can bind acetylated Lysines of histones using a conserved domain called bromodomain (Dhalluin et al. 1999; Yap & Zhou

2010). Bromodomains are found in many chromatin-related proteins including HATs, chromatin remodelers, nuclear scaffolding proteins, and the bromodomain and extra-terminal domain (BET) protein family (see chapter 1.2.4). Histone acetylation inhibits the formation of secondary and tertiary structures in the core nucleosomes, thereby de-condensing chromatin structure and recruiting histone readers (Verdin & Ott 2015). Hence, the complex action of writers and erasers of histone modifications regulate the accessibility of chromatin for transcription factors and other transcriptional co-activators.

Acetylated chromatin
Open and transcriptinally active

Deacetylated chromatin
Compact and transcriptionally repressed
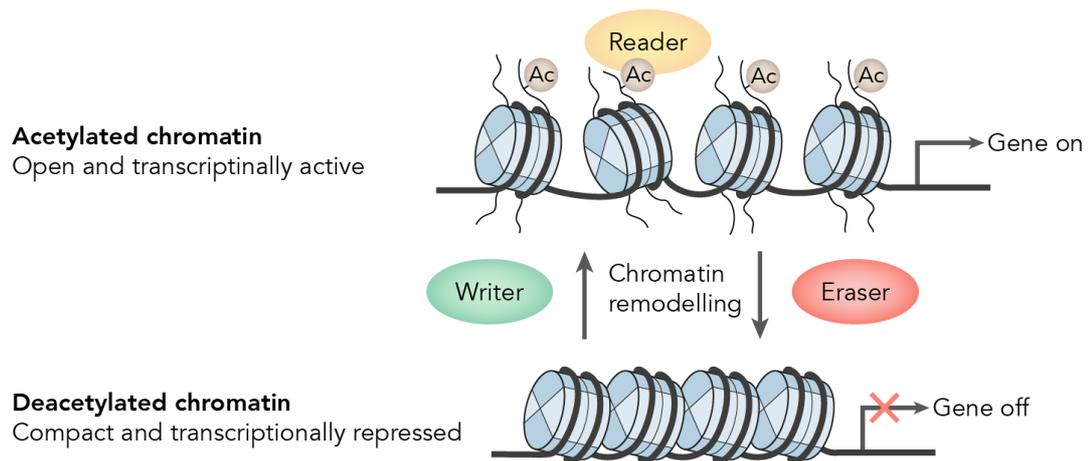
Figure 1-1 | Acetylation of histone tails induces chromatin remodeling to activate transcription. Histone marks are removed by eraser enzymes. Acetylation marks (Ac) are removed by histone deacetylases which leads to compaction of chromatin and results in transcriptional repression. Histone acetyltransferases are writers that acetylate histone tails to decondense chromatin and activate transcription (modified from Verdin & Ott, 2015).

1.2 Transcription of RNA Polymerase II

Histone modifications substantially contribute to gene activation and transcription of ribonucleic acid (RNA). Bacteria have developed only one enzyme that synthesizes RNA. This single RNA polymerase is composed of four catalytic subunits that are regulated by another subunit known as sigma. Different sigma factors bind to distinct promoter sequences and thereby regulate the transcription of unique sets of genes (Clancy 2008). In eukaryotes, three different RNA polymerases (Pol I, Pol II and Pol III) tran-

scribe RNA from the genomic DNA template (Roeder & Rutter 1969). Structurally, all three polymerases contain a ten-subunit catalytic core. However, Pol I, Pol II, and Pol III further contain other subcomplexes adding up to 14, 12, and 17 subunits in total, respectively (Vannini & Cramer 2012).

The three RNA polymerases characteristically differ in their gene targets and transcription initiation pathways, enhancing the complexity of gene regulation. Pol I transcribes the 35S precursor of the 28S, 18S and 5.8S ribosomal RNAs (rRNAs) (Viktorovskaya & Schneider 2015). Pol II transcribes messenger RNAs (mRNAs) from all protein-coding genes and most regulatory, non-coding RNAs (Cooper 2000; Deniz & Erman 2016). Pol III synthesizes transfer RNAs (tRNAs), cellular 5S rRNA and some other short RNAs like U6 small nuclear RNA (snRNA) (Arimbasseri & Maraia 2016). In addition to mRNA synthesis Pol II regulates the whole set of co-transcriptional RNA-processing events and is involved in chromatin-linked interactions (Saldi et al. 2016). Below, the mechanism of Pol II transcription will be elucidated in more detail.

1.2.1 Transcription cycle of RNA polymerase II

Transcription of Pol II dependent genes can be grouped into three major stages: initiation, elongation and termination. The transcriptional machinery is composed of a multitude of enzymes and protein complexes including general transcriptions factors (GTFs: TFIIA, TFIIB, TFIID, TFIIE, TFIIF, TFIIH), Pol II, the Mediator and several other co-activators, co-repressors, chromatin modifiers and remodelers (Gupta et al. 2016; Thomas & Chiang 2006).

Preinitiation

Transcription begins with the formation of the Preinitiation Complex (PIC), which itself is a stepwise process (Figure 1-2A-B). First TFIID containing the TATA-box binding protein (TBP) binds to the core promoter (Davison et al. 1983; Sawadogo & Roeder 1985). After the sequential entry of TFIIA and TFIIB that stabilize TFIID binding to the

promoter (Buratowski et al. 1989), Pol II and TFIIF are recruited. At last, TFIIE enters the PIC followed by TFIIH. Interestingly, an alternative model to this sequential PIC assembly pathway was described as the Pol II holoenzyme pathway. The Pol II holoenzyme pathway suggests that upon TFIID binding to the promoter, Pol II is recruited as a preassembled holoenzyme complex, containing a subset of GTFs and other proteins that are involved in chromatin remodeling, DNA repair and mRNA processing (Thomas & Chiang 2006). Both pathways may exist *in vivo* and depending on promoter context and specific signaling molecules either pathway could be used.

In vivo the initiation complex is further stabilized by the coactivator complex Mediator. The Mediator achieves this by cooperating with the GTFs TFIIB, TFIID and TFIIH (Plaschka et al. 2016). Given its multisubunit structure that makes various contacts with the polymerase, the Mediator serves as a scaffold to bridge transcription factors to Pol II. In yeast, conditional dissociation of a Mediator subcomplex lead to reduced global RNA levels (Linder et al. 2006; Thompson et al. 1993). This indicates that the Mediator substantially contributes to well-regulated transcription *in vivo* by increasing efficiency of PIC assembly.

The processes presented above were initially described based on biochemical studies. Recent advances in structural biology have confirmed and refined many of these models. Especially the advances in 3D electron microscopy have enabled researchers to unravel the composition of large complexes and determine the exact points of contact between different subcomplexes (Hantsche & Cramer 2016). Once it is assembled, the PIC adopts a "closed" state, unable to initiate transcription. To open the DNA up about 11 to 15 bp around the transcriptional start site (TSS) the XPB helicase subunit of TFIIH induces a torsional strain, positioning single-stranded DNA to the active site of Pol II. Pol II is now prepared to enter elongation and transcribe throughout a gene without dissociating from the DNA template (Gupta et al. 2016).

Initiation

When the DNA template is melted, the polymerase starts to produce the RNA transcript. However, this early transcription is unstable and often results in abortive transcription. Once the transcript has reached a length of about 5 nucleotides (nt) the polymerase can escape the promoter and enter the elongation phase. Interestingly, phosphorylation of the carboxy (C)-terminal domain (CTD) of Pol II by cyclin dependent kinase 7 (Cdk7), a subunit of TFIIH, prevents direct binding of the Mediator to Pol II (Søgaard & Svejstrup 2007). After Pol II has escaped from the promoter TFIID, TFIIA, TFIIH, TFIIE and Mediator were described to form a scaffold for a re-initiation complex that allows rapid recruitment of Pol II and assembly of another functional PIC (Yudkovsky et al. 2000).

Early elongation

While the RNA chain is being elongated via the so-called nucleotide addition cycle (for review see Hantsche & Cramer, 2016), the transcript reaches a critical length of 17-25 nt. At this stage, the nascent transcript needs to be protected from degradation by nuclear 5' -> 3' exoribonucleases like Xrn2. This is achieved by addition of a 5' cap structure. Recruitment of the capping machinery again is dependent on CTD phosphorylation (Figure 1-2C; see chapters 1.2.2 and 1.2.3). In eukaryotes the 5' guanine-N7 methyl cap is the first modification of nascent pre-mRNA. Capping occurs in three sequential enzymatic reactions of which the metazoan Capping Enzyme catalyzes the first two: (1) RNA triphosphatase cleaves the 5' triphosphate of the pre-mRNA. (2) The resulting diphosphate end is capped with guanosine monophosphate (GMP) by RNA guanylyltransferase to form 5' guanylylated-RNAs. (3) RNA guanine-N7 methyltransferase transfers a methyl group to the N7 position of the terminal guanine base to complete the synthesis of cap (for review see Ghosh & Lima, 2010).
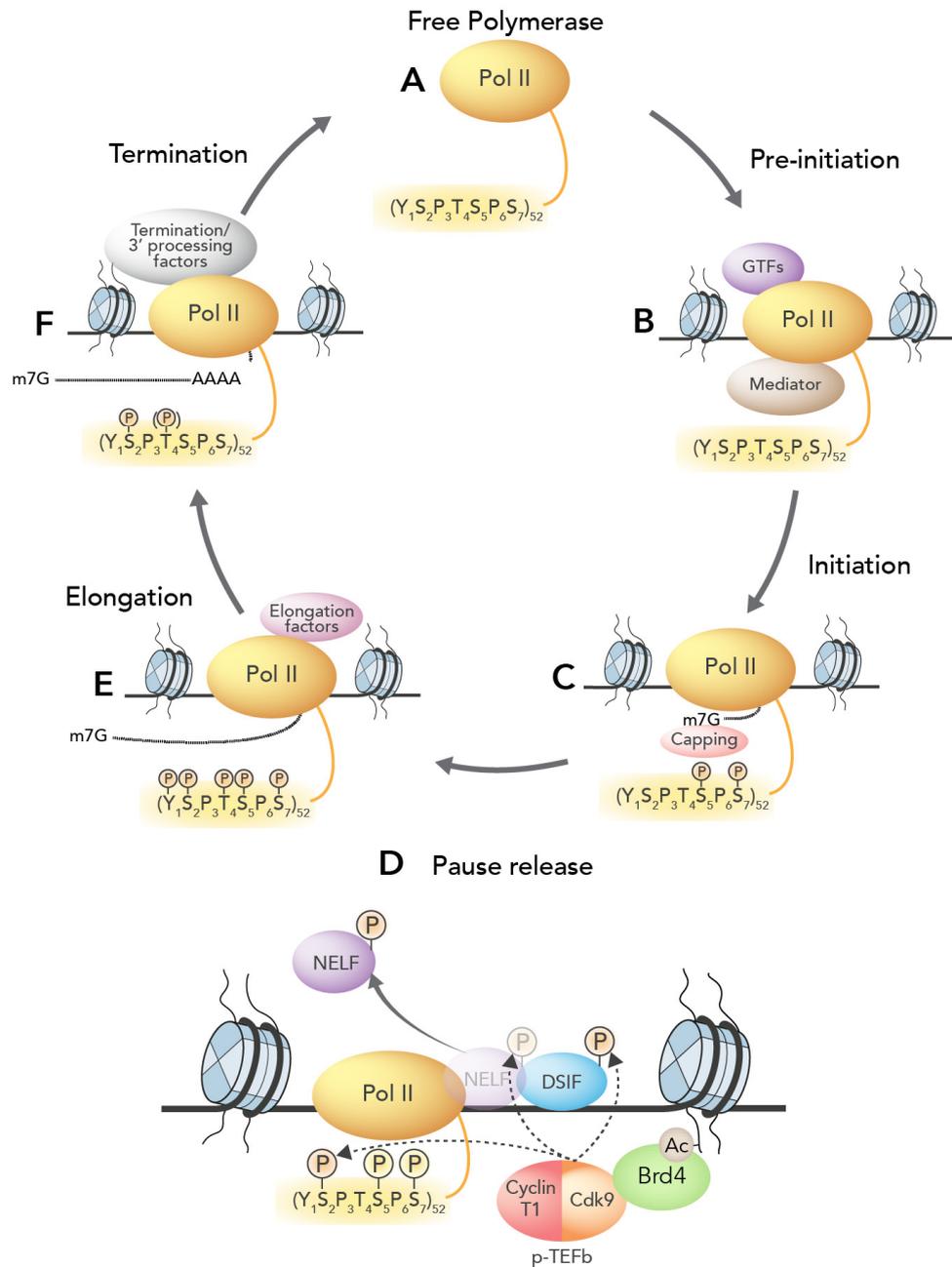
Figure 1-2 | Transcription cycle of RNA polymerase II. RNAPII with an hypo-phosphorylated CTD **(A)** is recruited to the pre-initiation complex **(B)**. At the initiation phase Ser5 and Ser7 are phosphorylated **(C)**. Ser5-P induces release of the pre-initiation complex as well as capping of the 5' mRNA end. Pol II pausing at the promoter proximal region is generated by DSIF and NELF. Release from the elongation block is facilitated by the kinase activity of P-TEFb, consisting of Cdk9 and CyclinT1. Cdk9 phosphorylates Ser-2, DSIF, and NELF, causing the dissociation of NELF and conversion of DSIF from a negative to a positive elongation factor **(D)**. Throughout elongation Thr4 and Tyr1 are also phosphorylated, as is Ser2 at increasing levels. **(E)**. When reaching termination of transcription the phosphorylations of Tyr1, Thr4 (in yeast), S5 and S7 are removed by phosphatases **(F)**. To enter a new cycle all remaining CTD phosphorylations must be removed again.

In higher eukaryotes including *Drosophila* and mammals, the elongating polymerase is stalled 20-80 bp downstream of the TSS. This rate-limiting step in early elongation is often referred to as promoter proximal pausing. Paused Pol II has been extensively studied on the *Hsp70* and *c-Myc* loci in *Drosophila* and human cell lines, respectively (Bentley & Groudine 1986; Eick & Bornkamm 1986; Rougvie & Lis 1988). In *C. elegans* pausing levels are strongly reduced and yeast appears to lack pausing completely, suggesting that promoter proximal pausing is exclusive for higher eukaryotes. Indeed, approximately 40%-46% and 70%-89% of active genes were identified as paused in mammalian and *Drosophila* cells, respectively (Kwak & Lis 2013). More recent studies observed Pol II pausing at 60%-95% of mammalian genes (Day et al. 2016; Jonkers et al. 2014), suggesting that this regulatory mechanism is indeed crucial for expression of most mammalian genes. Although many active genes are paused, the degree of pausing varies dependent on cis-acting DNA elements, nucleosome occupancy, and certain elongation factors.

Negative elongation factor (NELF) and DRB-sensitivity-inducing factor (DSIF, consisting of subunits Spt4 and Spt5) are the main pausing factors that block Pol II from further elongation (Renner et al. 2001; Wu et al. 2003) (Figure 1-2D). NELF is a 5-subunit complex and was reported to interact with RNA via its NELF-E subunit but also interacts with DSIF and Pol II (Yamaguchi et al. 1999). Interestingly, knockdown of NELF by RNAi reduced transcription rates of most genes (Amleh et al. 2009), indicating that pausing is not an inhibitory mechanism but a regulatory feature that allows stimulation of transcription. Accordingly, paused Pol II was reported to keep promoters free from nucleosomes (Gilchrist et al. 2010). Thus, promoter proximal pausing is a common characteristic of highly regulated, active genes and contributes to keeping the promoter accessible to transcription factors (reviewed in Jonkers & Lis, 2015).

The elongation block is released after recruitment of positive transcription elongation factor b (P-TEFb) which is a heterodimer composed of cyclin-dependent kinase 9 (Cdk9) and cyclin T1/T2 (Peng et al. 1998). Interestingly, the recruitment of P-TEFb

itself is highly regulated and can be facilitated e.g. by bromodomain protein 4 (Brd4) or orchestrated by the Super Elongation Complex (SEC) (see section 1.2.4). Cdk9 then phosphorylates NELF and the Spt5 subunit of DSIF (Fujinaga et al. 2004; Kim & Sharp 2001). This causes NELF to dissociate and converts DSIF into a positive elongation factor (Yamada et al. 2006). Together these tightly regulated events lead to the release of the paused polymerase into productive elongation (Fowler et al. 2014).

Productive elongation

During elongation various coactivators are recruited to the transcription machinery to promote the ongoing transcription as well as cotranscriptional RNA processing events (Figure 1-2E). Pol II not only pauses in the promoter proximal region but also around exons (Jonkers et al. 2014), highlighting that splicing is a co-transcriptional event. Co-transcriptional splicing is partly regulated by dynamic phosphorylations of the CTD. For example, recruitment of the U2AF65-Prp19 complex via phosphorylated CTD activated *in vitro* splicing (David et al. 2011). Accordingly, splicing defects and reduced recruitment of U2AF65 and U2 snRNP were observed in a CTD mutant that cannot be phosphorylated on Ser2 (Gu et al. 2013). The Mediator is probably involved in recruiting processing factors as well. Its Med23 subunit binds the splicing factors hnRNPL, SF3B, and Eval1, indicating a crosstalk between splicing and the Mediator. Besides spatial coupling of processing factors to the site of transcription many other factors influence co-transcriptional splicing, including the elongation rate (reviewed in Saldi et al. 2016).

The transcription elongation rate, the velocity Pol II is producing RNA, increases after the first few kilobases (kb) from ~0.5 kb per minute to 2-5 kb per minute after ~15 kb (Fuchs et al. 2014; Jonkers et al. 2014). However, elongation rates can vary, depending on nucleosome occupancy or histone marks that restrict or promote the speed of the polymerase (Bintu et al. 2012). For example ubiquitinylation of histone H2B and trimethylation of H3 at Lys36 are found within the gene body, potentially influencing

the speed of transcription (reviewed in Venkatesh & Workman, 2015). Further studies describe a correlation between H3K79me2 and H4K20me1 with high elongation rates and gene- or sequence-related features such as gene length and low complexity DNA sequence (Fuchs et al. 2014; Jonkers et al. 2014; Veloso et al. 2014). Together, these findings highlight the strong interdependence between histone marks and transcription elongation.

Termination

While transcriptional initiation is well characterized, less is known about the mechanism of termination. In eukaryotes two models have been proposed to describe termination: the allosteric model and the torpedo model. When the polymerase arrives at a functional poly-adenylation (poly(A)) site multiple events such as the activity of cleavage and polyadenylation factors (CPAs) trigger the release of the RNA transcript and the polymerase (reviewed in Proudfoot, 2016) (Figure 1-2F). In the allosteric model, Pol II senses a poly(A) site. Following the association with CPAs this leads to conformational changes that eventually cause termination of transcription. Alternatively, the torpedo model suggests that Pol II keeps transcribing after cleavage of the nascent transcript. Then, the 5'-3' exonuclease Xrn2 is recruited to the poly(A) site and starts degrading the uncapped 5' end of the Pol II associated transcript. When Xrn2 reaches the polymerase, the release of Pol II from the DNA template is triggered. While the detailed mechanism of this process is currently unclear, several regulatory factors of transcriptional termination have been identified.

One event that influences termination and selection among multiple poly(A) sites is Pol II pausing. By slowing down the Pol II elongation complex, CPA association with the poly(A) site and 3' processing are enhanced. Recognition of a poly(A) site alone can lead to pausing effects, conformational changes and increased termination (Kazerouninia et al. 2010; H. Zhang et al. 2015). Pausing can also be induced by formation of R loops, RNA:DNA hybrids that are established when the nascent transcript

hybridizes with the antisense DNA strand outside of the elongation complex (reviewed in Skourti-Stathaki & Proudfoot, 2014). Accumulating R loops can result in single- and double-strand breaks that are potentially mutagenic (Aguilera & García-Muse 2012). Therefore, R loops need to be resolved. In mammals Senataxin is not only required to resolve R loops but also promotes efficient termination (Skourti-Stathaki et al. 2011). Interestingly, Senataxin is recruited via SMN that recognizes a specific methylation mark on the Pol II CTD (Zhao et al. 2015). In summary, these events elucidate the complex regulation of transcriptional termination.

1.2.2 C-terminal domain of RNA Pol II (CTD)

RNA polymerase II is uniquely equipped with a repetitive structure at the C-terminus of the large subunit Rpb1 (Saldi et al. 2016). This C-terminal domain (CTD) consists of tandem heptad repeats with the consensus sequence of Tyrosine-Serine-Proline-Threonine-Serine-Proline-Serine (Tyr1-Ser2-Pro3-Thr4-Ser5-Pro6-Ser7). The CTD of budding yeast has a length of 26 repeats of which most repeats harbor the consensus sequence. Mammals have developed a longer, more diverse CTD with 52 repeats and several repeats in the proximal part of the CTD that vary from the consensus sequence. Interestingly, the CTD is dynamically modified throughout the transcription cycle. Phosphorylation of the Serine residues is the best-studied modification but also acetylation, methylation, ubiquitinylation and Proline-isomerization have been described. Given the complexity of potential modification patterns, the CTD is regarded as a binding platform for a multitude of transcription-associated factors. This forms the CTD into a 'switch panel' that controls the whole process of transcription.

1.2.3 Kinases phosphorylate the CTD throughout the transcription cycle

Cyclin-dependent kinases (Cdks) can be divided into two major groups. The activity of Cdks 1, 2, 3, 4, 5, and 6 is tightly connected to regulation of the cell cycle and cell division. The second group is involved in regulation of transcription and includes Cdks 7, 8, 9, 12, and 13 whereas Cdk10 and Cdk11 presumably contribute to both processes (Paparidis et al. 2017). As described below, all transcription-related Cdks have been reported as CTD kinases (Eick & Geyer 2013). Recently, it was suggested that Cdk11 phosphorylates the CTD as well (Pak et al. 2015). However, according to a previous *in vitro* study Casein Kinase 2 (CK2) but not Cdk11 facilitates CTD phosphorylation and Cdk11 is in fact a CK2 target (Trembley et al. 2003).

The dynamic modification patterns of the CTD throughout the transcription cycle have been revealed, using phospho-specific antibodies in chromatin immunoprecipitation (ChIP) and native elongating transcript sequencing (NET-seq) analyses (reviewed in Eick & Geyer 2013; Zaborowska et al. 2016). When Pol II enters the pre-inititation complex its CTD is hypo-phosphorylated, a state known as *IIa* form (Lu et al. 1991) (Figure 1-2A-B). The first modifications of the CTD are placed at the 5' end of the gene during the initiation phase. Here, Cdk7, a subunit of the general transcription factor TFIIH, phosphorylates Ser5 and Ser7 (Akhtar et al. 2009; Glover-Cutter et al. 2009; Kim et al. 2009; Lu et al. 1992; Rodriguez et al. 2000) (Figure 1-2C). The intact PIC and presence of the Mediator are prerequisites for phosphorylation of Ser7 (Ser7-P) by Cdk7 (Boeing et al. 2010). The same study suggests that additional, so far unknown kinases phosphorylate Ser7 in coding regions. Functionally, Ser7-P supposedly regulates transcription of small nuclear RNAs (Chapman et al. 2007; Egloff et al. 2007). Phosphorylation of Ser5 is required for successful release of Pol II from the PIC as well as for recruiting the 5' end capping enzyme which interacts with Ser5-P and Tyr1 (Cho et al. 1997; Ghosh et al. 2011; McCracken et al. 1997; Søgaard & Svejstrup 2007). Tyr1-P is

mostly found at the beginnings of coding genes, where it is also associated with anti-sense promoter transcription and active enhancers (Descostes et al. 2014). The only kinase with reported Tyr1-P activity so far is c-Abl (Baskaran et al. 1999), although the role of c-Abl as a CTD kinase remains unclear (Zaborowska et al. 2016). Together, the dynamic phosphorylations of the CTD are shifting Pol II into the hyperphosphorylated IIo form, a state that marks the polymerase as actively transcribing.

The level of Ser5-P gradually drops during elongation caused by phosphatase activity of RPAP2 and Ssu72 (Egloff et al. 2012; Krishnamurthy et al. 2004; Wani et al. 2014). Ssu72 dephosphorylates Ser7-P as well, and is essential for efficient termination (Zhang et al. 2012). Ser2 gets phosphorylated by Cdk9 (Cho et al. 2001; Marshall et al. 1996; Wood & Shilatifard 2006) which is regarded as a requirement for efficient elongation (Figure 1-2D). *In vitro* studies on CTD peptides point to a role of Cdk9 as a Ser5 kinase and suggest that Ser5-P but not Ser2-P marks the polymerase for efficient pause release and Ser7-P primes the CTD for this modification (Czudnochowski et al. 2012). Interestingly, inhibition of Cdk9 with the chemical inhibitor Flavopiridol caused increased promoter proximal pausing of Pol II, indicating that efficient pause release is blocked upon inhibition of Cdk9 (Jonkers et al. 2014). However, Flavopiridol is known to inhibit other kinases as well, including Cdk12 and Cdk13 that both have been reported to be Ser2 kinases (Bartkowiak et al. 2010). Conversely, the histone reader Brd4 was recently described to possess Ser2 kinase activity, in addition to its well-known role in P-TEFb activation (Devaiah et al. 2012). While the roles of Brd4 and Cdk13 as Ser2 kinases need to be further elucidated, several studies have analyzed the function of Cdk12 in more detail.

The majority of Cdk9 occupies the 5' region of a gene (Ghamari et al. 2013; Lin et al. 2011), but Cdk12 is mostly found at the 3' end (Bartkowiak et al. 2010). This suggests a mechanism in which Cdk9 is placing Ser2-P marks early in transcription, whereas Cdk12 is the major Ser2 kinase towards the 3' end of genes (reviewed in Bowman & Kelly, 2014). Nonetheless, two recent studies reported a role for Cdk9 in transcription

termination, hence at the 3' end of genes. Here Cdk9 possibly regulates Pol II pausing at the poly(A) site (Laitem et al. 2015) or as a regulatory kinase of Xrn2 (Sansó et al. 2016) (see "Termination" paragraph in chapter 1.2.1). Another CTD phosphorylation mark, Thr4-P, is highest at 3' ends and Polo-like kinase 3 (Plk3) is presumably the responsible kinase in human cells (Hintermair et al. 2012). Importantly, the CTD gets dephosphorylated to allow processive termination and recycling of Pol II for another transcription cycle (Cho et al. 2001; Lin et al. 2002). Together, these dynamic CTD modifications are connected to the different stages of the transcription cycle and Pol II activity.

1.2.4 Brd4 recruits Cdk9 to sites of active transcription

Brd4 is a member of the mammalian bromo and extra-terminal domain protein family (BET), which further comprises Brd2, Brd3, and testis-specific Brdt (reviewed in Taniguchi, 2016) (Figure 1-3A). The characteristic domains of mammalian BET proteins are conserved in orthologues including *Drosophila* fs(1)h and *Saccharomyces cerevisiae* Bdf1 and Bdf2. All four mammalian BET proteins feature two N-terminal bromodomains (BD1 and BD2). Bromodomains are common in chromatin-associated proteins and proteins equipped with bromodomains usually bind acetylated histone tails. This has also been observed for Brd4 (Dey et al. 2003). Interestingly, the histone binding specificity amongst the two bromodomains of Brd4 differs and is more similar for a single bromodomain of different BET proteins (Filippakopoulos et al. 2012). This is in line with the phylogenic representation of human bromodomains, where each BD1 and BD2 of the different BET proteins are grouped together (G. Zhang et al. 2015) (Figure 1-3A).

In addition to bromodomains, other Brd4 domains are similar important for supporting the function of this histone reader. Two p53 interacting domains were described, located in between BD2 and ET. Interestingly both domains, BID and PDID, could pull down p53 independently and have been proposed to provide regulatory functions to Brd4, triggered by phosphorylation by Casein Kinase II (Wu et al. 2013).
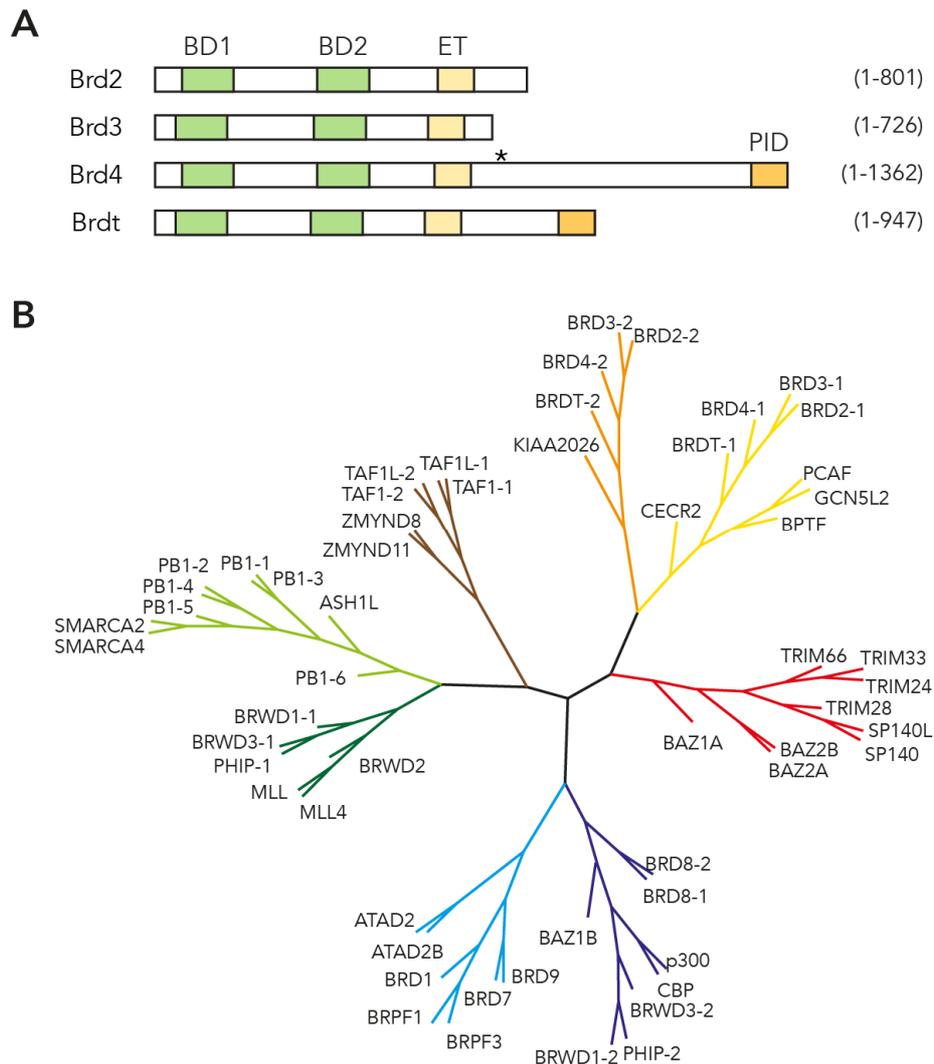
Figure 1-3 | The human BET protein family. (A) Domain structure of the human BET protein family. All BET members feature two tandem bromodomains (BD1 and BD2) at the N-terminus and an extraterminal (ET) domain. Brd4 harbors a P-TEFb interacting domain (PID) which is conserved in Brdt. The asterisk (*) marks the length of a second isoform Brd4 short (Brd4S) which lacks the C-terminal stretch from 723-1362. **(B)** In the phylogenic tree of human bromo-domains BD1 (yellow) and BD2 (orange) are grouped together although they are derived from different BET proteins (modified from Zhang et al. 2015a).

The ET domain supposedly regulates chromatin modifying enzymes and was report-ed to bind the argenine demethylase JMJD6 and the lysine methyltransferase NSD3 (Liu et al. 2013; Rahman et al. 2011). Additionally, interactions of the ET domain with nucle-osome remodelers SWI/SNF and CHD4 were described (Rahman et al. 2011). Brd4 is unique for a P-TEFb-interacting domain (PID) at its C-terminus, where it binds the ki-

nase subunit Cdk9. This domain is highly conserved in human testis-specific Brdt and *Drosophila* fs(1)h (Bisgrove et al. 2007). The kinase activity of Cdk9 is essential for transcriptional elongation of most mammalian genes (see chapters 1.2.1 and 1.2.3). Hence, the current model depicts Brd4 as a chromatin reader that binds to active chromatin via acetylated histone marks using its N-terminal bromodomains. The PID domain can then recruite and activate P-TEFb from its inactive complex that further comprises Hexim1/2, Larp7, MePCE and 7SK snRNA, which is also known as 7SK small nuclear ribonucleoprotein (snRNP) (Yang et al. 2005). Importantly, only the activated P-TEFb can join the transcriptional machinery and release Pol II from the elongation block (reviewed in dos Santos Paparidis et al. 2016) (Figure 1-2D).

Brd4 is the only somatic BET member capable of directly binding to Cdk9, since the PID domain is not present in the short isoform of Brd4 (Brd4-s), Brd2 or Brd3. However, BD2 of Brd4 might also bind P-TEFb via acetylated CyclinT1, suggesting a 2-step mechanism of P-TEFb activation by Brd4 that also involves the BD2 domain (Schröder et al. 2012). Interactions between P-TEFb and BD2 of BET proteins other than Brd4 have not been reported so far. Together, this highlights the importance of the PID for Brd4 function as it directly connects Brd4 to transcriptional regulation.

Given its role as P-TEFb activator, Brd4 facilitates transcription not only at coding genes but also at enhancers (Kanno et al. 2014; Liu et al. 2013). In fact, Brd4 has been described as a key factor characteristic for so-called super enhancers (Hnisz et al. 2013; Lovén et al. 2013). These enhancers are typically highly active and promote transcription of genes that define cell identity. Genome-wide ChIP-seq studies demonstrate co-occupancy of Mediator and Brd4 at super enhancers, highlighting the connection between the two transcriptional regulators that were co-purified previously (Jiang et al. 1998; Lovén et al. 2013). High Brd4 occupancy at enhancers suggests that Brd4 activates transcription of enhancer-associated genes. Indeed, inhibition of Brd4 with a small molecule drug resulted in transcriptional elongation defects that mainly affected genes regu-

lated by super-enhancers (Lovén et al. 2013). In summary, Brd4 is associated with the transcription of most active genes and is therefore a master regular of transcription.

1.2.5 Brd4 and cancer

In the year 2010 two small molecule inhibitors were developed that specifically target the bromodomains of BET proteins. These two inhibitors, JQ1 and I-BET, were the first of a new drug class called BET inhibitors (Filippakopoulos et al. 2010; Nicodeme et al. 2010). Importantly, both JQ1 and I-BET target the bromodomains of all BET family members including Brd2, Brd3, Brd4, and Brdt. JQ1, like all other BET inhibitors, binds to the histone-acetyl binding pocket of the bromodomains thereby blocking the binding to acetylated histone tails. Constantly, improved BET inhibitors are reported. For example, the novel inhibitor RVX-297 demonstrates differential binding to BD1 and BD2 domains of BET proteins, selectively targeting BD2 (Kharenko et al. 2016). Together, BET-inhibitors are a powerful tool to study Brd4 function.

Inhibition of Brd4 with JQ1 results in its eviction from active chromatin. Accordingly, Brd4 occupancy decreases at many genes after treating human cell lines with JQ1. At genes where Brd4 is the major recruiting factor of P-TEFb, this resulted in reduced gene expression, as described for the *c-Myc* oncogene (Delmore et al. 2011; Mertz et al. 2011). JQ1 lead to broad eviction of Brd4 from chromatin in B-cell tumors and repressed genes were enriched for c-Myc and E2F targets (Donato et al. 2016). Similar results were reported for I-BET, which inhibited transcription of *BCL2*, *c-Myc* and *CDK6* in promyelocytic leukemia cells (Dawson et al. 2011). It was known before that Brd4 has an implication in some forms of cancer, as the Brd4-NUT fusion oncogene was identified in aggressive forms of carcinomas (French et al. 2003). Brd4 further promotes expression of viral oncogenes from human papilloma virus (Yan et al. 2010). With these findings, it was recognized that BET-inhibitors very effectively decrease expression of several oncogenes along with anti-proliferative effects when tested in human cancer cell lines. Consequently, Brd4 was identified as a promising target for cancer therapy.

The therapeutic potential of Brd4 inhibition was rapidly evaluated. Screening of several cell lines for JQ1 sensitivity indicated that lymphoid and myeloid tumors are especially responsive to the inhibitor in terms of anti-proliferative effects (Mertz et al. 2011). This was confirmed in animal models for acute myeloid leukemia (AML) and multiple myeloma (MML), where JQ1 efficiently reduced tumor load (Delmore et al. 2011; Zuber, et al. 2011). Numerous studies have followed and demonstrated that a wide range of tumors, including breast cancer and prostate cancer, can potentially be drugged with BET inhibitors (Asangani et al. 2014; Shu et al. 2016). Based on the results obtained from cell culture experiments and animal studies, early excitement arose about this new drug class. Several ongoing clinical trials are evaluating the efficiency and safety of BET inhibitors for human patients (Andrieu et al. 2016). In a recent report the administered drug OTX015 showed promising anti-tumor activity in patients with advanced stages of NUT midline carcinoma (Stathis et al. 2016). However, more clinical trials will provide major insights whether BET inhibitors are indeed applicable in therapy of human cancer patients.

1.3 Scope of this thesis

Brd4 and Cdk9 together are key regulators of transcription elongation. Elongation is tightly controlled within the transcription cycle of RNA Pol II as illustrated by the phenomenon of promoter proximal pausing. Furthermore, both proteins have implications in the development and maintenance of human cancers. This has led to the development of specific inhibitors of Brd4 and Cdk9, most famously JQ1 and Flavopiridol, respectively. Although these inhibitors have provided many insights into the function of the two proteins, their specificity is limited. Is Brd4 indeed the protein that mediates the anti-tumor effects of JQ1? Which target genes are specifically regulated by Brd4? Do distinct domains of Brd4 have differential downstream effects? What is the impact of the Brd4-Cdk9 interaction on global gene regulation? Which genes depend on Cdk9 activity

for processive transcription? These questions shall be answered within the scope of this thesis. The aim of this thesis is to shed light on (i) the specificity of JQ1 for targeting Brd4, (ii) the role of distinct Brd4 domains on global transcription regulation, (iii) the role of Brd4 as Cdk9-recruiting protein, and (iv) the role of Cdk9 in the synthesis of nascent transcripts.

2 Results

2.1 Establishment of an inducible expression system for Brd4 mutants

BET inhibitor JQ1 is not specific for a single BET family member. So far this applies to all other available BET inhibitors as well, restricting their use to inhibit only one particular BET protein. However, many studies use JQ1 to study Brd4 function, based on the assumption that Brd4 is the main target of JQ1. Furthermore, JQ1 solely inhibits the bromodomain function of BET proteins. Any conclusions about other Brd4 domains drawn from JQ1 studies are therefore likely based on secondary effects. Due to these limitations of JQ1, I developed an alternative strategy to inhibit Brd4.

To block the function of Brd4 in a domain-specific way, I constructed dominant-negative mutants. To this end, full length Brd4 was divided into 9 overlapping fragments (f1-f9) of about 200 amino acids (aa) in length (Figure 2-1A). The HA-tagged constructs were cloned into the pRTS vector, which contains a bi-directional promoter allowing simultaneous expression of the Brd4 fragment and eGFP (Bornkamm et al. 2005). eGFP was used as a reporter for efficient induction. Vectors were stably transfected into Burkitt lymphoma Raji cells, because this cell line was reported to be highly sensitive to JQ1 (Mertz et al. 2011), suggesting that Raji cells are dependent on functional Brd4. Positively transfected cells were selected with hygromycin B and expression was induced by doxycycline (dox). Dox levels were carefully titrated to avoid toxic effects on the cells. Western analysis revealed that all Brd4 fragments f1-f9 were properly expressed, although at different levels (Figure 2-1B). Full-length Brd4 (Brd4-HA) and f7 yielded low signals compared to f1, f2, f4, f8 and f9 with intermediate and f3, f5 and f6 with high levels of expression. No HA signal was detected in cells transfected with a luciferase-

expressing construct (Raji-luc), which served as a control. Together, this repository of

inducible Brd4 fragments allowed screening for dominant-negative mutants.
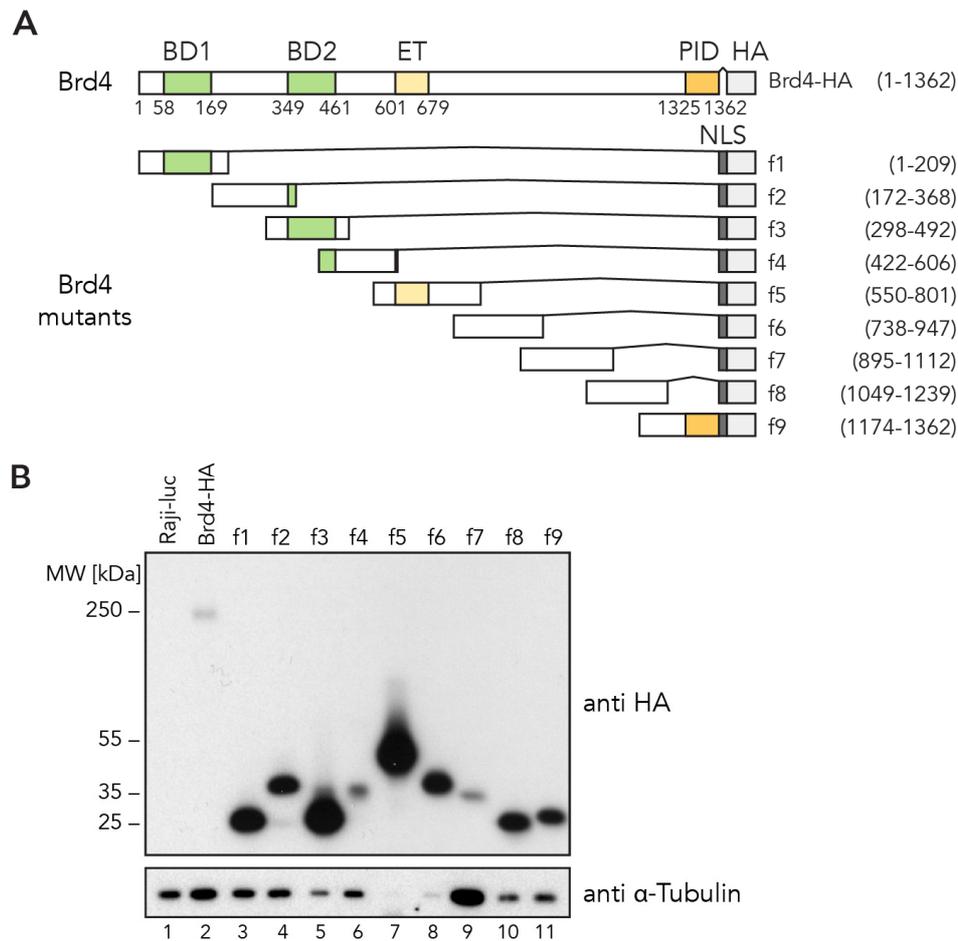
Figure 2-1 | Expression system for Brd4 mutants. (A) Schematic structure of recombinant full-length human Brd4 protein (Brd4-HA) and Brd4 fragments f1-f9. BD1/2 = bromodomain 1/2, ET = extra-terminal domain, PID = P-TEFb-interacting domain, HA = hemagglutinin tag, NLS = nuclear localization signal. **(B)** Expression levels of HA-tagged Brd4 mutants, assessed via Western analysis of the HA tag. α-Tubulin served as loading control. Samples were diluted with loading buffer prior to loading to visualize all signals on a single membrane (dilution ratios: lanes 2 and 9, 1:1; lanes 1, 3, 4, 6, 10 and 11, 1:10; lanes 5, 7 and 8, 1:20). Raji-luc cells expressed a non-tagged luciferase and served as negative control.

2.2 Expression of Brd4 fragments inhibits cell proliferation

I next investigated if overexpression of specific Brd4 domains can inhibit cell proliferation. For this purpose, I screened all cloned Brd4 constructs for a dominant-negative phenotype using proliferation assays. After induction of the Brd4 constructs, cell prolif-

eration was monitored for 8 days. Two days after induction I consistently detected that proliferation rates were (i) substantially reduced for cells expressing Brd4 fragments f3, f5, f9, (ii) intermediately reduced for f4 and f6, and (iii) not affected in the control cell line Raji-luc or other Brd4 fragments (Figure 2-2).
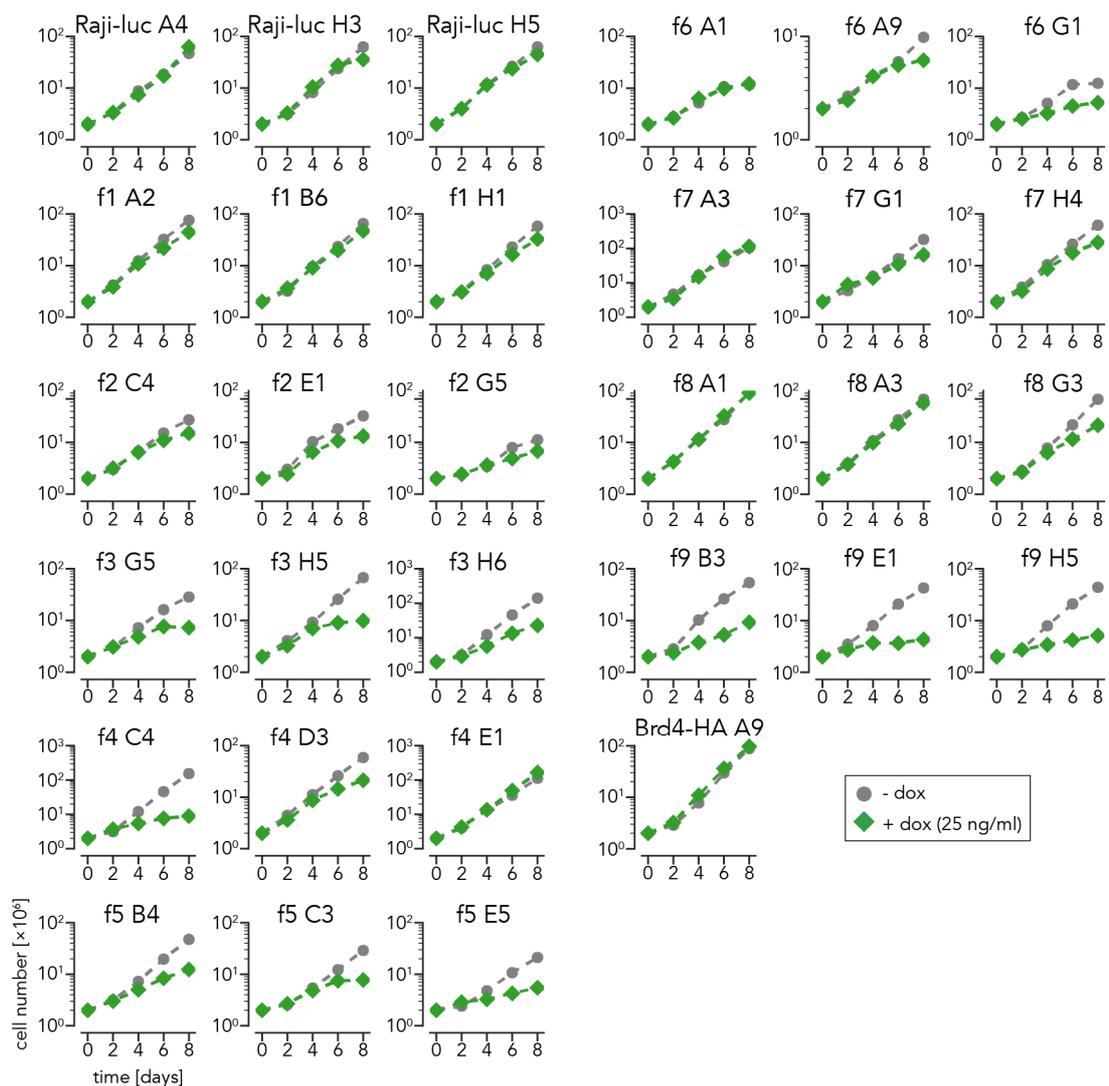
Figure 2-2 | Proliferation assay Brd4 mutants. Living cell numbers (log scale) of induced (25 ng/ml doxycycline, green) vs. non-induced (grey) cells were plotted against time. Induced cells expressed either luciferase (Raji-luc, negative control), Brd4 fragments f1 - f9, or recombinant full-length Brd4 (Brd4-HA). For each condition three biological replicates were analyzed, except Brd4-HA, for which I obtained only one inducible clone.
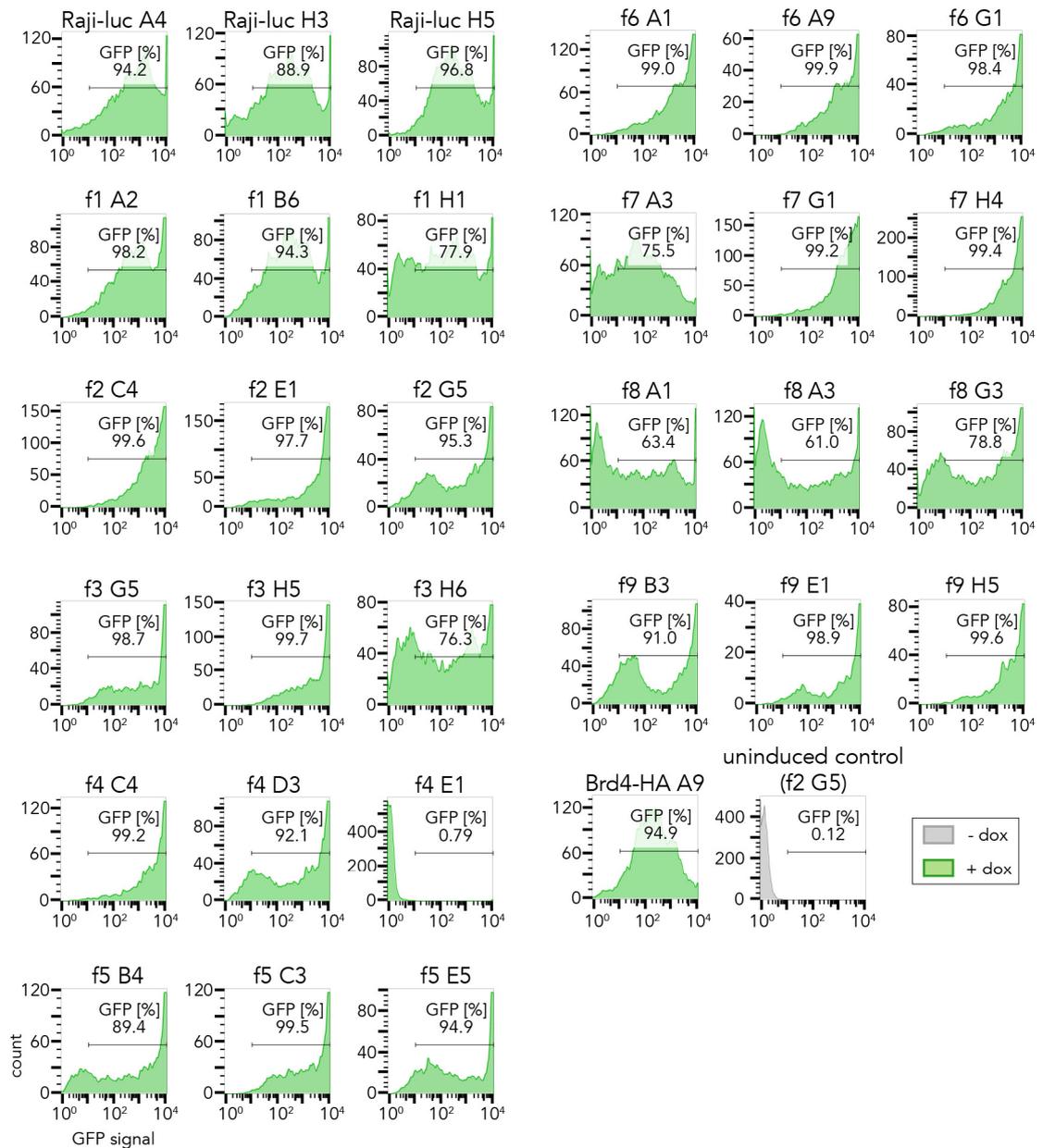
Figure 2-3 | Induction of Brd4 mutants used in the proliferation assay. Ratios of induced cells (green) were assessed by measuring GFP reporter signals using flow cytometry, as a control for the proliferation assay on day 8 (Figure 2-2). Uninduced Raji f2 cells served as negative control (grey). For most replicates induction levels of ~90% were measured, with the exception of f4 E1, which was GFP negative, suggesting a selection of a non-inducible subclone.

Proliferation rates were analyzed in three biological replicates. Here mutant f4 showed inconsistent proliferation defects, because for replicate f4 E1 no defect was observed. To verify efficient induction of the constructs in all cells, a prerequisite for dom-

inant-negative inhibition, I measured GFP reporter signals on day 8 via flow cytometry and found induction rates of ~ 90% for most samples (Figure 2-3). However, f4-E1 was not inducible on day 8 indicating that the dominant-negative conditions selected for a non-inducible subpopulation in this replicate. Notably, I could confirm the dominant-negative phenotype of Brd4 mutants in the non-small cell lung carcinoma cell line H1299 (Figure 2-4)
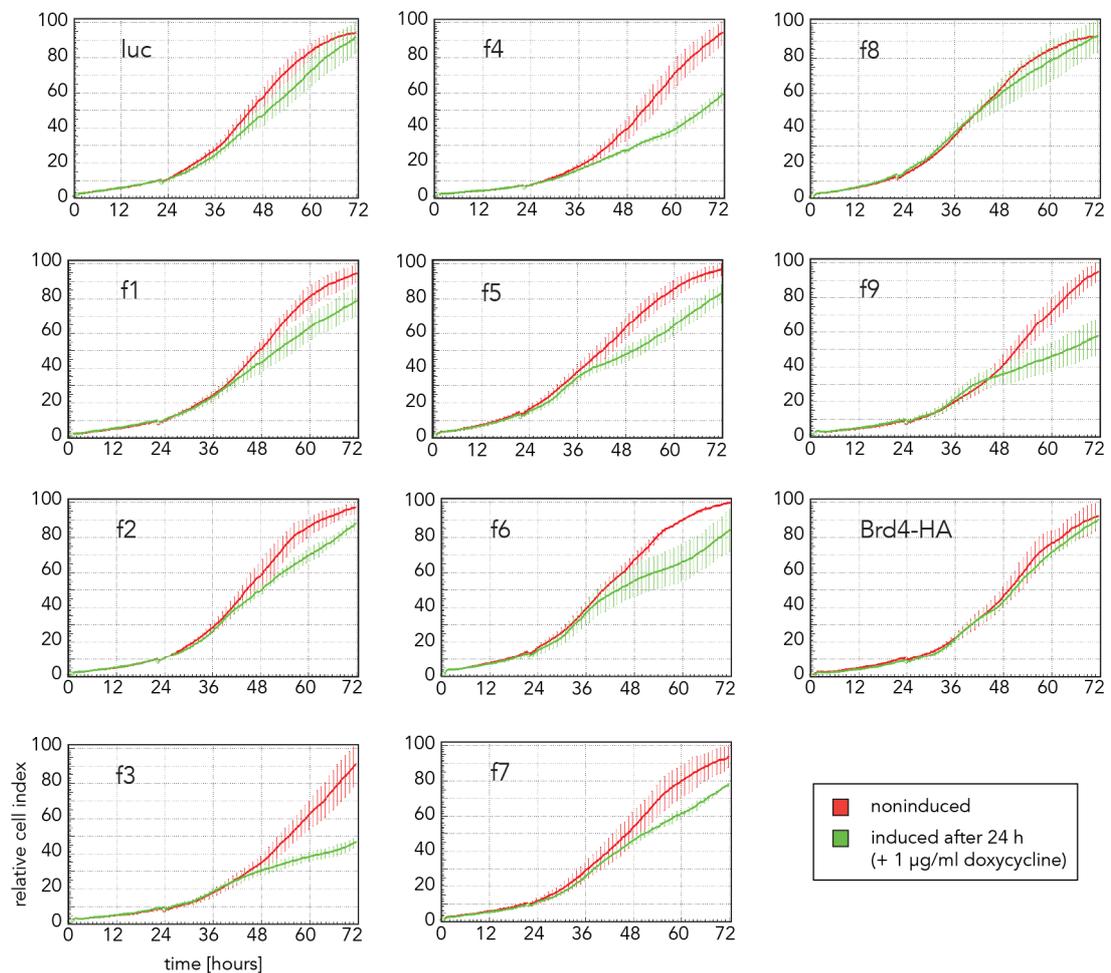
Figure 2-4 | Proliferation assay of dominant-negative Brd4 mutants in H1299 cells. Proliferation of H1299 cells that express Brd4 constructs or luciferase (control) was measured using the XCelligence system (Roche). Expression of the recombinant proteins was induced via 1 µg/ml doxycycline 24 h after seeding of the cells. The cell index of induced (green) and non-induced (red) cells was measured for additional 48 h and plotted against time. Error bars: standard deviation, n=2.

Unexpectedly, expression of f3 comprising BD2 strongly inhibited cell proliferation whereas f1 comprising BD1 did not. I constructed a Brd4 f-BD1 mutant (54-168 aa of full length Brd4) to test whether overexpression of the first bromodomain alone will cause proliferation defects comparable to other dominant-negative mutants. Indeed, expression of f-BD1 caused substantial growth defects in well-induced cells (Figure 2-5), indicating that the N-terminal or C-terminal regions that flank BD1 in mutant f1 suppress the dominant-negative activity of BD1 overexpression. This is consistent with crystal structures of Brd4 suggesting that the 20 residues preceding BD1 can loop backwards and block the acetylated lysine recognition site (Vollmuth et al. 2009). My findings support the speculative autoregulatory mechanism of the first bromodomain of Brd4 but more detailed investigations are necessary to shed light on the autoregulation of BET bromodomains.
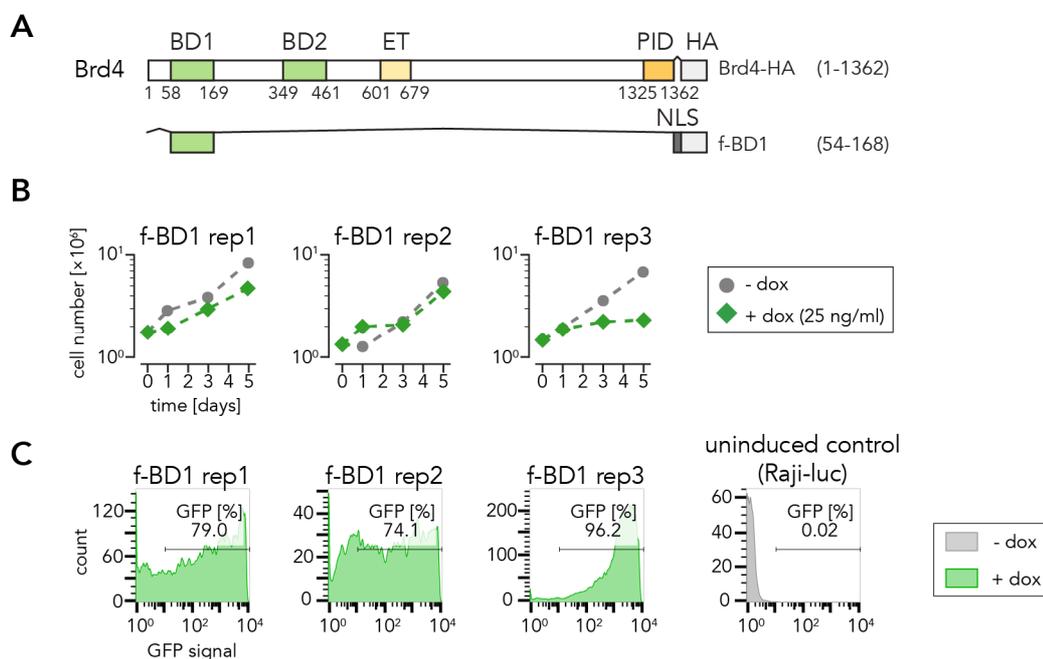
Figure 2-5 | Characterization of Brd4 f-BD1 mutant. (A) Schematic structure of recombinant full-length human Brd4 protein (Brd4-HA) and Brd4 fragments f-BD1 comprising 54-168 aa of full-length Brd4. BD1/2 = bromodomain 1/2, ET = extra-terminal domain, PID = P-TEFb-interacting domain, HA = hemagglutinin tag, NLS = nuclear localization signal. **(B)** Proliferation kinetics. Cells numbers were counted at least every second day over a period of 5 days in total for three replicates (rep 1-3). **(C)** The proportion of GFP-positive, induced cells was determined using flow cytometry.

For instance, mutations within the N-terminus of Brd4 could reveal those residues that facilitate autoinhibition of BD1. In summary, Brd4 fragments that comprise functional domains are potent dominant-negative inhibitors. Mutants f3 (inhibition of bromo-domain function) and f9 (inhibition of P-TEFb-interacting domain function) were considered as most interesting dominant-negative mutants for inhibition of Brd4 function (dnBrd4). In the following experiments the impact of these two mutants on the cellular transcriptome of Raji cells was compared with the impact of JQ1.

2.3 Raji and H1299 cells have differential sensitivity to JQ1

Human cancer cell lines differ in their response to JQ1 (Mertz et al. 2011). To assess the individual sensitivity of Raji and H1299 cells, I performed proliferation assays in the presence of JQ1. Cells were treated with increasing concentrations of JQ1 for 72 h and cell proliferation was determined using an MTS-based colorimetric readout. Proliferation of H1299 cells was reduced to 50% (GI_{50}) at a JQ1 concentration of ~ 2 μM, whereas the GI_{50} for Raji cells was determined as ~ 100 nM (Figure 2-6A). Repression of *c-Myc* is a well-described downstream effect of JQ1 and a major reason for the growth inhibitory effects of JQ1 in cancer cell lines (Mertz et al. 2011). Furthermore, the *c-Myc* gene is translocated into the immunoglobulin locus in Raji cells, leading to overexpression of this oncogene (Nishikura et al. 1985). Therefore, I determined c-Myc protein levels after treatment with 1 μM and 2.5 μM JQ1 for 4 h. In H1299 cells, JQ1 had no effect on c-Myc protein levels as determined by Western analysis (Figure 2-6B), although high concentrations of JQ1 were used. Conversely, c-Myc signals were markedly decreased in Raji cells. These cell line-specific effects suggest that JQ1 acts on biological processes that vary among different cell lines. Next, I tested the long-term effects of JQ1 on Raji-luc cells, which served as control cell line in the subsequent experiments. I detected complete inhibition of cell proliferation with 500 nM JQ1 (Figure 2-6C). Thus, I considered 500 nM JQ1 as suitable concentration for the following transcriptome analysis.
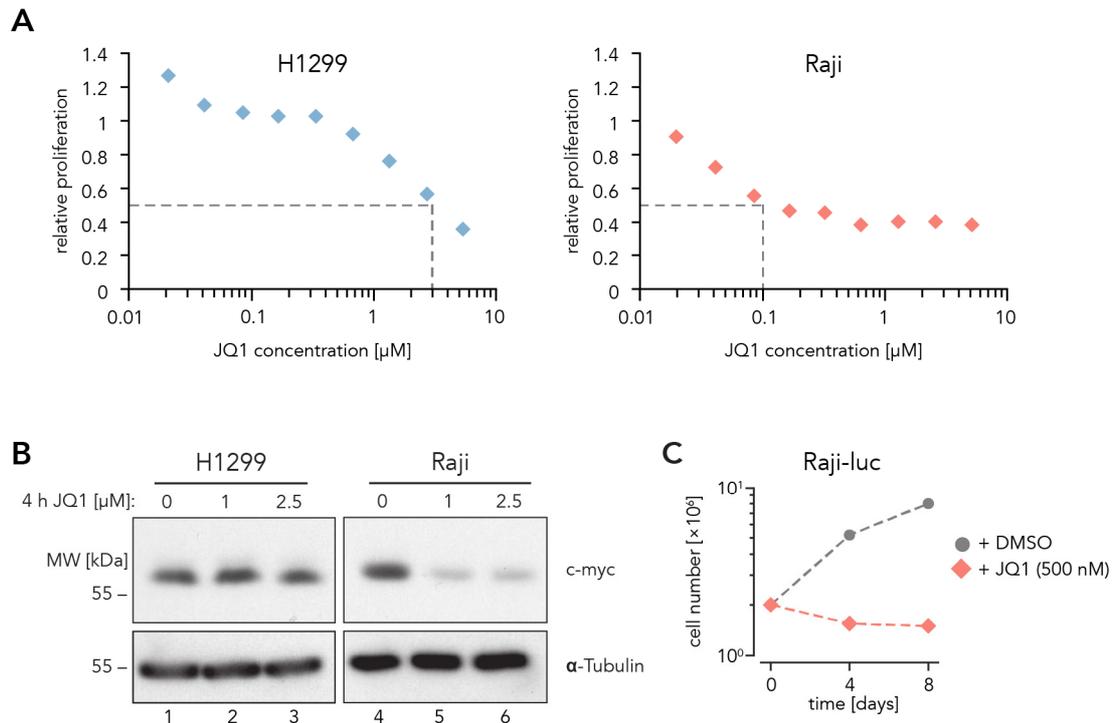
Figure 2-6 | Sensitivity of H1299 and Raji cells to JQ1 treatment. (A) Cell proliferation at increasing JQ1 concentrations (log scale) was determined using a colorimetric assay based on MTS metabolization. Measurements were performed for two biological replicates. **(B)** Cells were treated with 1 µM and 2.5 µM JQ1 for 4 h (DMSO as control). Protein levels of c-Myc were determined by Western analysis (3E10 anti-myc antibody, anti-α-Tubulin as loading control). **(C)** Induced Raji-luc cells were treated with 500 nM JQ1 (red) / DMSO (gray, control) for 8 days. Living cell numbers were counted and plotted against time.

2.4 Transcriptome analysis of dnBrd4 mutants and JQ1

2.4.1 Preparation and quality control of RNA-seq libraries

To characterize genes that are regulated by dnBrd4 mutants and to define the overlap between JQ1-regulated genes and dnBrd4-regulated genes, I performed RNA-sequencing (RNA-seq). In cooperation with Stefan Krebs (group of Helmut Blum, Gene Center), libraries of poly(A) enriched RNAs were prepared for five biological replicates of f3 and f9 dominant-negative Brd4 mutants, JQ1-treated Raji-luc cells, and DMSO-treated Raji-luc cells as control. All libraries were prepared 24 hours after inducing the

dnBrd4 mutants or 24 hours after adding JQ1. In parallel, sufficient induction was con-
firmed by flow cytometry analysis of eGFP expression (Figure 2-7).
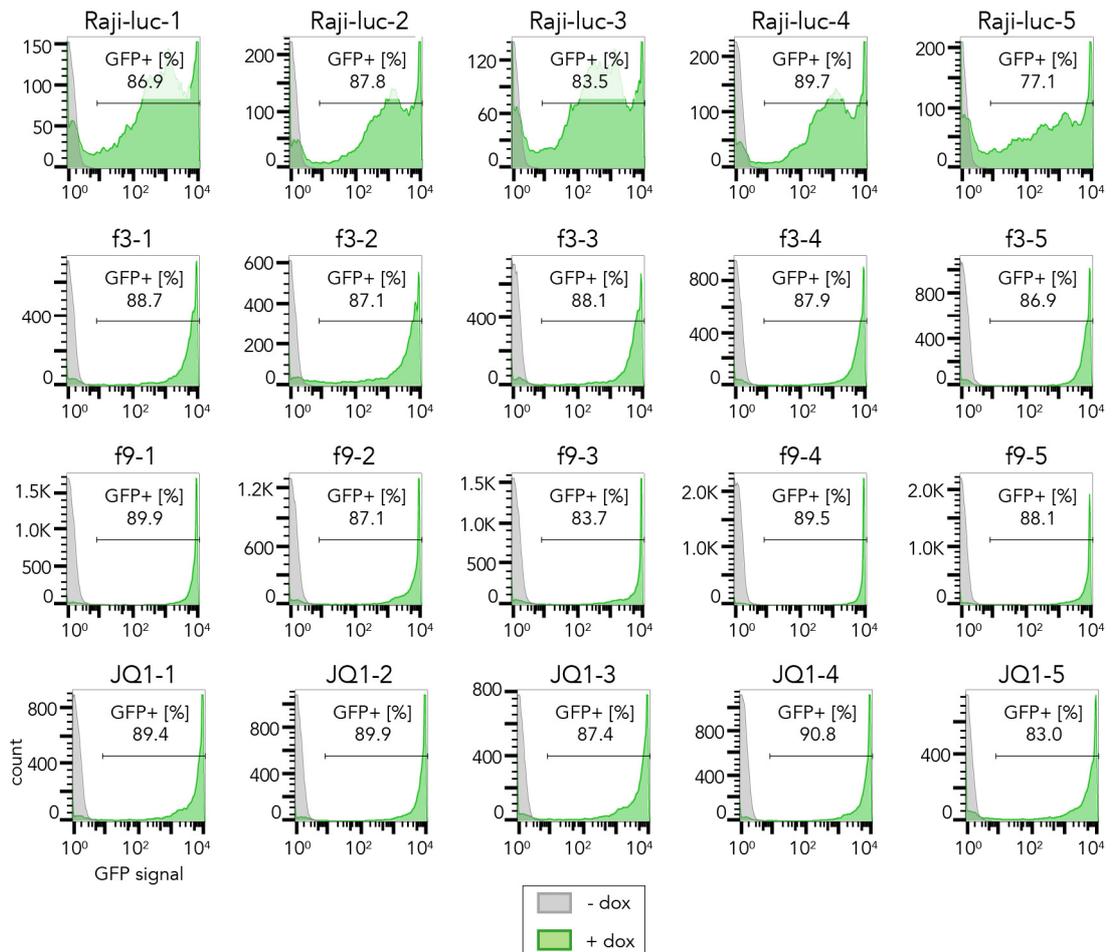
Figure 2-7 | Induction of Brd4 mutants used for RNA-seq. Ratios of induced cells (green) vs.
non-induced cells (grey) were assessed by measuring eGFP reporter signals using flow cytome-
try. Cells were induced by addition of 25 µg/mL doxycycline (dox).

RNA-seq data was analyzed by Michael Kluge (group of Caroline Friedel, LMU). As
quality control for low variation among the five biological replicates, principal compo-
nent analysis (PCA) was performed. Four clearly separated groups of samples were
identified by the PCA (Figure 2-8A), corresponding to the four investigated conditions.
Here, replicates of the same sample clustered closely together and were simultaneously
separated from other conditions. Furthermore, replicates of f3 and f9 clustered in close

proximity, suggesting higher similarities of their transcriptomes compared to the replicates of JQ1, which were more distant to all other conditions in the analysis.

Higher variation was observed for replicates 2 and 5 of condition f3 (f3-2 and f3-5), which did not cluster as closely with the rest of the f3 replicates. Similar results were obtained when performing hierarchical clustering analysis based on the Euclidean distance (Figure 2-8B). Here, f3-5 clustered with the remaining f3 replicates, while f3-2 clustered close to the DMSO-treated Raji-luc control group. Thus, replicate f3-2 was excluded from further analysis. In summary, this demonstrated high quality of the RNA-seq datasets, allowing for an in-depth differential expression analysis.
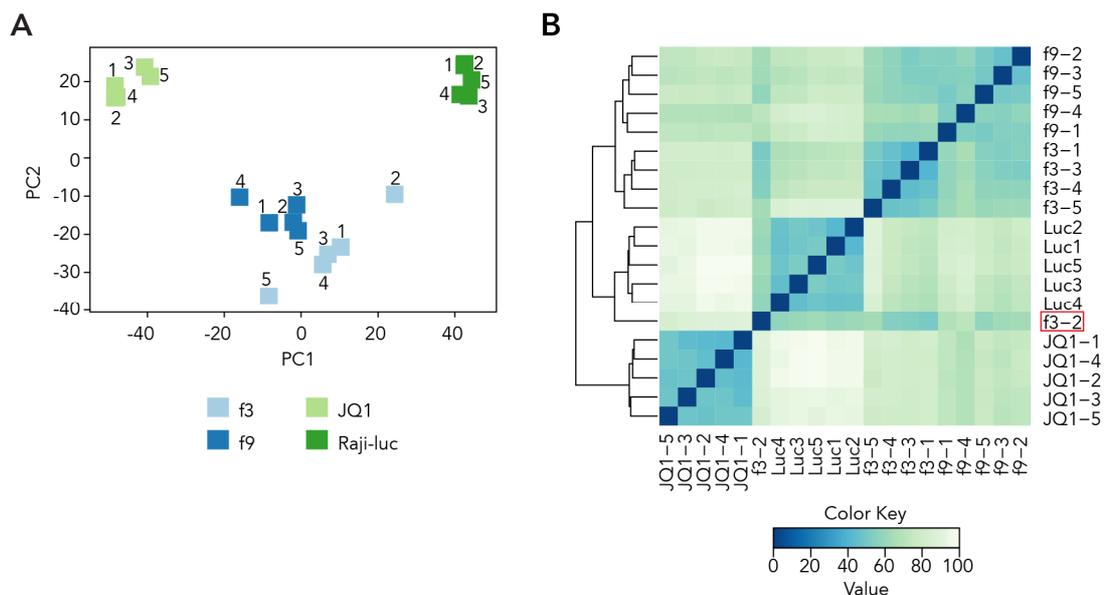
Figure 2-8 | Clustering analysis of RNA-seq samples. (A) Principal component analysis (PCA) of 20 RNA-seq samples; 5 replicates per condition. f3 replicate no. 2 (f3-2) did not cluster properly with the other f3. **(B)** Hierarchical clustering analysis based on the Euclidean distances between the normalized read counts. Replicate f3-2 (marked in red) clustered with the control group and was thus excluded from further analysis.

2.4.2 JQ1 and dnBrd4 mutant f3 regulate a common set of genes

Next I asked how JQ1 treatment and expression of dnBrd4 in mutant f3 affect the transcriptome. To this end, differential expression analysis relative to the DMSO-treated

Raji-luc control was performed and the overlap of differentially expressed (DE) genes (p-value ≤ 0.05, no fold-change cutoff) was calculated. Remarkably, 66% and 55% of expressed genes were significantly differentially expressed under JQ1 treatment and expression of the f3 mutant, respectively, indicating substantial deregulation of gene expression. More importantly, 4971 of 7745 JQ1-regulated genes (64%) were also regulated by f3 (Figure 2-9A, left).
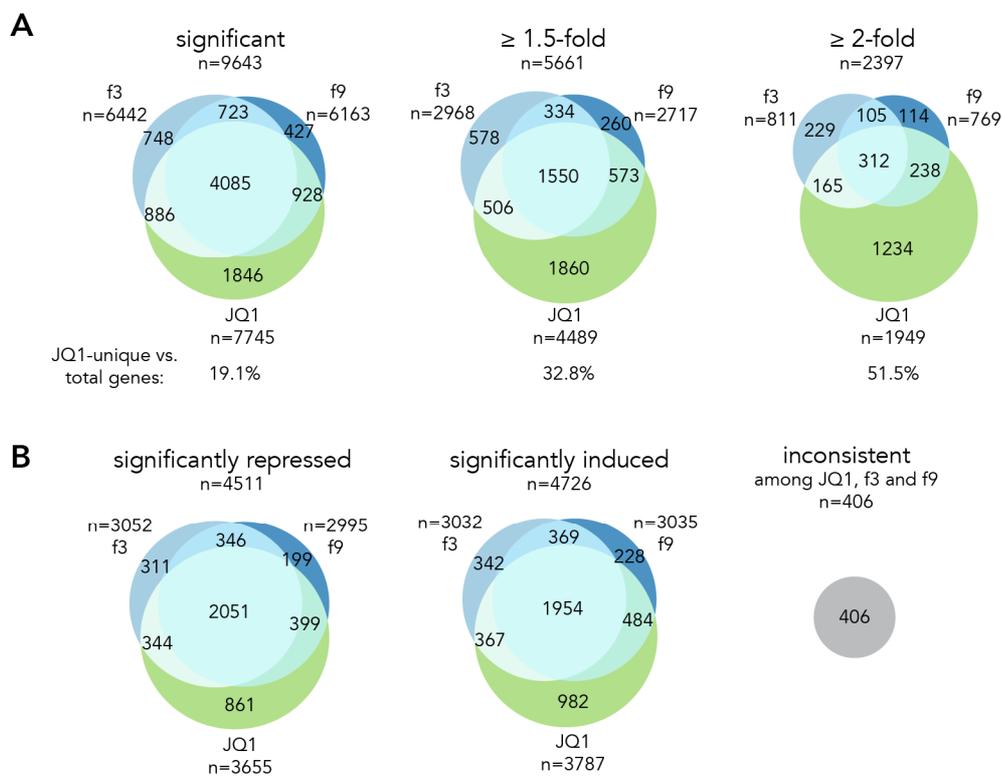
Figure 2-9 | Differential expression analysis. Differential expression analysis was performed using three different programs: limma, edgeR and DEseq2. Genes that were found significantly (p-value ≤0.05) differentially expressed with at least 2 out of the 3 programms (DE genes) were used for further analysis. **(A)** Significantly (p-value: ≤0.05) differentially expressed genes of f3, f9 and JQ1-treated Raji cells were plotted as Venn diagram to visualize commonly regulated genes (left). DE genes were further filtered by applying increasing fold-change filters (≥ 1.5-fold, center; ≥ 2-fold, right). The percentage of JQ1-unique genes (green) relative to the total number of DE genes that passed the filter was calculated. **(B)** DE genes were split into commonly repressed (left), commonly induced (center) and inconsistent genes (right). A gene was considered as inconsistently regulated when it was upregulated in one group and downregulated in another group.

This suggests that Brd4 fragment f3 comprising BD2 potentially inhibits Brd4 similar to JQ1 by blocking the bromodomain function. Notably, the direction of the change in gene expression was the same for DE genes of JQ1 and f3 conditions: 95 % of the common DE genes were consistently repressed (2395) or induced (2321) by both f3 and JQ1 (Figure 2-9B) and the rank correlation between corresponding fold-changes was 0.84. Thus, JQ1 and dnBrd4 f3 regulate the transcriptome of Raji cells in a very similar manner with the same set of genes being either repressed or induced.

2.4.3 Brd4 PID is linked to bromodomain function

Since both, JQ1 and f3, inhibit the bromodomain function of Brd4, I further investigated the consequences of inhibiting the P-TEFb interacting PID domain of Brd4. For this purpose I compared the transcriptomes of dnBrd4 mutants f9 and f3. Strikingly, f9 DE genes accounted for 4808 of f3 DE genes (75%) (Figure 2-9A, left) and rank correlation of significant fold-changes was 0.93. This demonstrates that dnBrd4 mutants f3 and f9 regulate a large set of common genes in a similar way, and further suggests that the gene regulatory activity of Brd4 requires the PID domain. Next I compared the transcriptomes of f9 and JQ1-treated cells. Here, f9 DE genes accounted for 5013 DE genes of JQ1-treated cells (65%) with a rank correlation of fold-changes of 0.9. This implies that disruption of the Brd4 PID function has similar effects on the transcriptome as JQ1. In summary, inhibition of BD2 and PID domains of Brd4 caused strongly overlapping changes in gene expression, suggesting that both domains are functionally linked.

2.4.4 JQ1 deregulates gene expression more strongly than dnBrd4 mutants

Interestingly, comparison of median fold-changes of regulated genes between the different conditions indicated that the effect of JQ1 on gene expression was more pronounced than for the dnBrd4 mutants. While median fold-changes for either up- or down-regulated genes were ~ 1.46 for the dnBrd4 mutants, under JQ1 treatment they were

~ 1.52 for up-regulated genes and 1.67 for down-regulated genes. Although these differences are small, they are highly statistically significant (Wilcoxon rank sum test, p-value $<10^{-5}$) and have a considerable effect on the number of DE genes identified at different fold-change cut-offs. When I successively applied $\geq$ 1.5-fold and $\geq$ 2-fold-change filters to the dataset of DE genes, the resulting Venn diagrams revealed that more JQ1-regulated genes (1949 at fold-change 2) passed these increasing filters compared to genes regulated by mutants f3 and f9 (811 and 759, respectively, Figure 2-9A). This indicates that JQ1 affects gene expression more strongly than dnBrd4 mutants f3 and f9.

2.4.5 Genes activated by Brd4 inhibition

Previous studies on transcriptomic changes induced by BET-inhibitors mainly focused on downregulated genes and thereby highlighted the activating function of Brd4. To investigate also the repressive role of Brd4, I compared up- and downregulated genes. Surprisingly, in all three groups around 50% of genes were upregulated (Figure 2-10), suggesting that Brd4 is not only activating transcription but is also involved in the repression of many genes. This repression of many genes is not necessarily due to direct transcriptional repression by Brd4, but possibly a downstream effect resulting from Brd4-mediated upregulation of transcriptional repressors. For instance, cyclin dependent kinase inhibitors *CDKN1B* and *CDKN2B*, which are significantly upregulated by f3, f9 and JQ1 (1.59-fold to 3.7-fold) (Table 2-1A), have been shown to be transcriptionally repressed by c-Myc (Herkert & Eilers 2010).
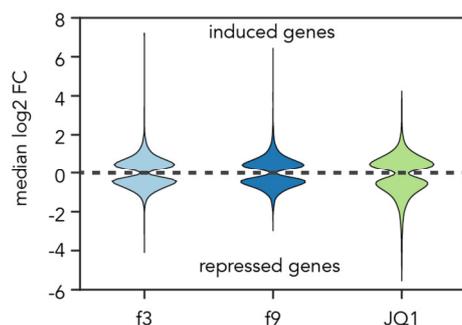
Figure 2-10 | Distribution of median log2 fold-change for DE genes. Induced genes were plotted above the dashed line, reduced genes below. Median log2 FCs were calculated using the log 2 FC values determined by the differential expression programs that found a statistical significant change (p-value: ≤0.05; at least 2 out of limma, edgeR, DEseq2).

Another interesting set of genes upregulated by f3, f9, and JQ1 are *AFF1*, *AFF4,* and *AF9*, members of the super-elongation complex (SEC) (Table 2-1B). Since SEC, like Brd4, binds P-TEFb (Lin et al. 2010; Lu et al. 2016), this suggests a balancing mechanism in which SEC is upregulated upon inhibition of Brd4. So far, little is known about transcriptional regulation of the corresponding genes, making it difficult to propose a detailed mechanism. Nevertheless, these regulatory circuits further exemplify the complex role of Brd4 in transcriptional gene regulation.

Table 2-1 | Differential expression analysis of representative genes. Representative genes were listed according to the median log2 fold changes (FC) determined for the JQ1 samples. Median log2 FCs were calculated using the log 2 FC values determined by the differential expression programs that found a statistical significant change (p-value: ≤0.05; at least 2 out of limma, edgeR, DEseq2). Upregulated genes are labeled in blue, downregulated genes are labeled in green. NS (not significant). **(A)** *c-Myc* and c-Myc-regulated genes. **(B)** Genes encoding for subunits of the super elongation complex (SEC).

A

Gene	median log2 FC			
	f3	f9	JQ1	
CDKN1B		0.67	1.09	1.16	induced
CDKN2B		1.89	1.88	1.53	
C-MYC		-1.14	-0.86	-1.21	repressed

B

super elongation complex (SEC)

Gene	median log2 FC			
	f3	f9	JQ1	
AFF1		1.07	0.67	1.12	
AFF2		0.70 NS		1.10	
AFF4		0.67	0.45	0.95	
MLLT3 (AF9)		0.99	0.75	0.92	
CDK9	NS	NS		0.34	induced
EAF1		-0.23 NS	NS		
MLLT1 (ENL)		-0.27	-0.28	-0.41	repressed
EAF2	NS	NS		-0.60	
AFF3	NS		-0.43	-1.27	

2.4.6 Brd4 DE genes are enriched for c-Myc target genes

C-Myc and c-Myc-regulated genes are well known downstream targets of JQ1 and are described as main mediators of the anti-proliferative effects of BET inhibition (Delmore et al. 2011; Mertz et al. 2011). I tested if c-Myc target genes are enriched in f3 and f9 DE genes in a comparable manner as JQ DE genes. To this end gene set enrichment analysis (GSEA) was performed using ranked lists of JQ1, f3, and f9 DE genes.

A

Enrichment plots: SCHUHMACHER_MYC_TARGETS_UP

B

Gene set	JQ1			Brd4 f3			Brd4 f9		
	n	NES	FDR q-val	n	NES	FDR q-val	n	NES	FDR q-val
ODONNELL_TARGETS_OF_MYC_AND_TFRC_DN	42	-2.53	< 0.001	42	-1.96	0.001	42	-2.24	< 0.001
YU_MYC_TARGETS_UP	39	-2.46	< 0.001	39	-1.69	0.006	39	-2.01	< 0.001
SCHUHMACHER_MYC_TARGETS_UP	72	-2.33	< 0.001	72	-2.75	< 0.001	72	-2.53	< 0.001
BILD_MYC_ONCOGENIC_SIGNATURE	144	-2.19	< 0.001	144	-2.57	< 0.001	145	-2.44	< 0.001
DANG_MYC_TARGETS_UP	128	-2.17	< 0.001	128	-2.64	< 0.001	128	-2.43	< 0.001
SCHLOSSER_MYC_TARGETS_AND_SERUM_RESPONSE_UP	45	-2.14	< 0.001	45	-2.42	< 0.001	45	-2.46	< 0.001
KIM_MYC_AMPLIFICATION_TARGETS_UP	134	-2.03	< 0.001	135	-2.05	< 0.001	143	-1.99	< 0.001
ACOSTA_PROLIFERATION_INDEPENDENT_MYC_TARGETS_UP	64	-1.86	0.002	63	-2.43	< 0.001	63	-2.38	< 0.001

Figure 2-11 | Gene set enrichment analysis (GSEA) of c-Myc target genes. (A) c-Myc signature enrichment plots in Raji-luc + 500 nM JQ1, Brd4 f3, and Brd4 f9 cells versus DMSO-treated Raji-luc cells as a control for all three conditions. Plots were prepared using the SCHUHMACHER_MYC_TARGETS_UP dataset (Schuhmacher et al. 2001) available at the Molecular Signatures Database (Liberzon et al. 2011). c-Myc target genes were enriched at the bottom of the ranked list of genes obtained from the previous DE analysis. **(B)** Table of selected c-Myc target gene sets enriched in all three samples (Acosta et al. 2008; Bild et al. 2006; Kim et al. 2006; O'Donnell et al. 2006; Schlosser et al. 2005; Yu et al. 2005; Zeller et al. 2003). n = number of genes in each set; NES = normalized enrichment score; FDR q-val = test of statistical significance.

I detected significant (FDR q-val < 0.001) enrichment of c-Myc target genes at the bottom of the ranked list, demonstrating that c-Myc-regulated genes are similarly downregulated in all three conditions (Figure 2-11A). Importantly, the enrichment for

c-Myc target genes was robustly reproduced for numerous other available gene sets (Figure 2-11B) (Acosta et al. 2008; Bild et al. 2006; Kim et al. 2006; O'Donnell et al. 2006; Schlosser et al. 2005; Schuhmacher et al. 2001; Yu et al. 2005; Zeller et al. 2003). In summary, the proliferation defects observed in f3 and f9 mutant cell lines are likely to be mediated by targeting c-Myc and c-Myc-regulated expression patterns. This further illustrates that the mechanisms of dominant-negative inhibition of Brd4 and BET inhibition using JQ1 largely overlap.

2.5 Establishment and validation of an analog-sensitive Cdk9 Raji cell line

Flavopiridol or i-Cdk9 are chemical inhibitors with high specificity for Cdk9. Frequently such inhibitors are used to study the cellular functions of Cdk9, assuming that unspecific effects on functionally related kinases like Cdk7 or Cdk12 are negligible. With the advent of the CRISPR/Cas9 gene editing technology, genetically manipulated kinases have been engineered in a way that allows highly specific inhibition of an individual kinase. This so-called 'analog-sensitive' (as) kinase technology is based on the mutation of a certain amino acid within the ATP-binding pocket of the kinase domain known as 'gatekeeper' (Lopez et al. 2014). Typically, the gatekeeper position is occupied by large amino acids like Phenylalanine. In analog-sensitive kinases the gatekeeper is mutated to a smaller amino acid. ATP-analogs with a bulky side chain can then be used to specifically target the analog-sensitive kinase, because their ATP-binding pocket is enlarged and can thus accommodate the analog while the wild type kinase cannot, as exemplified by a three-dimensional model for Cdk9 (Figure 2-12A-B).

Analog-sensitive Cdk9 Raji cell lines were engineered by Weihua Qin (Leonhardt Group, LMU Biocenter). In total two clones were identified that carried the designed Phenylalanine 103 to Alanine (F103A) mutation.
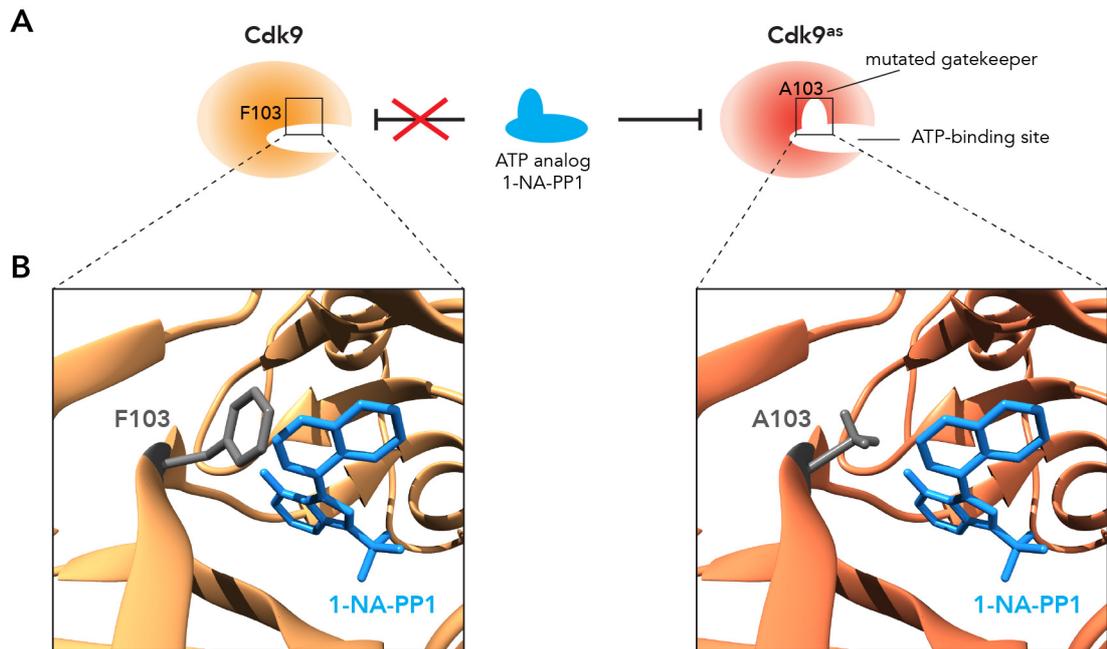
Figure 2-12 | Structure of engineered analog-sensitive Cdk9. (A) Schematic targeting strategy of the enlarged ATP-binding site of Cdk9[as] with the inhibitor 1-NA-PP1. Only when the gatekeeper residue F103 is mutated to alanine, the inhibitor can be accommodated. (B) Modeled 3D structure of the ATP-binding pocket occupied by 1-NA-PP1 of wild type Cdk9 (left, PDB: 3BLQ, Baumli et al. 2008) in comparison with Cdk9[as] (right). 3D modeling was performed using the USCF Chimera Software (Pettersen et al. 2004).The 3D model illustrates that F103 sterically interferes with 1-NA-PP1 whereas A103 allows the accommodation of the inhibitor.

One cell clone was homozygous for F103A (Cdk9[as]), the second clone was heterozygous for the gatekeeper mutation but additionally gathered a deletion within the second allele resulting in a premature STOP codon after the first N-terminal 100 amino acids (Cdk9[STOP/as]). Because it can be assumed that the Cdk9[STOP] allele is non-functional, both cell lines were considered to solely express analog-sensitive Cdk9.

2.5.1 Inhibition of analog-sensitive Cdk9 decreases cell proliferation

To further characterize the Cdk9as cell lines, I determined their sensitivity to the inhibitory Adenine analog 1-NA-PP1 in a proliferation assay. Cells were treated with increasing concentrations of 1-NA-PP1 for 72 h and cell proliferation was detected using an MTS-based colorimetric readout. Cell growth of both analog-sensitive cell lines was inhibited by $\geq 50\%$ at 1-NA-PP1 concentrations of 5 μM or higher (Figure 2-13A). Wild

type Raji cells were only slightly affected at very high concentrations. Given these re-
sults, 5 µM and 10 µM were considered as ideal concentrations of the inhibitor for the
following experiments.
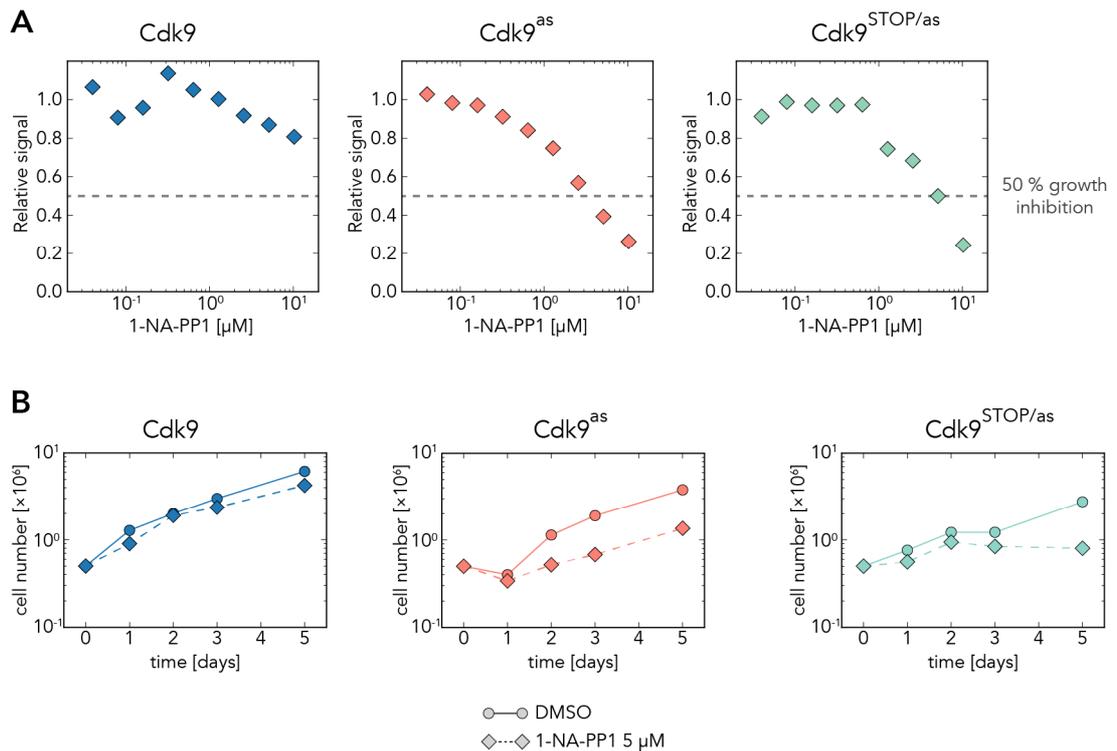
Figure 2-13 | Proliferation kinetics of Cdk9as cell lines. (A) Cell proliferation at increasing
concentrations of 1-NA-PP1 (log scale; relative to DMSO control) was determined using an
MTS-based colorimetric assay. Measurements were performed for two biological replicates
after 72 h of treatment. **(B)** Long-term cell proliferation was assessed in presence or absence of
5 µM 1-NA-PP1 (DMSO as control) over a time course of 5 days.

Next, I performed long-term proliferation kinetics to assess the overall growth be-
havior of CDK9as and CDK9[STOP/as] cells in comparison to wild type cells. The prolifera-
tion rates were measured by monitoring the living cell number for 5 days. Untreated
Cdk9as cell lines proliferated 2-3 times slower compared to the wild type (Figure 2-13B).
Inhibition of Cdk9as with 5 µM 1-NA-PP1 substantially reduced proliferation of the
mutated cell lines further, while wild type cells only responded weakly. This first charac-
terization of analog-sensitive Cdk9 cell lines revealed that inhibition of Cdk9as with

1-NA-PP1 in the low micromolar range decreases cell proliferation and that this effect is specific for the cells with an F103A mutation in the Cdk9 gene.

2.5.2 Inhibition of analog-sensitive Cdk9 reduces phosphorylation of Pol II CTD

Cdk9 phosphorylates the C-terminal domain (CTD) of RNA polymerase II (Pol II). Accordingly, inhibition of Cdk9 with Flavopiridol reduces CTD Ser2-P as determined by Western analysis and mass spectrometry (Schüller et al. 2016). However, it remains unclear whether inhibition of other CTD kinases including Cdk12 contributes to the loss of CTD phosphorylation. Analog-sensitive Cdk9 cell lines provide an approach to investigate the effects on CTD phosphorylation in a Cdk9-specific manner. I treated cells with 10 µM 1-NA-PP1 for 15 min, 2 h, and 8 h and assessed the effect on CTD phosphorylation using specific antibodies against the Pol II large subunit Rpb1 and phospho-specific CTD antibodies. After 15 min signals for the hyper-phosphorylated IIo form of Rpb1 were reduced while the hypo-phosphorylated IIa form was increased in both CDK9^{as} and CDK9$^{STOP/as}$ whereas no effect was detected for wild type cells (Figure 2-14, compare lanes 7 & 12 to lane 2). This suggests that the amount of phosphorylated Pol II CTD is dramatically reduced upon specific inhibition of Cdk9. Indeed, the IIo form of both phosphorylated Ser2 and Ser5 were reduced as well, which was more pronounced in CDK9$^{STOP/as}$ cells. Reduction of CTD phosphorylation was even more substantial after 2 h of treatment, whereas after 8 h a recovery of phosphorylation signals was observed. In CDK9^{wt} cells 1-NA-PP1 had no detectable effect on CTD phosphorylation at any time point. Interestingly, for Ser5-P signals an intermediate band became visible just below the reduced IIo form after 15' and 2 h. Levels of Cdk9 and α-Tubulin were determined as loading controls. This analysis after specific inhibition of Cdk9 demonstrates that functional Cdk9 contributes to phosphorylation of Pol II CTD. Inhibition of Cdk9 shift-

ed the IIo to the IIa form, which was paralleled by reduced Ser2-P signals and an altered

band pattern of Ser5-phosphorylated Pol II in western blot.
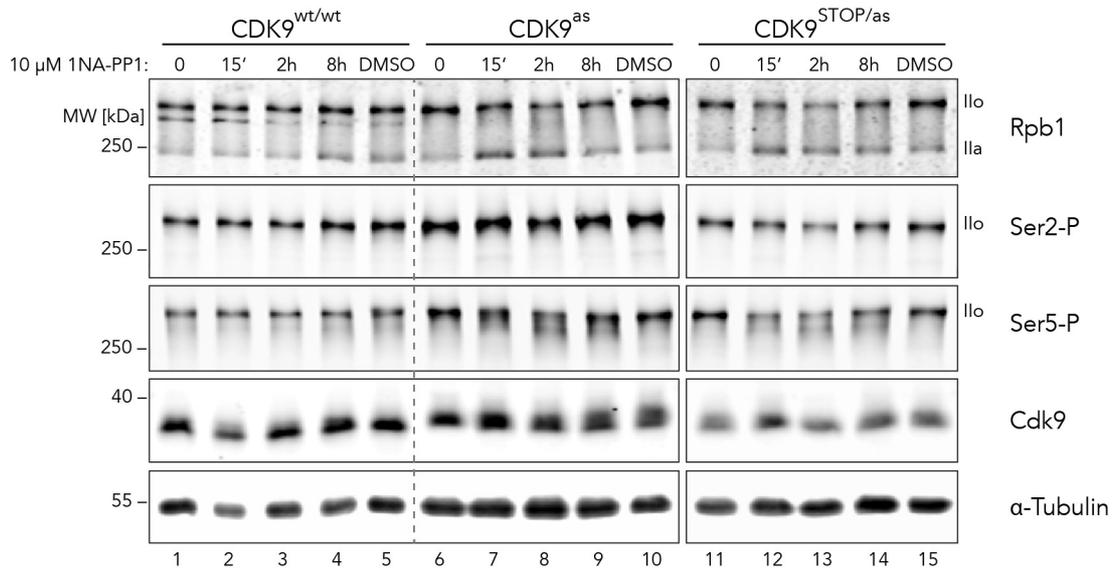
Figure 2-14 | Inhibition of Cdk9as with 1-NA-PP1 reduces CTD phosphorylation signals.
CDK9^{wt}, CDK9^{as}, and CDK9^{STOP/as} cells were treated with 10 µM 1-NA-PP1 for 15 min, 2 h, and
8 h. Untreated and DMSO-treated cells were used as controls. Phosphorylation levels of Pol II
CTD were assessed by means of Western analysis using antibodies against Pol II large subunit
Rpb1, CTD phosphorylated at Ser2 and Ser5. Cdk9 and α-Tubulin served as loading control.

2.5.3 Inhibition of Cdk9as is rescued via ectopic expression of wildtype Cdk9

Next I treated Cdk9as with lower concentrations of the inhibitor to determine how pro-
nounced the effect of Cdk9 inhibition on CTD phosphorylation is. While the effects af-
ter 15 min were barely detectable, Pol II phosphorylation signals were markedly reduced

after 2 h when using 2.5 µM or 5 µM 1-NA-PP1 (Figure 2-15A). This highlights that the

PP1 analog potently inhibits the CTD kinase activity of Cdk9as. Subsequently, I per-

formed a Cdk9 rescue assay to demonstrate that the reduction of CTD phosphorylation

is due to a loss of Cdk9 activity. To this end, Cdk9as cells were transfected with a plasmid

that allows inducible expression of wild type Cdk9-HA.
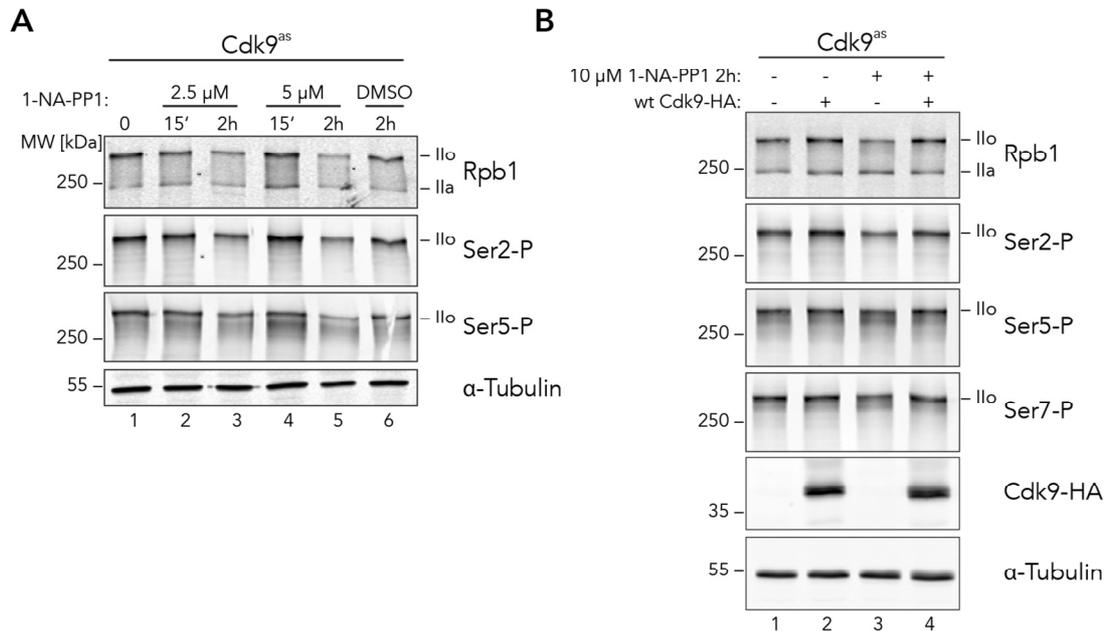
Figure 2-15 | Decreased CTD phosphorylation in Cdk9as cells is rescued by ectopic expression of wild type Cdk9. (A) CDK9[as] cells were treated with 2.5 µM and 5 µM 1-NA-PP1 for 15 min and 2 h each. CTD phosphorylation signals were subsequently detected in Western analysis. **(B)** CDK9[as] cells were transfected with an inducible wild type Cdk9-HA expression plasmid. Cells were treated with 1-NA-PP1 (DMSO as negative control) and the effect of ectopic wild-type Cdk9 expression on CTD phosphorylation was determined by means of Western analysis.

CTD phosphorylation signals were reduced upon 1-NA-PP1 treatment as observed in the previous experiments (Figure 2-15B, compare lanes 1 and 3). Induced expression of wt Cdk9-HA in untreated cells caused a moderate increase of Rpb1 IIo form and Ser2-P (lane 2), highlighting the potential role of Cdk9 as a Ser2 kinase. Notably, in presence of 1-NA-PP1, no reduction of CTD phosphorylation was detected after ectopic expression of wt Cdk9-HA (lane 4). This suggests that Cdk9 is specifically targeted by 1-NA-PP1 and induced expression of functional wild type Cdk9 rescues this phenotype.

2.6 Analysis of the transient transcriptome of Cdk9as cells

The outstanding role of Cdk9 to release paused polymerases from the elongation block has been investigated extensively. Still, the impact of Cdk9 function on the production of nascent RNA transcripts remains unclear, mainly due to the lack of specific Cdk9 in-

hibitors as well as proper sequencing technology. Specific inhibition of Cdk9 in analog-sensitive Raji cells in combination with the recently developed transient transcriptome sequencing (TT-seq) (Schwalb et al. 2016) provide a solution to these limitations.

2.6.1 Preparation and quality control of transient transcriptome sequencing (TT-seq) libraries

In collaboration with Saskia Gressel (group of Patrick Cramer, MPI Biophysical Chemistry, Göttingen), I prepared TT-seq libraries from Raji Cdk9[as] cells. Bioinformatics analysis was performed by Björn Schwalb (group of Patrick Cramer). Duplicates of cells were treated with 5 µM 1-NA-PP1 (DMSO as control) for 10 min (Figure 2-16A). This was followed by 5 min of incubation with 4-thiouridine (4sU), an uridine analog that allows labeling of newly synthesized RNAs (Dölken et al. 2008).
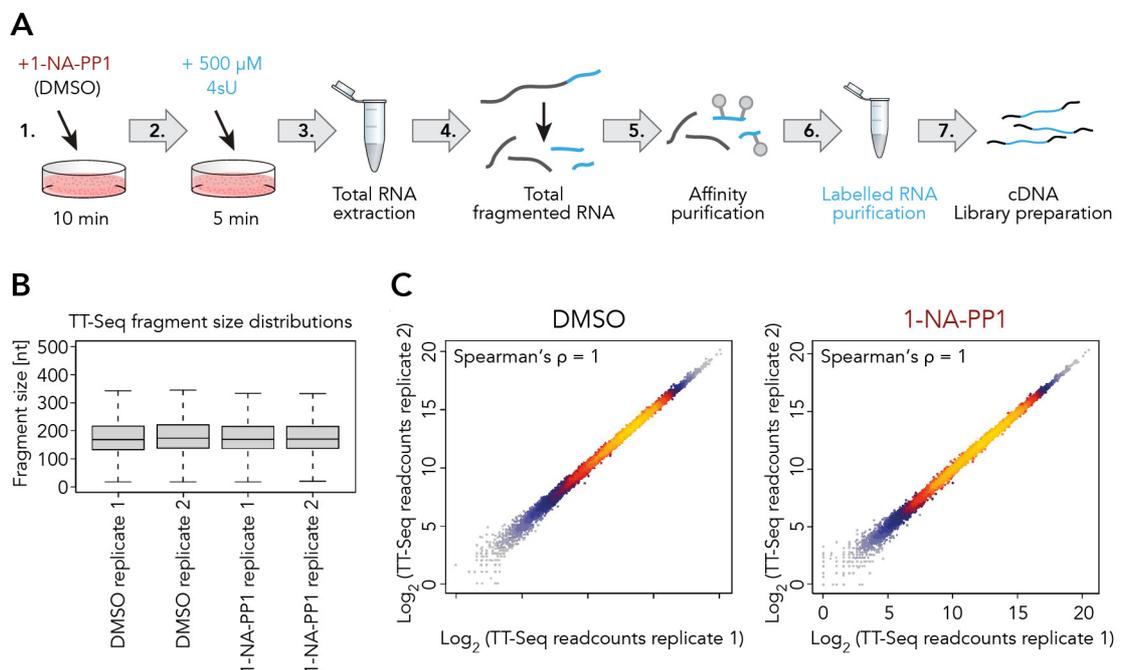
Figure 2-16 | Experimental setup and quality control of TT-seq. (A) Raji CDK9[as] cells were treated with 5 µM 1-NA-PP1 or DMSO for 10 min (1.). To label nascent RNAs, 4sU was added for 5 min (2.) and total RNA was extracted (3.). Extracted RNA was fragmented (4.) and affinity purification was performed (5.) to select for 4sU-labelled RNA (6.). This was followed by library preparation (7.). **(B)** TT-seq fragment size distributions were similar among all samples and the average fragment size was ~170 nt. **(C)** Scatter plots with color encoded density estimation comparing TT-seq readcounts of two replicates with DMSO (left) and 1-NA-PP1 (right) treatment (Spearman correlation coefficient 1 for both).

After extraction of the total RNA, the transcripts were fragmented to a size of ~ 170 nt (Figure 2-16B). This fragmentation step is crucial to remove the unlabeled 5' regions of the transcripts that were transcribed prior to labeling. 4sU-labeled RNA was subjected to thiol-specific biotinylation, affinity-purified and used to prepare cDNA libraries for transcriptome sequencing. TT-seq readcounts were highly reproducible amongst the two replicates for each condition, DMSO and 1-NA-PP1, as demonstrated by a Spearman correlation coefficient of 1 for both (Figure 2-16C). The high quality of the TT-seq data allowed for complete mapping of transcription units (TU) before and after inhibition of Cdk9. TUs were defined for each annotated gene as the combination of all transcript isoforms (UCSC RefSeq GRCh38).

2.6.2 Cdk9 inhibition decreases RNA synthesis in the 5'-region of genes

Cdk9 regulates pause release and is therefore expected to be critical for processive elongation of many genes. To characterize the role of Cdk9 for efficient RNA synthesis, the differential TT-seq reads were compared before and after 10 min inhibition of Cdk9 (Figure 2-17A). Reduced RNA synthesis was observed at the 5'-region of genes, as exemplified by the HEATR3 gene (Figure 2-17B). From ~20 kilobases (kb) on, nascent RNA levels were the same for both DMSO- and 1-NA-PP1-treated cells. This indicates that polymerases, that had already been engaged in productive elongation before inhibition of Cdk9, were unaffected and continued transcribing. In contrast, polymerases that had been paused at the promoter proximal region were blocked. This resulted in a so-called 'response window' that corresponds to the time of Cdk9 inhibition and was mapped to the 5'end of genes. Notably, the response is characterized by a marked decrease of nascent RNA production.
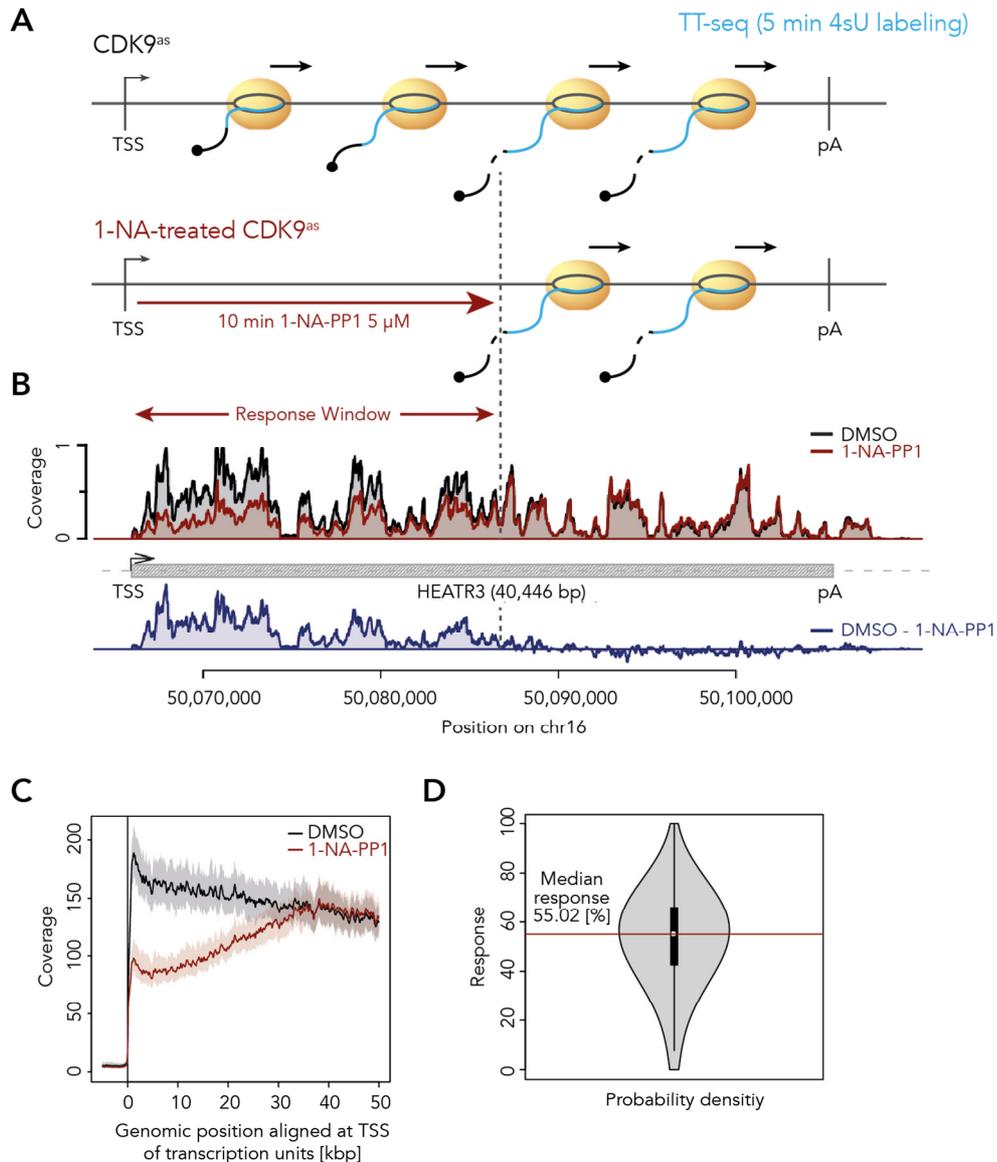
Figure 2-17 | Cdk9 inhibition decreases RNA synthesis in the 5'-region of genes. (A) Model of the inhibition of Cdk9as with 1-NA-PP1 (5 µM, 10 min) and subsequent 4sU labeling of nascent RNAs for 5 min. **(B)** Relative TT-seq signal (coverage) with 1-NA-PP1 or DMSO treatment at the HEATR3 gene (1-NA-PP1 in red / DMSO in black). The grey box depicts the transcript body from transcription start site (TSS, black arrow) to polyA site (pA). The response window is set from 200 bp downstream of the TSS and spans the region with decreased TT-seq signals after Cdk9 inhibition. **(C)** Comparison of the average TT-seq signal of expressed TUs (RPK of 20 or higher) aligned at the TSS with 1-NA-PP1 or DMSO treatment for 954 out of 2,539 investigated TUs ≥ 50 kb. Shaded areas around the average signal (solid lines) give confidential intervals of the average signal. **(D)** Response to 1-NA-PP1 treatment for 2,539 investigated TUs defined as 1 - (1-NA-PP1/DMSO) ×100 for a window from the TSS to 10 kb downstream excluding the first 200 bp depicted as a violin plot. The median response (55 %) is illustrated with a red line.

Since pausing does not occur at all genes at a similar level, next the response to Cdk9 inhibition was investigated genome-wide. To this end metagene analysis was performed, comparing the average TT-seq signal of expressed TUs (reads per kilobase [RPK] of 20 or higher) with 1-NA-PP1 or DMSO treatment. 954 out of 2,539 investigated TUs were aligned at the TSS (> 50 kb in length) for two merged replicates. The metagene analysis revealed that the 1-NA-PP1-induced reduction of RNA synthesis at the 5'-region of genes can also be observed genome-wide (Figure 2-17C). Moreover, the average width of the response window was 23 kb. To describe the response of genes to Cdk9 inhibition in a more quantitative way, response ratios were calculated for applicable TUs. Applicable TUs synthesized RNA, harbored a single TSS, and exceeded 10 kb in length (2,539 TUs). The response ratio of TUs varied between 0% to 100% (fully responding TUs) with a median of ~ 55% (Figure 2-17D). A remaining TT-seq signal in the response window reflects the subpopulation of polymerases that proceeds to productive elongation independent of Cdk9 kinase activity.

2.6.3 RNA polymerase II pausing delimits transcription initiation

Cdk9 inhibition decreased productive elongation of transcription within the response window but allowed normal transcription beyond this window. Therefore, I asked if initiation was affected upon inhibition of Pol II pause release. Based on the TT-seq data the elongation velocity was calculated and the mean was determined as 2.7 kb per minute (Figure 2-18A). TT-seq further enables calculation of the initiation frequency. In average 2.7 initiation events per cell per minute were calculated (Figure 2-18B). To correlate the TT-seq data with Pol II pausing, available mammalian NET-seq (mNET-seq) data derived from the nuclear chromatin fraction from HeLa cells was used (Nojima et al. 2015). In mNET-seq the 3'-end of nascent RNA that is still associated with the polymerase is sequenced and thus can be mapped to the genome. This allows determination of the precise position of transcribing polymerases.
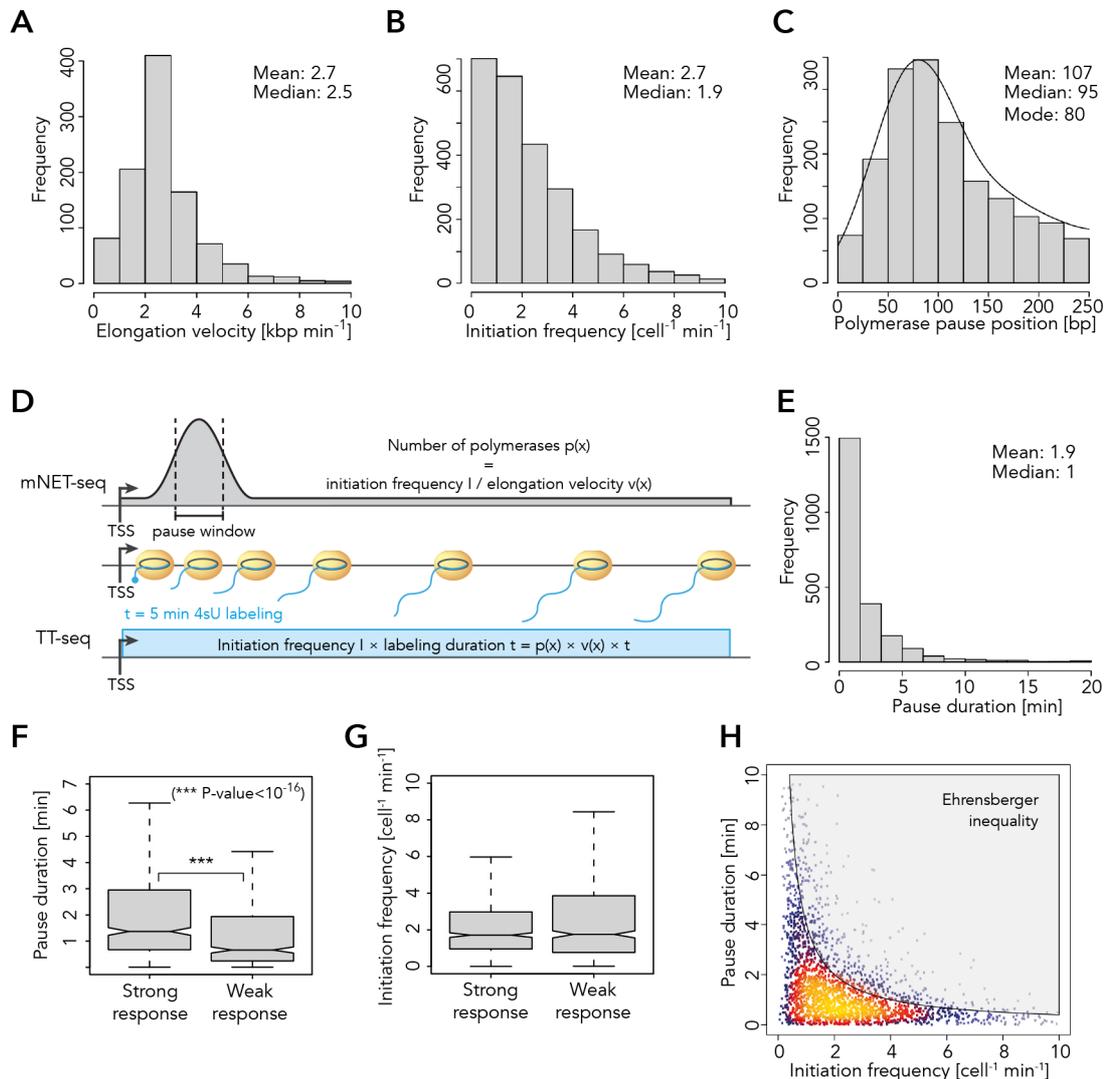
Figure 2-18 | RNA polymerase II pausing affects transcription initiation. (A-C) Histograms depicting the distribution of elongation velocity, initiation frequency [cell⁻¹min⁻¹], and pause position distance from the TSS. **(D)** Schematic representation of integrated measures to investigate the polymerase dynamics in the promoter-proximal region. Upper panel: mNET-seq signal as a product of initiation frequency (*I*) and elongation velocity (*v*) of the polymerase. Middle panel: Polymerase movement with 4sU labeled RNA fragments according to TT-seq with a RNA labeling time of 5 min. Fragment length is determined by elongation velocity of the respective polymerase. Lower panel: TT-seq signal strength equals initiation frequency. **(E)** Histogram depicting the distribution of pause duration. **(F-G)** Distributions of gene-wise pause duration and initiation frequency for TUs with a response ratio > 75% quantile (603 TUs) and TUs with a response ratio < 25% quantile (527 TUs). **(H)** Comparison of the initiation frequency to the pause duration for 2,284 common TUs with color encoded density estimation (Spearman correlation coefficient -0.54). Grey shaded area depicts impossible combinations of the two measures given the Ehrensberger inequality and a polymerase footprint of 50 bp (Ehrensberger et al. 2013).

90% of the TUs derived from the TT-seq approach showed Pol II pausing signals above background. Alignment of the pause sites relative to the TSS revealed that the pause position varies for the different TUs, with most pause sites located ~80 bp downstream of the TSS (Figure 2-18C).

Neither TT-seq nor mNET-seq data alone can provide information about the dynamics of Pol II pausing. To quantify the pause duration, both approaches were combined. The mNET-seq signal provides the number of polymerases within the pause window, which is determined by the initiation frequency I and the pause duration d (Figure 2-18D). As demonstrated, I could be obtained from TT-seq. Furthermore, d is proportional to the ratio of the mNET-seq signal over I, enabling the calculation of the pause duration d, which was on average 1.9 minutes (Figure 2-18E). Pause durations were significantly longer (Wilcoxon rank sum test, p-value $< 10^{-16}$) and initiation frequencies were lower for TUs that showed a strong reduction of RNA synthesis (Figure 2-18F-G). This led to the question whether pause duration is generally related to transcription initiation. Pause duration was plotted against initiation frequency of 2,284 common TUs and a robust anti-correlation between the two factors was observed (Spearman correlation coefficient -0.54) (Figure 2-18H), demonstrating that genes with shorter pausing exhibit higher initiation frequencies and more RNA synthesis. Together, combined analysis of independent mNET-seq and TT-seq data indicates that pause duration and initiation frequency for each gene are globally related.

To test directly if longer pause durations lead to lower initiation frequencies, TT-seq data after Cdk9 inhibition was further analyzed. Cdk9 inhibition resulted in significantly less labeled RNA between the TSS and the pause site (Wilcoxon rank sum test, p-value $< 10^{-15}$) (Figure 2-19A and C). Strikingly, initiation frequencies were significantly reduced as well after Cdk9 inhibition (Wilcoxon rank sum test, p-value $< 10^{-16}$) (Figure 2-19B-C). Because Cdk9 specifically targets paused Pol II, these results strongly suggest that pausing controls initiation.
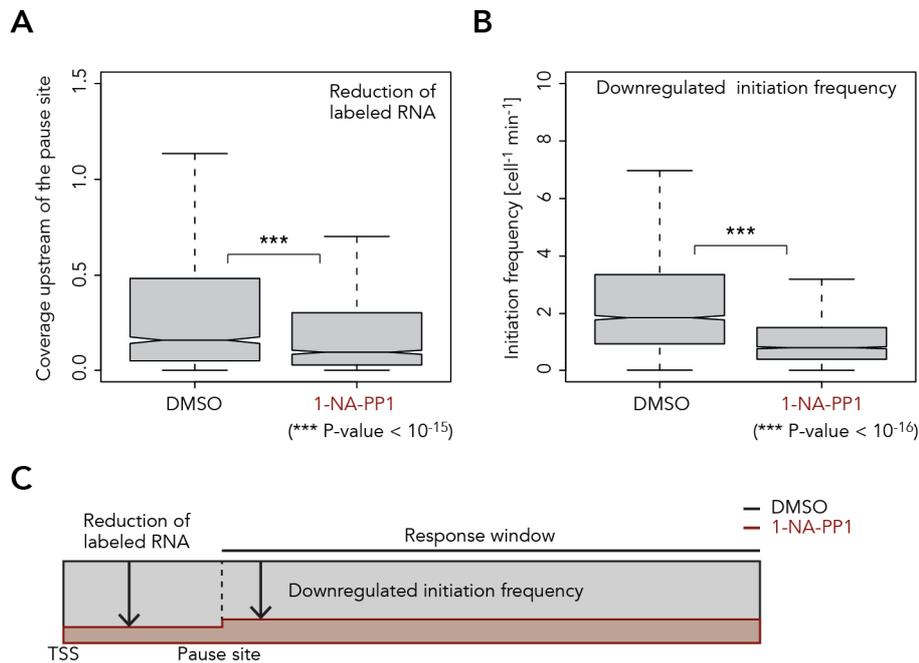
Figure 2-19 | Increasing pause duration suppresses transcription initiation. (A) Distribution of gene-wise mean TT-seq signal in the region between TSS and the pause site for DMSO (control) or 1-NA-PP1 treatment normalized to initiation frequency before treatment. **(B)** Comparison of gene-wise initiation frequencies after DMSO or 1-NA-PP1 treatment. **(C)** Schematic representation of the reduced labeled RNA levels within TSS and pause site as a consequence of downregulated initiation frequency.

2.6.4 Sensitivity to Cdk9 inhibition correlates with Brd4 occupancy

Paused Pol II is typically associated with negative elongation factors DSIF and NELF whereas Brd4 and Cdk9 regulate the release into productive elongation. To investigate which factors preferentially occupy pause windows with longer pause durations, ChIP-derived factor occupancies were correlated with the pause durations defined above. Importantly, this is possible because available ChIP-seq signals could be normalized with the inititation frequency, i.e. the number of polymerases released from the pause window per time (pause release rate). This normalization is crucial, because ChIP-derived factor occupancies are artificially high in pause windows with long pause durations (Ehrensberger et al. 2013). Correlation of normalized ChIP signals in the pause window with pause durations was positive for the factors NELFe, Cdk9, and Brd4.

Because Brd4 occupancy is high at enhancers (Lovén et al. 2013), long range chromatin interactions of strongly and weakly Cdk9-responding TUs were compared. Indeed, Cdk9-responding TUs showed a higher tendency to establish such chromatin interactions, as observed by Hi-C (Ma et al. 2015). Together these observations highlight that Brd4 and Cdk9 regulate the release of paused polymerases and that this regulation presumably involves chromatin looping to distant enhancers.
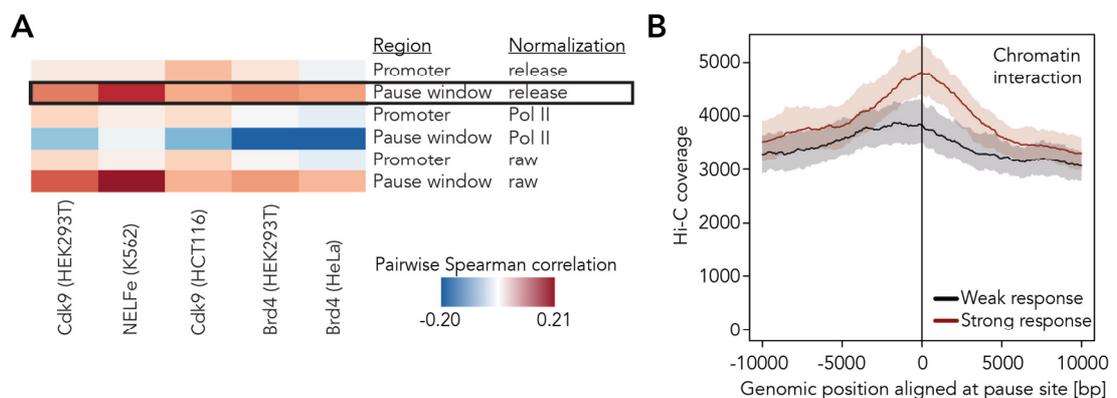
Figure 2-20 | Transcription- and chromatin-associated factors correlate with CDK9as response. (A) Pairwise spearman correlation (color encoded, -0.20 in blue to 0.21 in red) using ChIP measurements of Cdk9, NELFe and Brd4 of the promoter region (TSS – 250 bp to TSS) and pause window against the response to Cdk9 inhibition (see Figure 2-17) shown as a heatmap. Analysis was performed in three different ways: ChIP-derived occupancies were either normalized to pause duration (release), normalized to total Pol II (Pol II), or the raw signal was used (raw) (for references of ChIP measurements see Table 4-3). **(B)** Comparison of the average Hi-C signal (detecting long-range chromatin interactions) aligned at the pause site for strong responding TUs (response ratio > 75% quantile, 602 TUs) and weakly responding TUs (response ratio < 25% quantile, 528 TUs). Confidence intervals are provided as shaded areas around the average signal (solid lines).

3 Discussion

3.1 Dominant-negative mutants of Brd4 inhibit cell proliferation of tumor cell lines

Many studies have used small molecule inhibitors such as JQ1 to inhibit Brd4 and study its cellular function as well as its role in malignant diseases. However, the use of JQ1 is limited as this inhibitor also targets other proteins of the BET family and its mode of action is the disruption of bromodomain function alone. Thus, I aimed to inhibit Brd4 without using JQ1 or a similar inhibitor but to overexpress dominant-negative (dn) Brd4 mutants instead. I designed multiple Brd4 fragments that together cover the whole sequence of full-length Brd4. Besides the two N-terminal bromodomains other Brd4 domains support seminal functions as well (Figure 3-1).
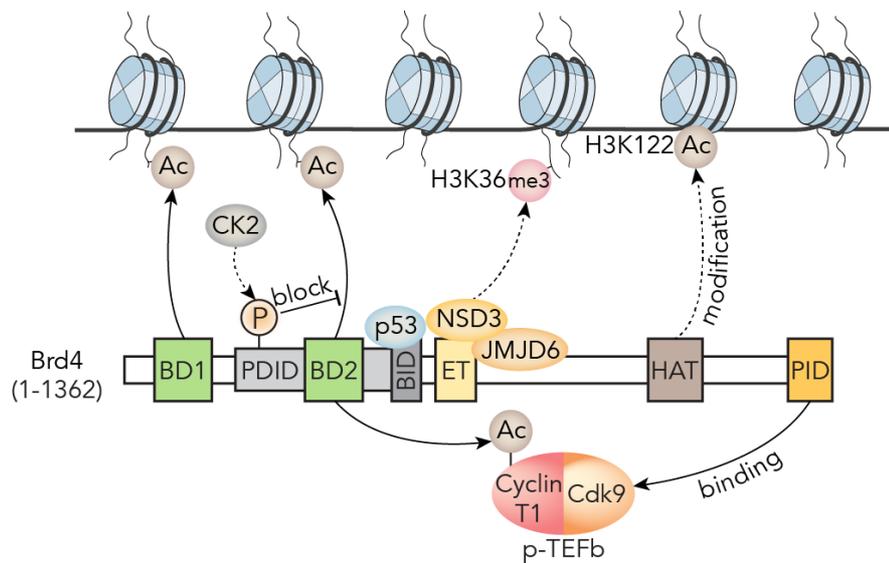
Figure 3-1 | Brd4 is a histone reader with many interaction partners. In addition to acetyl-lysine binding bromodomains, Brd4 comprises several other domains that interact with factors involved in transcription and chromatin regulation. PDID/BID bind p53 and binding of BD2 to acetylated histones is regulated by CK2-dependent phosphorylation of PDID. ET recruits histone demethylase JMJD6 and histone methyltransferase NSD3, which can trimethylate H3K36. The putative HAT domain was described to acetylate H3K122 (Devaiah et al. 2016). P-TEFb is recruited via dual binding of BD2 to acetylated CyclinT1 and PID to Cdk9.

Deletion of the C-terminal PID domain abolishes the interaction with Cdk9 (Bisgrove et al. 2007). The extra-terminal domain (ET) is essential for interaction with multiple proteins including NSD3 and JMJD6 (Rahman et al. 2011). Hence it is of great interest to additionally disturb the function of those domains using the approach of dn Brd4 mutants. Notably, all important domains of Brd4 could be specifically inhibited by distinct mutants, allowing a broader and yet more precise targeting approach compared to the use of JQ1. Screening of this set of potential dn Brd4 mutants for aberrant proliferation identified several mutants that exhibit a dominant-negative phenotype. Generally, all mutants that comprise one of the described Brd4 domains (BD1, BD2, BID/PDID, ET, and PID) markedly inhibited cell proliferation of Raji and H1299 cells.

The expression levels of the different Brd4 fragments varied substantially, raising the question whether the dn phenotypes I observed for some fragments are solely due to a general overexpression defect. Expression levels of f3, f5, and f6 were very high and in all three mutants I observed reduced proliferation in either Raji or H1299 cells or both. In contrast, f4 and f9 were expressed at markedly lower levels. However, this was sufficient to slow down proliferation in Brd4 mutants f4 and f9 as well. Notably, adequate expression of the fragments is a prerequisite to achieve dominant-negative inhibition of endogenous Brd4.

While JQ1 inhibits both bromodomains of Brd4, my dn approach allows targeting of BD1 (f1 and f-BD1) and BD2 (f3) separately. I detected reduced proliferation in f-BD1 and f3 mutant cells but not in the f1 mutant. Similar to f-BD1 and f3, a dual bromodomain construct (BD1/BD2) was reported as dn inhibitor before (Wang et al. 2012). Specifically, this mutant displaced full-length Brd4 from chromatin and induced a fragmented chromatin phenotype in a cervix carcinoma cell line. This suggests a comparable mode of inhibition for f-BD1 and f3, since both potentially disrupt the function of Brd4 bromodomains.

Nevertheless, BD1 and BD2 may fulfill separate roles, as demonstrated by the differential effects on cell proliferation of f1 and f3. This is supported by several other studies.

In the phylogenic tree of bromodomains, BD1 and BD2 domains of BET proteins represent individual branches (G. Zhang et al. 2015). Furthermore, the binding affinities to JQ1 and histone recognition preferences differ between the two domains. *In vitro* binding assays for Brd4 indicated best binding of BD1 to H3 and of BD2 to H4 acetylated lysine peptides (Vollmuth et al. 2009). In contrast, a more recent study observed that BD1 of Brd4 had a high affinity for acetylated H4 in particular while the binding affinity of BD2 was less preferential (Filippakopoulos et al. 2012). Both domains displayed efficient binding to JQ1 with dissociation constants (Kd) in the nanomolar range, but BD1 bound JQ1 stronger than BD2 did (Kd of about 50 nM and 90 nM, respectively) (Filippakopoulos et al. 2010).

Initial pulldown assays with Brd4 deletion mutants suggested that either bromodomain can interact with the CyclinT1 subunit of P-TEFb (Jang et al. 2005). Subsequently, BD2 of Brd4 was reported to bind acetylated CyclinT1 similarly well as acetylated H3 and H4 sequences (Vollmuth et al. 2009). These observations are highly interesting, since they describe another function of Brd4 bromodomains besides binding of histone tales. Moreover, they imply a second mode of interaction between Brd4 and P-TEFb, in addition to PID-Cdk9 binding. Indeed it has been proposed, that binding of BD2 to triple-acetylated CyclinT1 primes P-TEFb for full liberation from its inactive form upon a second Brd4 binding via the PID domain (Schröder et al. 2012). Together these diverse characteristics of BD2 may explain why the f3 mutant severely reduced cell proliferation.

Recently, two novel Brd4 domains were described that are involved in Brd4-p53 interactions (Wu et al. 2013). Phosphorylation-dependent interaction domain (PDID) spans amino acids 287-530 and encompasses BD2. Basic residue-enriched interaction domain (BID) is located between BD2 and ET, comprising amino acids 524–579. Although both domains are conserved in BET proteins, less is known about their function. Both domains independently interact with p53 as demonstrated in pulldown experiments (Wu et al. 2013). Further analyses revealed that PDID harbors an N-terminal

cluster of phosphorylation sites (NPS) that contains several serine residues that can be phosphorylated by casein kinase 2 (CK2). In their final model, Wu and colleagues postulate that in the non-phosphorylated state NPS binds BD2 and blocks Brd4 binding to acetylated chromatin. In this inactive state, p53 can already by recruited to BID. Upon CK2-dependent phosphorylation of NPS, the masking of BD2 by NPS is resolved and NPS will form an intramolecular contact with BID and simultaneously bind p53. This so-called phospho-switch activates Brd4-binding to acetylated chromatin and facilitates efficient transcription of p53 target genes including p21 and PUMA. Although mutant f3 comprises large parts of PDID it lacks the NPS region. Notably, mutant f4 harbors both NPS and BID. Thus the reduced proliferation phenotype in f4 is possibly mediated by disruption of the phospho-switch dependent recruitment of p53.

Mass-spectrometric studies of the Brd4 interactome have identified several proteins that interact with the extra-terminal ET domain of Brd4 and these interactions are conserved in Brd2 and Brd3 (Rahman et al. 2011). The ET-interacting proteins include argenine demethylase JMJD6 and the lysine methyltransferase NSD3. Both proteins are recruited to the promoter and gene bodies of Brd4-regulated genes in a Brd4-dependent way. Depletion of either NSD3 or Brd4 reduced the levels of H3K36 trimethylation (H3K36me3) in the gene body of CCND1 (CyclinD1), a Brd4-regulated gene. H3K36me3 is a well-described histone mark of actively transcribed chromatin (Kouzarides 2007). Assuming that the dn f5 mutant disrupts NSD3 recruitment via ET, this might reduce H3K36me3 levels and repress Brd4-regulated genes. Furthermore, it was demonstrated that JMJD6 binds to distant enhancers to control transcriptional pause release and that this association is dependent on Brd4 (Liu et al. 2013). Mutant f5 might abolish Brd4-dependent JMJD6 recruitment to these so-called anti-pause enhancers, thereby blocking the pause release of enhancer-regulated genes. Taken together, these hypothetical events provide possible mechanisms that lead to the anti-proliferative phenotype in mutant f5.

The Brd4 PID domain is essential for recruitment and activation of P-TEFb (Bisgrove et al. 2007). The dominant-negative effect of the f9 mutant which comprises the PID was therefore not surprising. Notably, expression of the f9 fragment caused the most robust proliferation defects in both Raji and H1299 as compared to all other Brd4 fragments including f3, which caused a comparably strong reduction of proliferation rates. Taking into account that expression levels in f9 were markedly lower than in f3, the PID containing f9 fragment can be considered the most potent dn inhibitor of Brd4 function analyzed in this screen. My findings highlight that the PID domain is crucial for regular Brd4 function which will be discussed in more detail in chapter 3.2.

In summary, the regions of the Brd4 protein whose overexpression lead to a dominant-negative phenotype precisely overlap with already reported domains. Future efforts should focus on the investigation of PDID/BID and ET domains, since our understanding about the functions of these certainly important domains is currently very limited. The contribution of the C-terminal region of Brd4, connecting ET and PID, to the overall function of Brd4 remains elusive. This region of Brd4 might provide secondary and tertiary structures that are essential for the correct three-dimensional organization of the protein. Furthermore, it was recently reported that Brd4 has histone acetyltransferase (HAT) activity that is distinct from other HATs (Devaiah et al. 2016). Interestingly, the putative HAT catalytic domain is located within the C-terminal stretch (1157-1197 aa in mouse Brd4), providing first insights into the function of this poorly understood region of the Brd4 protein.

3.2 Brd4 is the major mediator of the anti-tumor effects induced by JQ1 and regulates the transcriptome with its P-TEFb-interacting domain

Besides Brd4, JQ1 also targets the other somatic BET members Brd2 and Brd3 (Filippakopoulos et al. 2010). Thus JQ1 is not BET member specific and any JQ1-

mediated inhibition of Brd4 might be accompanied by inhibition of Brd2 and Brd3 as well. For example is has been demonstrated that knockdown of Brd2 alone or Brd3 alone inhibits transcription of certain cytokine genes that are also affected by Brd4 knockdown and inhibited by JQ1 (Belkina et al. 2013). Furthermore, JQ1 affects the regulatory function of Brd2, Brd3, and Brd4 on metabolic pathways in the pancreatic β-cell, as it was demonstrated by using BET-specific siRNAs (Deeney et al. 2016). Brd2 has implications on development of cancer as well. Transgenic mice overexpressing Brd2 restricted to lymphoid cells develop splenic B-cell lymphoma (Greenwald et al. 2004). Brd2 interacts with histone variant H2A.Z.2, a recently described mediator of cell proliferation and drug sensitivity in malignant melanoma (Vardabasso et al. 2015). Although increasing evidence supports the role of Brd2 and Brd3 as JQ1 targets, many studies still consider Brd4 as the major target of JQ1. Especially the anti-cancer effects of JQ1 have been mostly attributed to Brd4 due to its c-Myc activating function (Mertz et al. 2011; Zuber, Rappaport, et al. 2011). Therefore, dominant-negative Brd4 mutants provide an elegant way to specifically target Brd4 and compare the effects on cell proliferation and the cellular transcriptome to JQ1.

Similar to JQ1, dn Brd4 mutants inhibited cell proliferation of Raji and H1299 cells. This suggests that Brd4 function is essential in both cell lines although Raji cells were about 20 times more sensitive to the small molecule inhibitor than H1299. Comparison of c-Myc protein levels after JQ1 treatment revealed that c-Myc is a major downstream target of JQ1 in Raji but not in H1299 cells. Furthermore, the high enrichment of c-Myc targets in the Brd4-specific transcriptome datasets support the model that c-Myc down-regulation by either JQ1 or dnBrd4 inhibitors is largely responsible for the anti-proliferative effects observed in previous reports and the present study. This suggests that the effects of JQ1 treatment are cell line specific and at least in the case of c-Myc regulated by Brd4. Cell line specific activity of Brd4 has been reported in the context of so-called super enhancers, a highly active class of enhancers that are implicated in defining cell identity (Lovén et al. 2013) (see chapter 3.6). Hence, the contribution of Brd4 to

the anti-proliferative effects of JQ1 should be investigated carefully also on the transcriptome level.

Comparison of the transcriptome of mutant f3 with the transcriptome of JQ1-treated cells revealed major changes in gene expression in both transcriptomes and that the dominant-negative mutant f3 repressed and induced almost the same genes as JQ1. I further noticed that JQ1 induced higher changes in gene expression in affected genes than the f3 mutant. The functions of Brd2, Brd3, and Brd4 partially overlap as demonstrated for the regulation of cytokine genes using BET member-specific siRNA knockdowns (Belkina et al. 2013). Thus, higher JQ1-induced changes in gene expression may be explained by additional inhibition of Brd2 and Brd3 by JQ1 but not by dominant-negative Brd4. Alternatively, 500 nM JQ1 might simply be a more potent inhibitor than overexpressed Brd4 fragments, both in terms of stability and efficiency. However, the groups of regulated genes and the direction of their regulation, induction or repression, is largely identical among f3 and JQ1 datasets. Thus, mutant f3 confirms the current model that JQ1 may act mainly by inhibiting the interaction of the bromodomains of Brd4 and other BET proteins with acetylated histone tails.

Unlike f3, mutant f9 comprises a domain that is unique for Brd4 and neither present in Brd2 nor Brd3: P-TEFb-interacting domain (PID). Pol II undergoes promoter proximal pausing at 60% of mammalian genes (Day et al. 2016). At those genes, recruitment of P-TEFb is essential to release the polymerase from the elongation block. Brd4 recruits P-TEFb by binding Cdk9 via the PID domain. In fact, recruitment of P-TEFb might be facilitated in two steps. First, acetylated CyclinT1 is bound by BD2 of Brd4 which is followed by the described Cdk9-PID interaction, leading to full activation of P-TEFb (Schröder et al. 2012). Notably, by using mutants f3 and f9 both steps can be potentially targeted.

I found that changes induced in the transcriptome of mutant f9 largely overlapped with the changes that I observed for mutant f3 and JQ1 treated cells. The functional overlap of f9 with f3 and JQ1 is further confirmed by the almost identical impact of all

three inhibitors on the expression on c-Myc target genes. This result was not necessarily expected, because the contribution of the PID domain to the gene regulatory function of Brd4 has not been measured quantitatively before. The direct comparison of mutant f3 and f9 in my study demonstrates that BD2 and PID in Brd4 act as a functional unit and that the gene regulation by Brd4 largely depends on PID. However, it remains unclear whether the PID does interact only with P-TEFb or in addition with other factors. Here I found that a large set of genes activated by JQ1 and mutant f3 is found activated also by mutant f9 (for a detailed discussion on activated genes, see chapter 3.3). This may be due to downstream effects that are triggered by genes regulated by P-TEFb such as *c-Myc*. Nevertheless, I cannot exclude that the PID domain may have a second, not yet identified function that is important for transcriptional repression. Together, my results suggest that gene regulatory changes induced by JQ1 can also be induced by dominant-negative Brd4 mutants, and that the inhibition of the Brd4 PID domain is central for the function of BET-inhibitor JQ1.

The functional link observed between PID and bromodomains of Brd4 raises the question how the short isoform of Brd4 (Brd4-s), which lacks the PID (Bisgrove et al. 2007), is involved in transcriptional regulation and if inhibition of Brd4-s by JQ1 may also translate into a phenotype. Brd4-s might act as a dominant-negative inhibitor of full-length Brd4, as suggested by previous studies (Alsarraj et al. 2011; French et al. 2003). However, differential biochemical and nuclear localization properties indicate that the two isoforms of Brd4 may fulfill separate roles. Brd4-s localizes specifically to the transcriptionally inactive perinuclear region where it might be involved in gene re-pression (Alsarraj et al. 2013).

Overexpression of PID in mutant f9 potentially inhibits the recruitment of P-TEFb to Brd4 and acetylated chromatin. The inhibitory effect of PID expression or of synthet-ic peptides containing PID has been reported before. A synthetic peptide comprising the PID fused to the protein transduction domain of HIV-Tat abrogated Tat transactivation in a luciferase reporter assay (Bisgrove et al. 2007). Overexpression of the PID abrogated

binding of full-length Brd4 to P-TEFb but did not lead to defects in chromatin structure as observed for overexpression of BD1/BD2 dominant-negative inhibitor (Wang et al. 2012). Several studies have reported that the PID domain liberates P-TEFb from its inactive complex containing Hexim1 *in vitro* (Itzen et al. 2014) and in HEK293T cells (Schröder et al. 2012). Both studies strongly suggest that the PID competes with Hexim1 for binding of P-TEFb. Interestingly, JQ1 affects the cellular equilibrium between active and inactive P-TEFb and triggers the transient release of free P-TEFb together with elevated Hexim1 protein levels as a direct compensatory response (Bartholomeeusen et al. 2012). Activation of P-TEFb upon JQ1 treatment might be a cellular stress response but the underlying mechanism is poorly understood. However, transcriptome analyses confirm that JQ1 causes elevated Hexim1 expression (Donato et al. 2016; Mertz et al. 2011, this study). Upregulation of Hexim1 was observed in mutants f3 and f9 as well, underlining that the cellular response to JQ1 primarily depends on targeting Brd4.

3.3 Brd4 is both a transcriptional activator and repressor

In the original I-BET report it was carefully noticed that several genes are upregulated as a response to inhibition of BET proteins (Nicodeme et al. 2010). Although this activation may also be a downstream effect, the function of BET proteins as transcriptional repressors has been reported repeatedly. Brd2 forms nuclear complexes with Swi/Snf chromatin remodelers that co-activate and co-repress transcription (Denis et al. 2006). Direct interaction with a chromatin remodeler has been shown for Brd4 which binds CHD4 with its ET domain (Rahman et al. 2011). Interestingly, CHD4 is part of the mi-2/nucleosome and deacetylase (NuRD) complex which has been implicated in the repression of genes that are regulated by estrogen receptor α (Denslow & Wade 2007). Furthermore, a recent report demonstrated the repressive role of BET proteins for the transcriptional coactivator TAZ (Duan et al. 2016).

My results further establish that Brd4 inhibition results in both activation and re-pression of genes to a similar extent. Interestingly, I observed that *AFF1*, *AFF2* and *AF9*, encoding three major subunits of the super elongation complex (SEC), were upregulated by JQ1 as well as in mutants f3 and f9. SEC can also bind P-TEFb (Lin et al. 2010), sug-gesting a feedback loop and a crosstalk between Brd4 and SEC. In line with this, a recent model proposes recruitment of P-TEFb by Brd4 and SEC via different mechanisms (Lu et al. 2016). The upregulation of SEC might be a response to Brd4 inhibition to rescue RNA polymerase II (Pol II) elongation, in agreement with a recent study that demon-strated compensatory Pol II loading at JQ1-insensitive genes (Donato et al. 2016). Acti-vation of transcription might also be a response to the transient release of active P-TEFb (see final paragraph of chapter 3.2) which has been observed after JQ1 treatment but might also be a response to mutants f3 and f9 (Bartholomeeusen et al. 2012). Upregulat-ed transcription of SEC subunits further complements the report of Bartholomeeusen and colleagues, who detected increased protein levels of P-TEFb-SEC complexes in JQ1-treated cells. The observation that many genes are upregulated upon inhibition of Brd4 possibly results from a combination of both downstream effects and revoked transcrip-tional repression by Brd4.

3.4 Analog-sensitive kinase technology allows for immediate and specific inhibition of Cdk9

Cyclin-dependent kinase inhibitors like Flavopiridol, i-CDK9 or 5,6-dichlorobenzimidazole 1-β-D-ribofuranoside (DRB) have high specificities for Cdk9 (Lu et al. 2015; Wang & Fischer 2008). Amongst all Cdk9 inhibitors, Flavopiridol is the compound most often evaluated in clinical trials for cancer therapy (Morales & Giordano 2016). However, due to the lack of selectivity against other Cdks and many cases of adverse effects in the clinical trials, neither Flavopiridol nor any other Cdk9 in-hibitor has been allowed for clinical use. Besides clinical aspects, Cdk9 inhibitors are

valuable tools to study the role of Cdk9 in transcription regulation. Several studies have taken advantage of such inhibitors to assess the function of Cdk9 genome-wide. In global run-on sequencing (GRO-seq) experiments with Flavopiridol-treated nuclei from mouse embryonic stem cells (mESCs), it was shown that pause escape is dependent on Cdk9 kinase activity and occurs at all actively transcribed genes (Jonkers et al. 2014). Further it was demonstrated that transcription of non-paused genes is reduced as well upon inhibition of Cdk9 with DRB in HeLa nuclei (Laitem et al. 2015). Laitem and colleagues further describe a poly(A)-associated elongation checkpoint that is essential for efficient termination and can be targeted by DRB.

Unfortunately the described inhibitors target other CTD kinases as well, including Cdk7, Cdk12, and Cdk13 (Bensaude 2011; Bösken et al. 2014; Greifenberg et al. 2016). Thus, it is not possible to study the kinase activity of one single kinase using such inhibitors. Therefore, I applied the analog-sensitive kinase technology in combination with CRISPR/Cas9 gene editing. Analog-sensitive kinases harbor a so-called 'gatekeeper mutation' within the ATP-binding pocket. This mutation allows the accommodation of bulky Adenine analogs and provides an elegant way to specifically inhibit the analog-sensitive kinase. First reports on analog-sensitive kinases lead to detailed insights on the function of cell cycle kinases including Cdk1 and Cdk2 (Bishop et al. 2000; Kraybill et al. 2002). However, this strategy has also been applied on the study of CTD kinases. Research on analog-sensitive Cdk7 human colon carcinoma cells revealed that Cdk7 is involved in Cdk1/CyclinB assembly as well as in the activation of Cdk2/cyclin complexes (Larochelle et al. 2007). The same cell line was used to study the role of Cdk7 in transcription (Glover-Cutter et al. 2009). Inhibition of Cdk7 suppressed promoter proximal pausing and abrogated recruitment of NELF. Furthermore it was demonstrated that Cdk7 not only phosphorylates Ser5 of Pol II CTD but additionally phosphorylates Ser7.

Analog-sensitive kinase technology alternatively allows the use of modified ATP analogs that do not inhibit the kinase but allow the incorporation of labeled phosphates to identify protein targets of a specific kinase. In an *in vitro* phosphorylation assay using a

purified Cdk9as in total cell extracts, the substrates of Cdk9 were determined (Sansó et al. 2016). This screen identified the 'torpedo' exonuclease Xrn2 as a Cdk9 substrate providing an explanation for the role of Cdk9 in transcription termination that was discussed above (Laitem et al. 2015). Interestingly, in the report by Laitem et al. an exogenously expressed Cdk9as was used to confirm that the termination defects are at least partly due to Cdk9 inhibition by DRB.

The studies on analog-sensitive Cdk9 mentioned above relied on complex knockdown knock-in approaches with ectopic expression of mutated kinases. Therefore, engineering the endogenous Cdk9 gene using CRISPR/Cas9 to derive an analog-sensitive cell line, as it was used in the present work, represents a much more elegant way to specifically target Cdk9. Untreated Cdk9as Raji cells proliferated 2-3 times slower as wild type Raji. This phenotype could be explained by reduced kinase activity upon mutation of the gatekeeper, which resides within the ATP-binding pocket and potentially causes less effective binding or hydrolysis of ATP. Reduced kinase activity is a common observation in AS kinases and can be overcome by compensatory mutations (Lopez et al. 2014). An alternative explanation for the reduced proliferation rates of CDK9as cells might be its clonal origin, since construction of the cell lines involved single cell cloning. Nevertheless, the CDK9as cell line is viable and stably proliferates over weeks. Thus I consider the introduced F103A mutation as well tolerated.

Results from previous reports suggest that mainly phosphorylation of Ser2 shifts the Rpb1 protein band from the hypo-phosphorylated IIa form to the hyper-phosphorylated IIo form (Chapman et al. 2007; Medlin et al. 2005). Indeed, I found that inhibition of Cdk9 resulted in a substantial loss of the slower migrating IIo form. This was also observed in Western blots probing for Ser5-P polymerase. Here an intermediate band appeared that supposedly represents Pol II that has lost Ser2-P but is still phosphorylated at Ser5. These results strongly indicate that Cdk9 functions as a Ser2 kinase *in vivo* and that Ser5 kinase activity is limited to *in vitro* assays. I speculate that Cdk9 can potentially phosphorylate Ser5 *in vivo* as well. However, due to extensive Ser5 phos-

phorylation facilitated by the pre-initiation machinery including Cdk7, most Ser5 residues are already phosphorylated at this stage and may prohibit further phosphorylation by Cdk9. Furthermore association with additional factors including DSIF might influence the selectivity of Cdk9 in favor of Ser2.

The present work represents the second study of CRISPR/Cas9 engineered CTD Ser2 kinases together with a recent report that described the production of a Cdk12 analog-sensitive HeLa cell line (Bartkowiak et al. 2015). Similar to inhibition of Cdk9, specific targeting of Cdk12 resulted in reduced cell proliferation and disturbed CTD phosphorylation patterns, as observed using modification-specific antibodies. The reported and yet to be developed analog-sensitive cell lines will be key to unravel the specific functions of kinases that are involved in transcription and phosphorylation of the CTD.

3.5 Pausing controls transcription initiation

Several next-generation sequencing-based methods have elucidated the dynamics of Pol II along the locus of a transcribed gene (Liu et al. 2015). Chromatin immunoprecipitation using Pol II specific antibodies in combination with deep sequencing (ChIP-seq) demonstrated that in metazoan cells most genes display high Pol II occupancy 20-60 bp downstream of the TSS (Muse et al. 2007; Zeitlinger et al. 2007). This Pol II peak reflects polymerases that are paused in the promoter proximal region. The same peak is typically observed when performing mammalian native elongating transcript sequencing (mNET-seq). Here, 3′ ends of nascent transcripts associated with RNA polymerase are sequenced and visualized transcription at nucleotide resolution (Nojima et al. 2015). GRO-seq-based approaches can directly detect transcriptionally engaged Pol II via incorporation of the nucleotide analog bromo-UTP (BrUTP) into the nascent RNA. GRO-seq is performed in isolated nuclei and might not reflect the biological situation of an intact cell. Nevertheless, it allows assessment of dynamic transcriptional processes by deriving pause duration or elongation rates (Jonkers et al. 2014).

In this work I performed transient transcriptome sequencing (TT-seq) which is a 4sU-labeling RNA-seq approach (Schwalb et al. 2016). TT-seq informs on the synthesis of nascent RNA and can be combined with mNET-seq data to calculate pause durations. The calculated pause durations were in the range of minutes which is generally consistent with previous reports (Jonkers et al. 2014). In contrast, production of a transcript from an average protein-coding human gene takes more than 30 minutes. Hence, decreasing the pause duration will not increase RNA synthesis per time. To achieve more RNA synthesis, higher initiation frequencies are required. Gene activation can increase Pol II occupancy in the promoter proximal region (Boehm et al. 2003), highlighting that pausing is a rate-limiting step. Together this suggests that shorter pause durations will result in higher initiation rates.

Indeed, TT-seq analysis revealed that strongly paused genes have lower initiation frequencies. Furthermore the initiation frequency is lower when Cdk9-mediated pause release is inhibited, indicating that pausing directly delimits the transcription initiation rate. This is in line with a kinetic model of transcription, predicting that paused polymerases restricts further initiation events (Henriques et al. 2013) and might be explained by steric interference of paused Pol II which blocks initiation. Phosphorylation of Ser5 by Cdk7 is a hallmark of transcription initiation. Studies of a Cdk7as cell line in combination with recombinant Cdk9as demonstrated that Cdk9 kinase activity and Cdk9-dependent downstream events require proper initiation facilitated by Cdk7 (Larochelle et al. 2012). In conclusion, these results suggest that a basal initiation rate is a prerequisite for promoter proximal pausing which in return delimits further initiation events. This enables the cell to alter the synthesis rate of a given RNA by increasing or decreasing the number of initiating polymerases. Moreover, pausing can promote initiation by keeping the promoter proximal region nucleosome-free (Gilchrist et al. 2010).

Abortive transcription during early elongation has been well described (reviewed in Shandilya & Roberts 2012). Furthermore, Pol II can also undergo premature termination within the gene body, as indicated by localization of decapping and termination

factors 500 bp downstream of the TSS (Brannan et al. 2012). However, if and how premature termination also occurs at the pause site has not been conclusively addressed yet. If this was the case, the levels of RNA transcribed from the region between TSS and pause site should be elevated for strongly paused genes. In the present work, less labeled RNA was observed in the short region between TSS and pause site for transcription units with long pause durations. This implies that paused Pol II does generally not terminate, consistent with the finding that in the paused state, Pol II is stably engaged with the DNA template (reviewed in Adelman & Lis 2012).

3.6 The combined actions of Brd4 and Cdk9 regulate the release of paused Pol II

The present work highlights the importance of the P-TEFb-interacting domain of Brd4 (see chapter 2.4.3). Thus, the function of Brd4 is linked to the pause release of Pol II which is facilitated by the kinase activity of Cdk9, the catalytic subunit of P-TEFb. Brd4 recruits P-TEFb as response to various stimuli including serum stimulation, pro-inflammatory signals, and disease signals such as in MLL (Dawson et al. 2011; Nicodeme et al. 2010; Zippo et al. 2009). These and other findings demonstrated that in addition to classical paused, immediate early genes like *c-Myc*, *FOS* or *JUNB* (Lu et al. 2015), Brd4 regulates a diverse set of genes dependent on the cellular and environmental context (Liu et al. 2015). The potential of Brd4 to regulate cell-type specific events has been associated with so-called super enhancers. Super enhancers are highly active and can be differentiated from regular enhancers by high occupancy of Mediator subunit Med1 or Brd4 (Lovén et al. 2013). They regulate gene sets that typically define the identity of a cell, as it was demonstrated for many cell and tissue types including B-cells, embryonic stem cells, heart and lung tissue (Hnisz et al. 2013). Thus, Brd4 is crucial for maintaining developmental integrity. Accordingly, it was demonstrated that Brd4 controls the self-renewal ability and pluripotency of mESCs (Di Micco et al. 2014). Similar

results were obtained when investigating the distinct roles of Brd2 and Brd4 in adaptive immunity. Interestingly, Brd2 and Brd4 facilitate activation of genes essential for Th17 cell development, emphasizing the ability of Brd4 to potentiate specific transcriptional programs (Cheung et al. 2017).
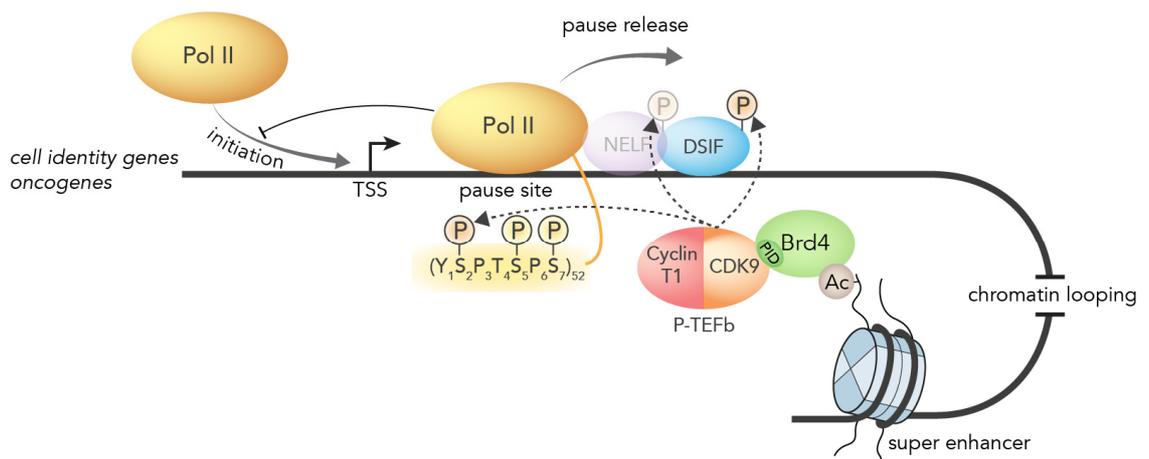
Figure 3-2 | Transcription is regulated by Brd4-mediated recruitment of P-TEFb. Model of Pol II pause release. Pol II is blocked at the pause site by negative elongation factors NELF and DSIF. This limits further transcription initiation. The elongation block is released upon Cdk9-dependent phosphorylation of NELF, DSIF, and Pol II CTD at Ser2. Subsequently the pause site is cleared, allowing further initiation events. Cdk9, the catalytic subunit of P-TEFb, is recruited to active chromatin by the PID domain of Brd4, which binds to acetylated histone tales, using its two N-terminal bromodomains. This mechanism presumably occurs frequently at super enhancers, where Brd4 promotes expression of cell-type specific genes ('cell identity genes') and tumor oncogenes.

The supposed role of Brd4 as a master regulator of cell identity is intriguing. Indeed, I observed that > 50% of expressed genes were deregulated upon JQ1 treatment or expression of dnBrd4 mutants. This demonstrates that Brd4 regulates a substantial portion of actively transcribed genes. Positive correlation of Cdk9-sensitive genes with Brd4 occupancy further indicates that these genes are regulated by the combined action of Brd4 and Cdk9. Strongly paused genes were enriched for higher order chromatin interactions, that are formed e.g. by enhancers. Together, I propose a model in which Brd4 and Cdk9 together regulate transcription of genes whose expression has to be rapidly in-

duced and tightly controlled (Figure 3-2). Promoter proximal pausing is the control mechanism that delimits transcription of the discussed genes. Presumably, the activity of Brd4 is governed by enhancers and super enhancers, which coordinate cell-specific expression patterns.

3.7 Outlook

The dominant-negative approach presented in this work has refined the roles of Brd4 domains BD2 and PID in detail. However, additional dnBrd4 mutants should be analyzed on the transcriptome level, especially mutants that comprise other domains of Brd4 including BD1, ET, and BID/PDID. The non-bromodomain regions ET and BID/PDID are of particular interest, because our understanding of these domains is still very limited. Similarly the roles of the other BET members Brd2 and Brd3 can be elucidated using dominant-negative mutants of Brd2 and Brd3. Transcriptome data of dnBrd2/3 mutants should be compared to the data obtained for dnBrd4 and JQ1 to untangle the functional diversity of the BET protein family.

The analog-sensitive Cdk9 cell line has proven a powerful tool to study the role of Cdk9 in transcription. Analog-sensitive kinases can further be used to identify the target proteins that are phosphorylated by an individual kinase using mass spectrometry. This has already be done in an *in vitro* approach for Cdk9as (Sansó et al. 2016). However, in this particular study, the assay was performed using whole cell extracts, thereby risking unspecific phosphorylation events that do not take place *in vivo*. Therefore, the Cdk9as cell line presented here should be used to study the phospho-proteome of Cdk9 *in vivo* to discover new target proteins and verify those that were identified before.

Together with Roland Schüller, I have previously established a combined genetic and mass-spectrometric approach to measure heptad-specific phosphorylation of RNA Pol II CTD (Schüller et al. 2016). I plan to combine this strategy with specific inhibition of Cdk9as to identify and quantitate the Cdk9-specific target residues within the CTD.

In vivo this was not possible before, since conventional Cdk9 inhibitors such as Flavo-piridol have off-target effects. Particularly, other CTD kinases are sensitive to Flavopiri-dol as well. For a detailed comparison of all known Cdks that have putative CTD kinase activity (Cdk7, Cdk8, Cdk9, Cdk12, and Cdk13), CRISPR-engineered cell lines express-ing analog-sensitive versions of these kinases should be constructed. Analysis of the transcriptome, phospho-proteome and CTD phosphorylation pattern in the analog-sensitive cell lines will help to dissect the individual functions of the respective kinases.

4 Materials and Methods

4.1 Material

4.1.1 Chemicals

1,4-Dithiothreitol (DTT)	Carl Roth GmbH&CoKG, Karlsruhe
1 kb DNA ladder	Invitrogen, Karlsruhe
1-NA-PP1	Calbiochem, Merck Millipore, Darmstadt
4-thiouracil (4sU)	Sigma-Aldrich Chemie GmbH, München
Agarose	Invitrogen, Karlsruhe
Bromophenol blue (BPB)	Sigma-Aldrich Chemie GmbH, München
Dimethyl sulfoxide (DMSO)	Sigma-Aldrich Chemie GmbH, München
DMEM medium (Gibco)	Life Technologies, Eggenstein
Doxycycline	Sigma-Aldrich Chemie GmbH, München
DPBS (Gibco)	Life Technologies, Eggenstein
Ethylendiaminetetraacetic acid (EDTA)	Carl Roth GmbH&CoKG, Karlsruhe
Ethanol (EtOH), absolute	Merck, Darmstadt
Ethidium bromide (EtBr)	Fluka Chemie GmbH, Buchs
Fetal bovine serum (FBS)	PAA Laboratories, Pasching, Österreich
Glycerol 86%	Carl Roth GmbH&CoKG, Karlsruhe
Glycine	Carl Roth GmbH&CoKG, Karlsruhe
HL-dsDNase	ArcticZymes, Tromsø, NO
Hygromycin B	Amresco, Solon, OH, USA
Isopropanol, absolute	Carl Roth, Karlsruhe
L-glutamine 200mM (Gibco)	Life Technologies, Eggenstein
Methanol (MeOH), absolute	Merck, Darmstadt
Neomycin (G148)	Promega Corp., Wisconsin, USA
Opti-MEM (Gibco)	Life Technologies, Eggenstein
Orange G	Sigma-Aldrich Chemie GmbH, München

Penicillin/Streptomycin 10k U/ml (Gibco)	Life Technologies, Eggenstein
Phenylmethanesulfonyl fluoride (PMSF)	ICN Biomed. Inc., Fountain Pkwy, USA
Polyacrylamide 30% (PAA)	Carl Roth GmbH+Co.KG, Karlsruhe
Powdered milk, blotting grade	Carl Roth GmbH+Co.KG, Karlsruhe
Prestained Protein Ladder Plus	Fermentas, St. Leon-Rot
QIAzol	Qiagen GmbH, Hilden
RPMI medium 1640 (Gibco)	Life Technologies, Eggenstein
Sodium dodecyl sulfate (SDS)	Carl Roth GmbH+Co.KG, Karlsruhe
Tetramethylethylenediamine (TEMED)	Carl Roth GmbH+Co.KG, Karlsruhe
Tetracycline	Promega Corp., Wisconsin, USA
Tris(hydroxymethyl)aminomethane (TRIS)	Merck, Darmstadt
TRIzol	Thermo Fisher Scientific, Waltham
Trypan blue	Invitrogen, Karlsruhe
Tween-20	Sigma-Aldrich Chemie GmbH, München

4.1.2 Consumables and kits

AFAmicro tubes	Covaris Ltd., Brighton, UK
Agar plates	Greiner GmbH, Frickenhausen
Amaxa Mouse ES Cell Nucleofector Kit	Lonza, Köln
Ampure XP beads	Beckman-Coulter, München
CellTiter 96Aqueous one solution	Promega Corp., Wisconsin, USA
Cover slides	Menzel, Braunschweig
Cryovials 1.5 ml	Nunc GmbH, Wiesbaden
Direct-zol kit	Zymo Research, Freiburg
DNA Mini/Maxi kits	Qiagen GmbH, Hilden
E-Plates 16-wells	OMNI Life Science, Bremen
ECL detection reagent	GE healthcare, München
Gene Pulser cuvettes	Bio-Rad Laboratories GmbH, München
Gel blotting Paper GB003	Schleicher & Schuell, Deutschland
Hybond N+ nylon membrane	GE Healthcare, München

KAPA HiFi DNA Polymerase	Kapa Biosystems, Wilmington, MA, USA
Laboratory glassware	Duran Productions GmbH & Co. KG, Mainz
mRNA-SENSE kit	Lexogen, Vienna, AT
Nitrile gloves duoSHILD	SHIELD Scientific, Bennekom, NL
NucleoSpin gel extraction kit	Macherey Nagel, Düren
Ovation Universal RNA-Seq System	NuGEN, Leek, NL
Parafilm	Carl GmbH+Co.KG, Karlsruhe
Pasteur pipettes	Hirschmann Laborgeräte, Eberstadt
Pipette tips ART 10, 20, 200, 1000	MolecularBio-Products, San Diego
Plastic ware for cell culture	Greiner Bio-One, Frickenhausen
Reaction tubes 1.5 ml, 2 ml	Eppendorf Deutschland, Wesseling-Berzdorf
Reaction tubes 15 ml, 50 ml	Becton Dickinson Biosiences, Heidelberg
RNA nano chip kit	Agilent Technologies, Waldbronn
Scalpel	Braun, Tuttlingen
Sterile filters	Merck Millipore, Darmstadt
Streptavidin beads	Miltenyi Biotec, Bergisch Gladbach
T4 DNA Ligase	New England Biolabs, Frankfurt a.M.

4.1.3 Technical instruments

-80°C freezer Hera Freeze	Thermo Fisher Scientific, Waltham
-20°C freezer Eco Plus	Siemens, München
AQUAline AL 12 waterbath	LAUDA, Lauda-Königshofen
Bacteria shaker (Series 25)	New Brunswick ScientificCo., NJ, USA
BioAnalyzer	Agilent Technologies, Waldbronn
Bio-Rad PowerPac 300	Bio-Rad Laboratories GmbH, München
Branson Sonifier 250	Heinemann Ultraschall- und Labortechnik
Countess automated cell counter (Invitrogen)	Thermo Fisher Scientific, Waltham
Electrophoresis equipment	Bio-Rad Laboratories GmbH, München
Electroporator (eukaryotic cells)	Bio-Rad Laboratories GmbH, München
Eppendorf Centrifuge 5417R	Eppendorf Deutschland, Wesseling-Berzdorf

Eppendorf Thermomixer C	Eppendorf Deutschland, Wesseling-Berzdorf
Fridge KU 1710 Vario	Liebherr, Biberach
FACS Aria II flow cytometer	BD Biosciences, Heidelberg
FACS Calibur flow cytometer	BD Biosciences, Heidelberg
Focused ultrasonicator S220	Covaris Ltd, Brighton, UK
Fuchs-Rosenthal chamber	GLW Gesellschaft für Laborbedarf GmbH
Gilson Pipettes 2, 10, 20, 200,1000	Gilson, Bad Camberg
Hypercassette	Amersham Biosciences, Freiburg
Illumina HiAeq 1500	Illumina Inc., San Diego, CA, USA
iMac 27-inch, Late 2013	Apple Inc., Cupertino, CA, USA
Inkubator Heraeus 6000	Heraeus Sepatech GmbH, Osterode
Incubator HERA cell 150	Heraeus Sepatech GmbH, Osterode
Laminar Flow Hood	BDK Luft-und Reinraumtechnik GmbH
Magnet stirrer M23	GLW, Würzburg
Microwave NNV 689W	Panasonic, Hamburg
Mighty Small Transphor Unit TE 22	GE Healthcare, München
Mighty Small II SE260 Electrophoresis Unit	Amersham Biosciences, Freiburg
MiniSpin Plus centrifuge	Eppendorf Deutschland, Wesseling-Berzdorf
Multi-calimatic pH-meter	Knick GmbH+Co.KG, Berlin
Nanodrop 1000	Thermo Fisher Scientific, Waltham
Odyssey imaging system	LI-COR Biosciences GmbH, Bad Homburg
PipetMan P	Gilson, Bad Camberg
Power supply Peqlab EV202	VWR Life Science, Erlangen
Primo Vert light microscope	Carl Zeiss Jena GmbH, Göttingen
Rollermixer SRT 6	Stuart Equipment, Staffordshire, UK
Rotanta 460 R centrifuge	Hettich, Tuttlingen
Rotina 380 centrifuge	Hettich, Tuttlingen
Scanmaker i800 plus	Microtek, Taiwan
Sunrise Photometer	Tecan Group Ltd., Männedorf, CH
UV lamp Peqlab VL-4. LC	VWR Life Science, Erlangen

Vi-CELL XR cell counter   Beckman Coulter, München

Vortexer Reax 2000   Heidolph Instruments GmbH, Schwabach

xCELLigence RTCA DP   Roche Diagnostics, Mannheim

4.1.4 Software

Adobe Illustrotor CS6   Adobe Systems, Dublin, IRL

Adobe Photoshop CS6   Adobe Systems, Dublin, IRL

FlowJo 2 V.10.0.8r1   FlowJo LLC, Ashland, OR, USA

Image J 2.0.0-rc-43/1.50g   Wayne Rasband, Maryland, MD, USA

MacVector 14.5.2   MacVector Inc., Cambridge, UK

Magellan v7.2   Tecan Group Ltd., Männedorf, CH

Mendeley Desktop 1.17.6   Elsevier Inc., New York, NY, USA

Microsoft Office 2010, 2011   Microsoft, Washington, DC, USA

RTCA 2.0 Software (xCELLigence)   Roche Diagnostics, Mannheim

UCSF Chimera 1.8.1   University of California (Pettersen et al. 2004)

4.1.5 Buffers and solutions

0.7% Agarose-TAE-Gel for DNA   2.1 g Agarose

                                        300 mL 1x TAE

                                        boil in microwave

                                        cool to 65°C

                                        EtBr (375 ng/µL)

10 x DNA Loading Dye   20 g Sucrose

                                        100 mg Orange G

                                        add 50 mL H_2O

Laemmli-Buffer (2x)   2% SDS

                                        100 mM DTT

                                        10 mM EDTA

                                        10% Glycerol

	60 mM Tris/HCl pH 6,8
	0.01% BPB
	1 mM PMSF
LB-medium	20 mM $MgSO_4$
	10 mM KCl
	1% Bacto-Tryptone
	0.5% Bacto-yeast extract
	0.5% NaCl
LB-agar	20 mM $MgSO_4$
	10 mM KCl
	1% Bacto-Tryptone
	0.5% Bacto-yeast extract
	0.5% NaCl
	1.2% Bacto-agar
Milk powder solution	5% powdered milk in 1 x TBST
PBS	137 mM NaCl
	2.7 mM KCl
	4.3 mM $Na_2HPO_4*6H_2O$
	1.4 mM KH_2PO_4
SDS-PAGE separating gel (6.5%)	4.3 mL PAA 30%
	10 mL 2xTris/SDS pH 8.8
	5.5 mL H_2O
	1167 µL APS
	17 µL TEMED

SDS-PAGE separating gel (10.5%)	7 mL PAA 30%
	10 mL 2xTris/SDS pH 8.8
	2.8 mL H_2O
	167 µL APS
	17 µL TEMED
SDS-PAGE separating gel (12.5%)	8.3 mL PAA 30%
	10 mL 2xTris/SDS pH 8.8
	1.5 mL H_2O
	167 µL APS
	17 µL TEMED
SDS-PAGE stacking gel (4%)	2 mL PAA 30%
	15 mL 2xTris/SDS pH 6.8
	5.4 mL H_2O
	90 µL APS
	20 µL TEMED
SDS-PAGE-running buffer (10x)	60.4 g Tris/Base
	288 g Glycin
	5 ml SDS 20%
	add 2 L H_2O
1x Tris acetate EDTA (TAE)	40 mM Tris Acetate
	1 mM EDTA
	adjust pH to pH 8.0
1x Tris buffered saline (TBS)	10 mM NaCl
	1 mM Tris/HCl pH 7.5

Tris EDTA (TE)	10 mM Tris
	1 mM EDTA
	adjust pH to 8.0
2x Tris/SDS pH 6.8	7.56 g Tris/Base
	2.5 mL SDS 20%
	add 250 mL H_2O
	pH 6.8 (with HCL)
2x Tris/SDS pH 8.8	22.68 g Tris/Base
	2.5 mL SDS 20%
	add 250 mL H_2O
	pH 8.8 (with HCL)
Western-transfer buffer (10x)	60.4 g Tris/Base
	288 g Glycin
	5 mL SDS 20%
	200 mL methanol
	add 2 L H_2O
Western-blocking-reagent	10% (v/v) TBS
	0.1% (v/v) Tween 20
	5% (w/v) powdered milk

4.1.6 Antibodies

Primary antibodies	source	clone	species	usage
anti α-Tubulin	Sigma (T9026)	T6557	mouse	WB 1:20,000
anti Brd4	Bethyl (A301-985A)	polyclonal	rabbit	WB 1:10,000
anti Cdk9	Santa Cruz (sc-484)	polyclonal	rabbit	WB 1:2,000
anti Cdk12	Sanza Cruz (sc-81834)	R12	mouse	WB 1:5,000
anti CTD Ser2-P	Dr. E Kremmer	3E10	rat	WB 1:10

anti CTD Ser5-P	Dr. E Kremmer	3E8	rat	WB 1:10
anti CTD Ser7-P	Dr. E Kremmer	4E12	rat	WB 1:10
anti GAPDH	Dr. E Kremmer	5C4	rat	WB 1:5,000
anti HA	Roche Diagnostics	3F10	rat	WB 1:20
anti Rpb1	Dr. E. Kremmer	Pol3.3	mouse	WB 1:5

Secondary antibodies	source	usage
HRP anti mouse IgG	Promega	WB 1:5,000
HRP anti rabbit IgG	Promega	WB 1:5,000
HRP anti rat IgG+IgM	Jackson Laboratories	WB 1:5,000
IRDye 800 anti mouse IgG	Rockland Inc.	WB 1:10,000
Alexa Fluor 680 anti rat IgG	Invitrogen	WB 1:20,000

4.1.7 Oligo nucleotides

PCR primers	sequence (5' to 3')	modification
BRD4 wt for	CCACCATGTCTGCGGAGAGCG	5' phospho
BRD4 f2 for	CCACCATGATGATAGTCCAGGCAAAAG	-‖-
BRD4 f3 for	CCACCATGACCACCATTGACCCCATTC	-‖-
BRD4 f4 for	CCACCATGGTCCGATTGATGTTCTCCAAC	-‖-
BRD4 f5 for	CCACCATGAAGCACAAAAGGAAAGAGGAAGTGG	-‖-
BRD4 f6 for	CCACCATGCACCATCATCACCACCATCAG	-‖-
BRD4 f7 for	CCACCATGACCCAAACACCCCTGCTC	-‖-
BRD4 f8 for	CCACCATGCACAAGTCGGACCCCTAC	-‖-
BRD4 f9 for3	CCACCATGGCCCCTGACAAGGACAAA	-‖-
BRD4 wt rev	GAAAAGATTTTCTTCAAATATTGAC	-‖-
BRD4 f1 NLS rev	TACCTTTCTCTTCTTTTTTGGCTGGGTCTGCGGAGGAG	-‖-
BRD4 f2 NLS rev	TACCTTTCTCTTCTTTTTTGGCTTCTTGGCAAACATCTC	-‖-
BRD4 f3 NLS rev	TACCTTTCTCTTCTTTTTTGGGCTATCGCTGCTGCTGTC	-‖-
BRD4 f4 NLS rev	TACCTTTCTCTTCTTTTTTGGCTTGTCCTCTTCCTCCGAC	-‖-
BRD4 f5 NLS rev	TACCTTTCTCTTCTTTTTTGGAATGAAGGGTGGGGGCGAGG	-‖-

BRD4 f6 NLS rev	TACCTTTCTCTTCTTTTTTGGGGAAGGGAGTAGCGGCGT	-||-
BRD4 f7 NLS rev2	TACCTTTCTCTTCTTTTTTGGCTCCTTCACCACCACGAAGG	-||-
BRD4 f8 NLS rev	TACCTTTCTCTTCTTTTTTGGCTTCTCACGCTCCTCTTTC	-||-
BRD4 wtNLS rev	TACCTTTCTCTTCTTTTTTGGGAAAAGATTTTCTTCAAATATTGAC	-||-
CDK9 for	CCACCATGGCAAAGCAGTACG	-||-
CDK9 rev	GAAGACGCGCTCAAACTCC	-||-

Seq. primers	**sequence (5' to 3')**
BRD4 862 for	CAGCCTGTGAAGACAAAG
BRD4 2300 for	CCAAACCGAAAGTCCAGGC
BRD4 f5 for 387	CTATGTCACCTCCTGTTTGC
BRD4 f7 rev 368	ATGTGGGTGGAAAACTGC
BRD4 f7 rev 555	GGAATGTATCATAAGCGGG
CDK9 screen for	CCCCGTAGCTGGTGCTTCCTCG
CDK9 screen rev	CCCCAGCAGCCTTCATGTCCCTAT
CMV profor	GGCGGTAGGCGTGTA
hGH_rev	TATTAGGACAAGGCTGGTGGGCAC
rgGlob-irv	AACAATCAAGGGTCCCC

gRNA primers	**sequence (5' to 3')**
CDK9 gRNA for	CACCGGCTCGCAGAAGTCGAACACC
CDK9 gRNA rev	AAACGGTGTTCGACTTCTGCGAGCC

CDK9 targeting donor oligo   sequence (5' to 3')

AAAGTGTGTTGGGTGTGGTTTTCTTGACTTTTTCTTCTTTCTATTCCTGCCTCAGCTTC
CCCCTATAACCGCTGCAAGGGTAGTATATACCTGGTcgcgGACTTCTGCGAGCATGACC
TTGCTGGGCTGTTGAGCAATGTTTTGGTCAAGTTCACGCTGTCTGAGATCAAGAGGGTG
ATGCAGATGCTGCTTAACGGCCT

4.1.8 Bacteria

DH10B

E.coli strain purchased from *Invitrogen GmbH, Karlsruhe.* Used for the cloning of all plasmid DNA, including the sub-cloning vector pSfi-Express and end-cloning vector pRTS-1.

4.2 Methods

4.2.1 Plasmids

All plasmids (Table 4-1) were stored in TE buffer at -25°C. Sanger sequencing was performed to verify the correct sequences of the expression cassettes (Sequiserve GmbH, Vaterstetten). The raw sequencing data was edited and aligned using the MacVector software in combination with the ClustalW alignment algorithm. All pRTS-1-based plasmids can be stably transfected in human cell lines Raji and H1299, where the vector is episomally maintained by the Epstein-Barr Virus (EBV) gene EBNA1.

Table 4-1 | Plasmids used in this study.

Name	Backbone plasmid	Resistance	Reference
wtBRD4-HA (1-1362)	pRTS-1	Ampicilline	Bornkamm et al. 2005
f1-BRD4-HA (1-209)	-||-	-||-	-||-
f2-BRD4-HA (172-368)	-||-	-||-	-||-
f3-BRD4-HA (298-492)	-||-	-||-	-||-
f4-BRD4-HA (422-606)	-||-	-||-	-||-
f5-BRD4-HA (550-801)	-||-	-||-	-||-
f6-BRD4-HA (738-947)	-||-	-||-	-||-
f7-BRD4-HA (895-1112)	-||-	-||-	-||-
f8-BRD4-HA (1049-1239)	-||-	-||-	-||-

f9-BRD4-HA (1174-1362)	-||-	-||-	-||-
f-BD1-BRD4-HA (54-168)	-||-	-||-	-||-
CDK9-HA	-||-	-||-	-||-
pFLAG-CMV2-BRD4 (1-1362)	pFLAG-CMV2	-||-	Bisgrove et al. 2007
FLAG-CDK9	pFLAG-CMV2	-||-	Wang et al. 2008
pSpCas9-CDK9 gRNA-GFP	PX458	-||-	Ran et al. 2013

4.2.2 Brd4 and Cdk9 cloning strategy

HA-tagged Brd4 constructs were cloned into the pRTS-1 vector (Bornkamm et al. 2005; Hölzel et al. 2007). Nine different primer pairs were designed to amplify subfragments f-BD1 and f1-f9 of the *BRD4* open reading frame (ORF) via polymerase chain reaction (PCR) with a pFLAG-CMV2-BRD4 (1-1362) plasmid as template DNA (Addgene #22304; Bisgrove et al. 2007). A CCACC Kozak sequence followed by a start codon, and a SV40 nuclear localization signal (PKKKRKV) were added during the PCR using the designed primers. A PCR product containing the full-length ORF of *BRD4* was amplified in the same manner but lacking the NLS.

Next, a C-terminal HA tag, STOP codon and two *SfiI* restriction sites that flanked the whole ORF were added via blunt-end ligation of the PCR product with sub-cloning construct pSfi-Express. After *SfiI* restriction digest the fragment was ligated with the pRTS-1 vector, which features a doxycycline-inducible, bidirectional promoter, also expressing eGFP (Figure 4-1). A pRTS-1 construct containing the luciferase gene served as vector control. HA-tagged Cdk9 was cloned in the same manner, using FLAG-CDK9 (Addgene #28100; Wang et al. 2008) as template DNA for the initial PCR.
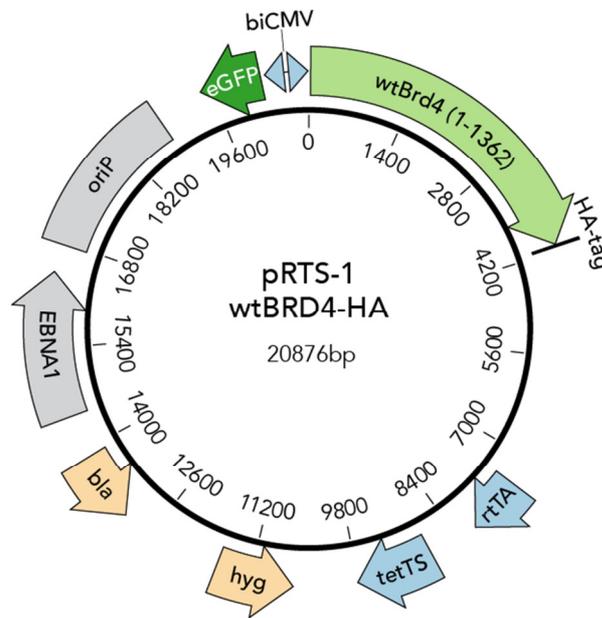
Figure 4-1 | Schematic vector map of the pRTS-1 wtBRD4-HA plasmid. An rtTA-responsive, bidirectional CMV promoter (biCMV) is flanked by eGFP and the gene of interest, here full-length Brd4 followed by a C-terminal HA-tag. EBNA1, the EBV gene EBNA1; bla, β-lactamase gene conferring bacterial resistance to ampicilline; oriP, the bacterial origin of replication; hyg, the hygromycin phosphotransferase gene conferring eukaryotic resistance to hygromycine; rtTA, tetracycline controlled transcriptional activator; tetTS, tetracycline-controlled transcriptional silencer (Bornkamm et al. 2005).

4.2.3 Ligation of DNA constructs

For ligation, the PCR or restriction digest product was first purified via agarose gel electrophoreses and extracted using the NucleoSpin gel extraction and PCR purification kit (Macherey Nagel) according to the manufacturer's protocol. The purified DNA fragment was diluted in H_2O, mixed with the linear vector DNA, incubated at 50°C for 5 min and immediately stored on ice. Then T4 ligase buffer and T4 DNA ligase were added and the mixture was incubated at 16°C over night (o/n).

4.2.4 Construction of analog-sensitive Cdk9 Raji cells

Analog-sensitive Cdk9 Raji cells were constructed by Weihua Qin (AG Leonhardt, LMU Munich) as described before (Mulholland et al. 2015) with slight modifications. The amino acid sequence of the Cdk9 kinase domain (UniProt, P50750-1) was aligned with

the sequence of the kinase domains of well-studied kinases to identify the gatekeeper residue of Cdk9 (F103; Table 4-2) (Lopez et al. 2014).

Table 4-2 | Sequence alignment of selected domains. Selected kinase domains were aligned to identify the gatekeeper residue (highlighted in orange) of Cdk9 (F103). Sequences of the kinase domains were retrieved from the UniProt database (The UniProt Consortium 2017) and sequence alignment was performed using the Clustal Omega 1.2.4 online tool (Sievers et al. 2011). * fully conserved residue; : strong conservation; . weak conservation

Kinase	Aligned sequence of kinase domain	Gatekeeper
c-Src	RHEKLVQLYAVV----------SEEPIYIVTEYMSKGSLLDFLK---------GETGKY	T341
Cdk1	RHPNIVSLQDVL----------MQDSRLYLIFEFLSM-DLKKYLD--------SIPPGQY	F80
Cdk2	NHPNIVKLLDVI----------HTENKLYLVFEFLHQ-DLKKFMD-------ASALTG--	F80
Cdk7	SHPNIIGLLDAF----------GHKSNISLVFDFMET-DLEVIIK--------DNSLV--	F91
Cdk8	KHPNVISLQKVF--------LSHADRKVWLLFDYAEH-DLWHIIKFHRASKANKKPVQ--	F97
Cdk9	KHENVVNLIEIC--RTKASPYNRCKGSIYLVFDFCEH-DLAGLLS-------NVLVK--	F103
Cdk12	IHRSVVNMKEIVTDKQDALDFKKDKGAFYLVFEYMDH-DLMGLLE--------SGLVH--	F813
	* .:: : . . :: :: .* :.	

Next, the guide RNA (gRNA) for guiding Cas9 to targeting site was designed using the optimized CRISPR Design tool available online at http://crispr.mit.edu/ (Zhang Lab MIT, 2015). The gRNA was cloned into the px458 backbone, which then expressed both gRNA and GFP-Cas9 (Addgene #48138; Ran et al. 2013). A single strand (ss) DNA oligo carrying an F to A mutation was synthesized and served as targeting donor to replace the gatekeeper residue F to A, thereby producing a *BstUI* cleavage site (Figure 4-2A). The gRNA and donor DNA were mixed 1:1 and transfected into Raji cells using the amaxa mouse ES cell nucleofector kit (Lonza). After two days of expression, GFP-positive cells were sorted into 96 well plates (12×) by means of FACS (Becton Dikinson). Survival clones were collected and genomic DNA was isolated for PCR screening. The targeting region was amplified by PCR and the PCR product was digested with BstUI to identify positive clones (Figure 4-2B). Finally, positively selected clones were verified by sequencing.
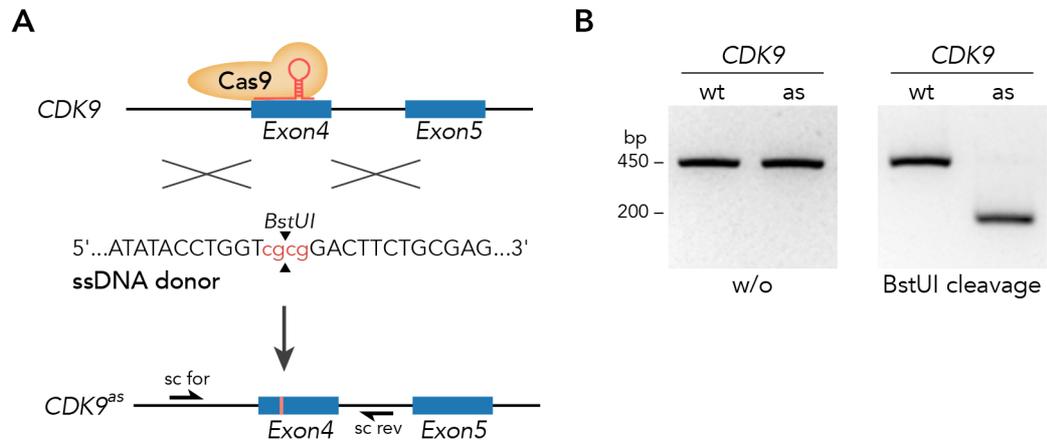
Figure 4-2 | Construction of analog-sensitive Cdk9^{as} (F103A) using CRISPR/Cas9.
(A) A ssDNA oligo served as donor to replace the gatekeeper residue F to A, which further introduced a *BstUI* restriction site. **(B)** The targeting region of survival clones was amplified with screening (sc) primers and the PCR product digested with *BstUI*. The digested DNA was detected in an agarose gel. CRISPR/Cas9 targeting of Cdk9 was carried out by Weihua Qin (Leonhardt group, LMU Munich).

4.2.5 Bacterial cell culture

4.2.5.1 Transformation of competent cells

Competent DH10B bacteria cells were transformed by mixing 50 µL of DH10B either with the whole ligation product or with 5 µg of purified plasmid DNA, followed by incubation for 20 min on ice. Next, a heat shock was performed for 30 s at 42°C and the cells were directly put on ice for 2 min. 400 µL LB medium were added and the cells were incubated at 37°C. After 90 min the cells were plated on selective agar plates. The plates were stored at 37°C o/n.

4.2.5.2 Miniprep of bacterial plasmid DNA

On the next day multiple clones were picked for o/n miniculture for which the clones were incubated in LB medium (2 mL total miniculture volume each). The miniculture was followed by miniprep, which started with the centrifugation of 1.5 ml miniculture (16,400 rpm; 4°C; 1 min), resuspension of the cell pellet in 150 µL buffer P1 and incubation at RT for 5 min. Buffer P1, P2 and P3 were taken from the QIAGEN Plasmid Maxi

kit but an alternate protocol was used. The cells were then lysed by adding 150 µL buffer P2 followed by mixing and 5 min incubation at RT. Next, 150 µL of cold buffer P3 was added to neutralize the lysate which was then mixed and incubated on ice. After 30 min the samples were centrifuged (16,400 rpm; 4°C; 5 min) and the SN was transferred into a new 1.5 mL microcentrifuge tube. The SN was mixed with 450 µL isopropanol, incubated for 5 min, and again centrifuged (16,400 rpm; 4°C; 5 min). The resulting pellet was washed with 1 mL 70% ethanol and after drying it for 5 min on air it was resuspended in 200 µL H_2O.

4.2.5.3 Maxiprep of bacterial plasmid DNA

Maxiculture was set up by inoculating 400 mL LB medium (50 µg/mL kanamycin) with 500 µL of the miniculture of chosen clones. All maxipreps were performed using the QIAGEN Plasmid Maxiprep kit. Briefly, the o/n maxiculture was harvested by cetrifuging at 3600 rpm for 15 min at 4°C. The bacterial pellet was resuspended in 10 mL buffer P1. Subsequently, 10 mL of buffer P2 were added to the resuspended cells and mixed thoroughly by inverting 10 times. After 5 min incubation 10 mL of prechilled buffer P3 were added and the mixture was inverted again. Next the suspension was centrifuged for 30 min at 4,000 rpm at 4°C. Meanwhile, a QIAGEN tip was equilibrated by applying 10 mL buffer QBT and allowing the column empty by gravity flow. Next, the supernatent of the mixture was applied to the tip and the flow-through was discarded. The tip was washed twice with 30 mL wash buffer QC. The DNA was eluted by adding 15 mL elution buffer QF and the eluted DNA was collected in a fresh 50 mL vessel. 10.5 mL isopropanol were added and centrifuged at 4,000 rpm for 30 min at 4°C. The supernatant was discarded and 5 mL 70% ethanol were added and centrifuged at 4,000 rpm at 4°C to wash the DNA pellet. The supernatant was decanted and the pellet was air-dried for 10 min. Finally the DNA was collected by resuspending in 300 µL TE buffer.

4.2.6 Human cell culture

4.2.6.1 Cell lines

Raji

This EBV-positive B-cell line was established from the left maxilla of a 12 year-old African boy with Burkitt's lymphoma in 1963 (Pulvertaft 1964). Identity of Raji cells (DSMZ no.: ACC 319) was verified by determining genetic characteristics using PCR-single-locus-technology (Eurofins Genomics). Raji cells harbor a t(8;14) translocation that places the c-*Myc* gene into the highly active immunoglobulin locus, leading to overexpression of the oncogene (Taub et al. 1984).

H1299

The non-small cell lung cancer cell line H1299 (ATCC-no.: CRL-5803) was established from a metastatic site of a lung lymph node of a 43 years Caucasian male. The cells grow adherent and display an epithelial morphology. Genetically, H1299 cells have a homozygous partial deletion of the *TP53* gene, thus lacking expression of the p53 protein (Bodner et al. 1992).

4.2.6.2 Cell culture conditions

Cells were cultured in RPMI (Raji) or DMEM (H1299) supplemented with 10 % fetal calf serum, 2 mM L-glutamine, and 1% penicillin streptomycin at 37°C, 5 % CO_2 (Raji) or 8 % CO_2 (H1299).

4.2.6.3 Stable transfection of Raji and H1299 cells

Raji and H1299 cells were stably transfected using Qiagen PolyFect in combination with Opti-MEM medium. To this end, 6 µg of plasmid DNA and 16 µL PolyFect solution were diluted in 400 µL Opti-MEM each. After 5 min the two solutions were mixed and incubated for 30 min at RT. Meanwhile the cells were washed once with PBS and covered with 8 mL Opti-MEM. Next the transfection mix was added to the cells, followed

by 7 h 30 min incubation at 37°C. Then, the Opti-MEM medium was replaced by standard growth medium supplemented with 100 μM hygromycin B for 1 week, which was increased to 200 μM for 3 additional weeks. Expression of recombinant proteins was induced by adding 25 ng/mL or 1,000 ng/mL doxycycline to Raji or H1299 cell culture medium, respectively. These concentrations were determined for each cell line individually, because doxycycline itself caused proliferation defects when used at high concentrations.

4.2.7 Cell proliferation assays

Cell culture density was measured using different systems. Proliferation of H1299 cells was monitored via the xCELLigence system. Triplicates of H1299 cells were seeded in 16-well E-Plates at a density of 5,000 cells per well and the cell index was monitored. After 24 h cells were induced with doxycycline (1 μg/mL) or treated with JQ1 (1 μM) and the cell index was compared with non-treated cells for additional 48 h.

Because the xCELLigence system cannot be applied to suspension cells, a Vi-CELL XR cell counter was used to measure proliferation of Raji cells transfected with Brd4 constructs. The long-term impact of JQ1 on Raji cells was detected with a Countess automated cell counter. For this, cells were mixed with an equal amount of 0.4% trypan blue solution and applied to counting chamber slides which were inserted into the Countess cell counter.

Cell proliferation at increasing JQ1 or 1-NA-PP1 concentrations was assessed using the CellTiter 96 AQueous One Solution Cell Proliferation Assay System. Cells were seeded in duplicates in a 96-well plate and increasing concentrations of JQ1/1-NA-PP1 or DMSO (control) were added. After 72 h MTS tetrazolium compound was added to each well for one hour. Then the quantity of the MTS formazan product was measured as absorbance at 490 nm with a Sunrise photometer which was operated using the Magellan data analysis software. Relative signals were calculated by dividing the JQ1/1-NA-PP1 signals by the corresponding DMSO signals.

4.2.8 Flow cytometry

The bi-directional promoter of the pRTS-1 vector drives expression of eGFP in addition to the inserted construct. This allows for quantification of the positively transfected, eGFP-positive cell population by means of flow cytometry. Raji cells were washed, re-suspended in phosphate buffered saline (PBS), and submitted to an XCalibur flow cytometer. For data acquisition, non-induced cells were gated for lymphocytes from which the eGFP-negative gate was defined for the following measurements. FlowJo 2 software was used for data analysis.

4.2.9 Western analysis

Cells were lysed in 2x laemmli buffer, boiled at 95 °C for 5 min, and sonified (10 pulses, output 5, duty cycle 50%) before submission to discontinuous sodium dodecyl sulfate-polyacrylamide gel electrophoresis (SDS-PAGE). SDS-PAGE was run at 30 mA constant per gel for about 2 h. Next, transfer to nitrocellulose membrane was prepared using the wet blot principle. The separating gel was laid onto one wet layer whatman paper and the water-soaked membrane was carefully applied onto the gel. After placing a final slice of whatman paper on top, the stack was taken into a transfer chamber filled with transfer buffer and eventually transfer was started (450 mA constant; 1.5 h).

Prior to primary antibody incubation, unspecific binding of antibodies was blocked by 1 h incubation of the membrane with 5% milk (w/v) in Tris-buffered saline plus 1% Tween (TBS-T). Blocking was followed by primary Ab incubation at 4°C o/n. The membrane was washed three times in TBS-T for 5 min before the secondary Ab was added. The membrane was incubated with HRP-conjugated secondary antibodies. Importantly, the membrane was washed three times in TBST and rinsed once in H_2O prior to detection. The signals were visualized via enhanced chemiluminescence using the Amersham ECL Western Blotting Detection Reagent. For this, equal amounts of ECL substrate reagents A and B were mixed and 1 ml of this mixture was spread onto the

membrane. ECL signals were captured by exposing film to the membrane. This last step was performed in the dark room where the films were also developed.

Alternatively, fluorophor-coupled secondary antibodies were used and incubated for 1.5 h at room temperature. After washing, these blots were visualized using the Odyssey system (Licor). This allows for multiplexing of two different secondary antibodies, because the emitted fluorescence differs in wavelength (anti mouse: 680 nm; anti rat: 800 nm). Signals were measured by scanning the TBS-T-soaked membrane with the Odyssey scanner, producing digital images as a result.

4.2.10 Poly(A) RNA-seq library preparation

24 hours after induction/JQ1 treatment, cells were washed twice in DPBS, resuspended in TRIzol reagent and short-term stored at -80 °C until library preparation. Library preparation and RNA sequencing was done in collaboration with Stefan Krebs from the LAFUGA group of Helmut Blum at the Gene Center (LMU Munich). Total RNA was isolated using the Direct-zol kit. The quality of total RNA was controlled using a nanodrop ND1000 photospectrometer: The ratios of absorbance at 260 nm and 280 nm ranged from 1.93 to 1.97 and 260/230 ratios ranged from 2.1 to 2.2. RNA integrity was checked on an Agilent BioAnalyzer 2100 with the Agilent RNA nano chip kit: RNA integrity numbers (RIN) ranged from 9.7 to 10 (scale 1 to 10; 10 for highest quality).

Next 1 µg of total RNA was used for preparation of Illumina-compatible strand-specific cDNA (RNA-seq) libraries using the mRNA-SENSE kit from Lexogen. Briefly, polyA RNA was bound to oligo dT beads; starter and stopper heterodimer oligos were annealed to captured mRNA. Starter oligos served as primer for cDNA synthesis which continued until stopper. Stopped cDNA and stopper were ligated to yield a cDNA fragment flanked by Illumina P5 and P7 sequences. This was followed by PCR amplification, which introduced barcodes and adaptor sequences to the libraries. PCR products were purified with Ampure XP beads, followed by quantification and quality control with Agilent BioAnalyzer 2100 using a DNA 1000 chip. Samples were sequenced on Il-

lumina HiSeq 1500 in single end mode with 76 bp read length and i7 index read. The sequencing depth was ~ $2x10^7$ reads per sample.

4.2.11 Bioinformatics analysis of Brd4/JQ1 RNA-seq data

Bioinformatics analysis was performed by Michael Kluge from the research group of Caroline Friedel at the Institute for Informatics (LMU Munich) as described in Decker et al. 2017. After trimming adapters from sequencing reads using cutadapt (Martin 2011), reads were mapped to the human reference genome GRCh38 as well as rRNA sequences using ContextMap 2 (Bonfert et al. 2015). Read counts per gene were determined using featureCounts (Liao et al. 2014) on the Ensembl gene annotation (release 84). Reads were assigned to a gene if they overlapped with an exon of the gene by at least 25 bp and mapped uniquely to that gene. ~ 80% of reads could be mapped per sample. Genes were included in downstream analyses if the average read count across all samples was ≥ 25 (~ 11,700 genes).

Before gene expression analysis, principal component analysis (PCA) and hierarchical clustering of samples were performed. For PCA, read counts were normalized using limma (Smyth 2005). Hierarchical clustering analysis was based on the Euclidean distances between the normalized read counts. Differential expression analysis for each condition against the control was performed with limma, edgeR and DESeq2 (Love et al. 2014; Robinson et al. 2010). Multiple testing correction was performed using the Benjamini–Hochberg method (Benjamini & Hochberg 1995). Genes were selected for further analysis if they were identified as differentially expressed by at least two of the three methods (multiple testing corrected p-value ≤ 0.05, Supplementary Table 1).

4.2.12 Transient transcriptome sequencing (TT-seq) of Cdk9as cells

TT-seq experiments were performed essentially as described before in Schwalb et al. 2016 together with Saskia Gressel from the group of Patrick Cramer (MPI for Biophysical Chemistry, Göttingen). Two independent biological replicates were prepared. Brief-

ly, for TT-seq experiments, 3.3 x 10^7 Raji B cells were treated for 15 minutes with solvent (DMSO) or 5 μM of 4-Amino-1-tert-butyl-3-(1'-naphthyl)pyrazolo[3,4-d]pyrimidine (1-NA-PP1). Labeling was performed with the addition of 500 μM of 4-thiouracil (4sU) for 5 min at 37 °C and 5 % CO2. Cells were harvested by centrifugation at 3,000 x g for 2 min. Total RNA was extracted using QIAzol according to the manufacturer's instructions. RNAs were sonicated to generate fragments of <1.5 kb using AFAmicro tubes in a Covaris S220 Focused-ultrasonicator. 4sU-labeled RNA was purified from 150 μg total fragmented RNA. Following thiol-specific biotinylation, labeled RNA was separated using streptavidin beads. Prior to library preparation, 4sU-labeled RNA was purified and quantified. Enrichment of 4sU-labeled RNA was analyzed by RT-qPCR as described before in (Schwalb et al. 2016). Input RNA was treated with HL-dsDNase and used for strand-specific library preparation according to the Ovation Universal RNA-Seq System. The size-selected and pre-amplified fragments were analyzed on a Fragment Analyzer before clustering and sequencing on the Illumina HiSeq 1500.

4.2.13 Bioinformatics analysis of TT-seq data

Bioinformatics analysis of the TT-seq data was performed by Björn Schwalb (Cramer group) as described recently (Gressel et al. 2017). Briefly, baired-end 50 base reads with additional 6 base reads of barcodes were obtained for each of the samples, i.e. 2 replicates of TT-Seq with 1-NA-PP1 treatment and 2 replicates of TT-Seq with DMSO treatment. Reads were demultiplexed and mapped with STAR 2.3.0 (Dobin et al. 2013) to the hg20/hg38 (GRCh38) genome assembly (Human Genome Reference Consortium). Quality filtering of SAM files was performed using Samtools (Li et al. 2009). Here alignments with MAPQ smaller than 7 (-q 7) were skipped and only proper pairs (-f99, -f147, -f83, -f163) were selected. Further data processing was carried out using the R/Bioconductor environment.

Spike-in (RNAs) normalization strategy was used essentially as described before in (Schwalb et al. 2016) to allow observation of global shifts and antisense bias determina-

tion (ratio of spurious reads originating from the opposite strand introduced by the RT reactions) in TT-seq signal. Read counts for all spike-ins were calculated using HTSeq (Anders et al. 2015). Sequencing depth calculations resulted in no detectable global differences. For each annotated gene, transcription units (TUs) were defined as the union of all existing inherent transcript isoforms (UCSC RefSeq GRCh38). Read counts for all features were calculated using HTSeq (Anders et al. 2015) and corrected for antisense bias. Read counts per kilobase (RPK) were calculated upon bias corrected read counts falling into the region of a transcribed unit divided by its length in kilobases.

Calculation of the number of transcribed bases: For each sample aligned duplicated fragments were discarded. Of the resulting unique fragment isoforms only those were kept that exhibited a positive inner mate distance. The number of transcribed bases (tb_j) for all samples was calculated as the sum of the coverage of evident (sequenced) fragment parts (read pairs only) for all fragments with an inner mate interval not entirely overlapping a Refseq annotated intron (UCSC RefSeq GRCh38, ~ 98% of all fragments) in addition to the sum of the coverage of non-evident fragment parts (entire fragment).

Calculation of response ratios. For each condition (DMSO or 1-NA-PP1) the antisense bias corrected number of transcribed bases was calculated for all expressed TUs exceeding 10 kb in length. Of all remaining TUs only those were kept harboring one unique TSS based on all Refseq annotated isoforms (UCSC RefSeq GRCh38). Response ratios were calculated for a window from the TSS to 10 kb downstream for each TU.

Estimation of elongation velocity. For each condition TUs exceeding 35 kb in length were used and truncated by 5 kb as described above. Of all remaining TUs only those were kept harboring one unique TSS given all Refseq annotated isoforms (UCSC RefSeq GRCh38). For each TU the elongation velocity [kb/min] was calculated, given that the difference of transcribed bases obtained by the 1-NA-PP1 treatment equals the number of transcribed bases per nucleotide times the number of nucleotides traveled, corrected by the amount of the response.

Determination of pause site. For all expressed TUs exceeding 10 kb in length with one unique TSS given all Refseq annotated isoforms (UCSC RefSeq GRCh38) the pause site was calculated in a window from TSS to 500 bases for all non-negative mNET-seq coverage values (Nojima et al. 2015).

For estimation of (productive) initiation frequency (pause release rate) all expressed TUs exceeding 10 kb in length and harboring one unique TSS were used. For each TU the (productive) initiation frequency [$cell^{-1}min^{-1}$] was calculated based on the labeling duration of 5 min and the length of the TU. Note that analysis was restricted to regions of non-first constitutive exons (exonic bases common to all isoforms).

Pause durations were calculated for all expressed TUs exceeding 10 kb in length with one unique TSS. The pause duration d_i [min] was calculated as the residing time of the polymerase in a window +/- 100 bases around the pause site (see above). Pause duration d_i was derived from the pause release rate and the number of polymerases (mNET-seq coverage values, Nojima et al. 2015) in a window +/- 100 bases around the pause site. For pause sites below 100 bp downstream of the TSS the first 200 bp of the TU were considered.

Ehrensberger inequality. The inequality from (Ehrensberger et al. 2013) states that new initiation events into productive elongation are limited by the velocity of the polymerase in the promoter-proximal region and the footprint of the polymerase on the DNA template (50 bp).

Table 4-3 | External datasets used for analysis.

Experiment	Factor	Cell type	GEO ID	Source	Authors
DNase Hi-C		K562	GSE56869	Nat Methods 2015	Ma, Duan
mNET-seq	Pol II	Hela S3	GSE60358	Cell 2015	Nojima, Proudfoot
ChIP-seq	NELF-E	K562	GSE31477	ENCODE 2011	Struhl
ChIP-seq	CDK9	HEK293T	GSE51633	Cell 2013	Liu, Rosenfeld
ChIP-seq	CDK9	HCT116	GSE70408	Cell 2015	Chen, Shilatifard
ChIP-seq	Brd4	HEK293T	GSE51633	Cell 2013	Liu, Rosenfeld
ChIP-seq	Brd4	Hela	GSE51633	Cell 2013	Liu, Rosenfeld

V Bibliography

Acosta, J.C., Ferrándiz, N., Bretones, G., … León, J. 2008. "Myc Inhibits p27-Induced Erythroid Differentiation of Leukemia Cells by Repressing Erythroid Master Genes without Reversing p27-Mediated Cell Cycle Arrest." *Molecular and Cellular Biology* **28**(24):7286–95.

Adelman, K. & Lis, J.T. 2012. "Promoter-Proximal Pausing of RNA Polymerase II: Emerging Roles in Metazoans." *Nature Reviews. Genetics* **13**(10):720–31.

Aguilera, A. & García-Muse, T. 2012. "R Loops: From Transcription Byproducts to Threats to Genome Stability." *Molecular Cell* **46**(2):115–24.

Akhtar, M.S., Heidemann, M., Tietjen, J.R., … Ansari, A.Z. 2009. "TFIIH Kinase Places Bivalent Marks on the Carboxy-Terminal Domain of RNA Polymerase II." *Molecular Cell* **34**(3):387–93.

Allis, C.D. & Jenuwein, T. 2016. "The Molecular Hallmarks of Epigenetic Control." *Nature Reviews Genetics* **17**(8):487–500.

Alsarraj, J., Faraji, F., Geiger, T.R., … Hunter, K.W. 2013. "BRD4 Short Isoform Interacts with RRP1B, SIPA1 and Components of the LINC Complex at the Inner Face of the Nuclear Membrane." *PloS One* **8**(11):e80746.

Alsarraj, J., Walker, R.C., Webster, J.D., … Hunter, K.W. 2011. "Deletion of the Proline-Rich Region of the Murine Metastasis Susceptibility Gene Brd4 Promotes Epithelial-to-Mesenchymal Transition- and Stem Cell-like Conversion." *Cancer Research* **71**(8):3121–31.

Amleh, A., Nair, S.J., Sun, J., … Li, R. 2009. "Mouse Cofactor of BRCA1 (Cobra1) Is Required for Early Embryogenesis." *PLoS ONE* **4**(4):2–9.

Anders, S., Pyl, P.T., & Huber, W. 2015. "HTSeq--a Python Framework to Work with High-Throughput Sequencing Data." *Bioinformatics (Oxford, England)* **31**(2):166–69.

Andrieu, G., Belkina, A.C., & Denis, G. V. 2016. "Clinical Trials for BET Inhibitors Run ahead of the Science." *Drug Discovery Today: Technologies* **19**:45–50.

Arimbasseri, A.G. & Maraia, R.J. 2016. "RNA Polymerase III Advances: Structural and tRNA Functional Views." *Trends in Biochemical Sciences* **41**(6):546–59.

Asangani, I. a, Dommeti, V.L., Wang, X., … Chinnaiyan, A.M. 2014. "Therapeutic Targeting of BET Bromodomain Proteins in Castration-Resistant Prostate Cancer." *Nature* **510**(7504):278–82.

Bartholomeeusen, K., Xiang, Y., Fujinaga, K., & Peterlin, B.M. 2012. "Bromodomain and Extra-Terminal (BET) Bromodomain Inhibition Activate Transcription via Transient Release of Positive Transcription Elongation Factor B (P-TEFb) from 7SK Small Nuclear Ribonucleoprotein." *The Journal of Biological Chemistry* **287**(43):36609–16.

Bartkowiak, B., Liu, P., Phatnani, H.P., … Greenleaf, A.L. 2010. "CDK12 Is a Transcription Elongation-Associated CTD Kinase, the Metazoan Ortholog of Yeast Ctk1." *Genes & Development* **24**(20):2303–16.

Bartkowiak, B., Yan, C., & Greenleaf, A.L. 2015. "Engineering an Analog-Sensitive CDK12 Cell Line Using CRISPR/Cas." *Biochimica et Biophysica Acta* **1849**(9):1179–87.

Baskaran, R., Escobar, S.R., & Wang, J.Y. 1999. "Nuclear c-Abl Is a COOH-Terminal Repeated Domain (CTD)-Tyrosine (CTD)-Tyrosine Kinase-Specific for the Mammalian RNA Polymerase II: Possible Role in Transcription Elongation." *Cell Growth & Differentiation : The Molecular Biology Journal of the American Association for Cancer Research* **10**(6):387–96.

Baumli, S., Lolli, G., Lowe, E.D., … Johnson, L.N. 2008. "The Structure of P-TEFb (CDK9/cyclin T1), Its Complex with Flavopiridol and Regulation by Phosphorylation." *The EMBO Journal* **27**(13):1907–18.

Belkina, A.C., Nikolajczyk, B.S., & Denis, G. V. 2013. "BET Protein Function Is Required for Inflammation: Brd2 Genetic Disruption and BET Inhibitor JQ1 Impair Mouse Macrophage Inflammatory Responses." *Journal of Immunology (Baltimore, Md. : 1950)* **190**(7):3670–78.

Benjamini, Y. & Hochberg, Y. 1995. "Controlling the False Discovery Rate: A Practical and Powerful Approach to Multiple Testing." *Journal of the Royal Statistical Society. Series B*

(Methodological) **57**(1):289–300.

Bensaude, O. 2011. "Inhibiting Eukaryotic Transcription: Which Compound to Choose? How to Evaluate Its Activity?" *Transcription* **2**(3):103–8.

Bentley, D.L. & Groudine, M. 1986. "A Block to Elongation Is Largely Responsible for Decreased Transcription of c-Myc in Differentiated HL60 Cells." *Nature* **321**(6071):702–6.

Bild, A.H., Yao, G., Chang, J.T., … Nevins, J.R. 2006. "Oncogenic Pathway Signatures in Human Cancers as a Guide to Targeted Therapies." *Nature* **439**(7074):353–57.

Bintu, L., Ishibashi, T., Dangkulwanich, M., … Bustamante, C. 2012. "Nucleosomal Elements That Control the Topography of the Barrier to Transcription." *Cell* **151**(4):738–49.

Bisgrove, D. a, Mahmoudi, T., Henklein, P., & Verdin, E. 2007. "Conserved P-TEFb-Interacting Domain of BRD4 Inhibits HIV Transcription." *Proceedings of the National Academy of Sciences of the United States of America* **104**(34):13690–95.

Bishop, A.C., Ubersax, J.A., Petsch, D.T., … Shokat, K.M. 2000. "A Chemical Switch for Inhibitor-Sensitive Alleles of Any Protein Kinase." *Nature* **407**(6802):395–401.

Bodner, S.M., Minna, J.D., Jensen, S.M., … Gazdar, A.F. 1992. "Expression of Mutant p53 Proteins in Lung Cancer Correlates with the Class of p53 Gene Mutation." *Oncogene* **7**(4):743–49.

Boehm, A.K., Saunders, A., Werner, J., & Lis, J.T. 2003. "Transcription Factor and Polymerase Recruitment, Modification, and Movement on dhsp70 in Vivo in the Minutes Following Heat Shock." *Molecular and Cellular Biology* **23**(21):7628–37.

Boeing, S., Rigault, C., Heidemann, M., … Meisterernst, M. 2010. "RNA Polymerase II C-Terminal Heptarepeat Domain Ser-7 Phosphorylation Is Established in a Mediator-Dependent Fashion." *The Journal of Biological Chemistry* **285**(1):188–96.

Bonfert, T., Kirner, E., Csaba, G., … Brunk, B. 2015. "ContextMap 2: Fast and Accurate Context-Based RNA-Seq Mapping." *BMC Bioinformatics* **16**(1):122.

Bornkamm, G.W., Berens, C., Kuklik-Roos, C., … Feuillard, J. 2005. "Stringent Doxycycline-Dependent Control of Gene Activities Using an Episomal One-Vector System." *Nucleic*

Acids Research **33**(16):e137.

Bösken, C.A., Farnung, L., Hintermair, C., … Geyer, M. 2014. "The Structure and Substrate Specificity of Human Cdk12/Cyclin K." *Nature Communications* **5**:3505.

Bowman, E. a & Kelly, W.G. 2014. "RNA Polymerase II Transcription Elongation and Pol II CTD Ser2 Phosphorylation." *Nucleus* **5**(3):224–36.

Brannan, K., Kim, H., Erickson, B., … Bentley, D.L. 2012. "mRNA Decapping Factors and the Exonuclease Xrn2 Function in Widespread Premature Termination of RNA Polymerase II Transcription." *Molecular Cell* **46**(3):311–24.

Brownell, J.E., Zhou, J., Ranalli, T., … Allis, C.D. 1996. "Tetrahymena Histone Acetyltransferase A: A Homolog to Yeast Gcn5p Linking Histone Acetylation to Gene Activation." *Cell* **84**(6):843–51.

Buratowski, S., Hahn, S., Guarente, L., & Sharp, P.A. 1989. "Five Intermediate Complexes in Transcription Initiation by RNA Polymerase II." *Cell* **56**(4):549–61.

Chapman, R.D., Heidemann, M., Albert, T.K., … Eick, D. 2007. "Transcribing RNA Polymerase II Is Phosphorylated at CTD Residue Serine-7." *Science (New York, N.Y.)* **318**(5857):1780–82.

Cheung, K.L., Zhang, F., Jaganathan, A., … Zhou, M.-M. 2017. "Distinct Roles of Brd2 and Brd4 in Potentiating the Transcriptional Program for Th17 Cell Differentiation." *Molecular Cell* 1–13.

Cho, E.J., Kobor, M.S., Kim, M., … Buratowski, S. 2001. "Opposing Effects of Ctk1 Kinase and Fcp1 Phosphatase at Ser 2 of the RNA Polymerase II C-Terminal Domain." *Genes & Development* **15**(24):3319–29.

Cho, E.J., Takagi, T., Moore, C.R., & Buratowski, S. 1997. "mRNA Capping Enzyme Is Recruited to the Transcription Complex by Phosphorylation of the RNA Polymerase II Carboxy-Terminal Domain." *Genes and Development* **11**(24):3319–26.

Clancy, S. 2008. "RNA Transcription by RNA Polymerase: Prokaryotes vs Eukaryotes." *Nature Education* **1**(1):125.

Cooper, G. 2000. *The Cell : A Molecular Approach*. 2nd ed. Washington ;Sunderland Mass.: ASM Press ;;Sinauer Associates.

Czudnochowski, N., Bösken, C. a, & Geyer, M. 2012. "Serine-7 but Not Serine-5 Phosphorylation Primes RNA Polymerase II CTD for P-TEFb Recognition." *Nature Communications* **3**(may):842.

David, C.J., Boyne, A.R., Millhouse, S.R., & Manley, J.L. 2011. "The RNA Polymerase II C-Terminal Domain Promotes Splicing Activation through Recruitment of a U2AF65-Prp19 Complex." *Genes & Development* **25**(9):972–83.

Davison, B.L., Egly, J.M., Mulvihill, E.R., & Chambon, P. 1983. "Formation of Stable Preinitiation Complexes between Eukaryotic Class B Transcription Factors and Promoter Sequences." *Nature* **301**(5902):680–86.

Dawson, M.A., Prinjha, R.K., Dittmann, A., … Kouzarides, T. 2011. "Inhibition of BET Recruitment to Chromatin as an Effective Treatment for MLL-Fusion Leukaemia." *Nature* **478**(7370):529–33.

Day, D.S., Zhang, B., Stevens, S.M., … Pu, W.T. 2016. "Comprehensive Analysis of Promoter-Proximal RNA Polymerase II Pausing across Mammalian Cell Types." *Genome Biology* **17**(1):120.

Decker, T.-M., Kluge, M., Krebs, S., … Eick, D. 2017. "Transcriptome Analysis of Dominant-Negative Brd4 Mutants Identifies Brd4-Specific Target Genes of Small Molecule Inhibitor JQ1." *Scientific Reports* **7**(1):1684.

Deeney, J.T., Belkina, A.C., Shirihai, O.S., … Denis, G. V. 2016. "BET Bromodomain Proteins Brd2, Brd3 and Brd4 Selectively Regulate Metabolic Pathways in the Pancreatic β-Cell." *PloS One* **11**(3):e0151329.

Delmore, J.E., Issa, G.C., Lemieux, M.E., … Mitsiades, C.S. 2011. "BET Bromodomain Inhibition as a Therapeutic Strategy to Target c-Myc." *Cell* **146**(6):904–17.

Denis, G. V., McComb, M.E., Faller, D. V., … Costello, C.E. 2006. "Identification of Transcription Complexes That Contain the Double Bromodomain Protein Brd2 and Chromatin Remodeling Machines." *Journal of Proteome Research* **5**(3):502–11.

Deniz, E. & Erman, B. 2016. "Long Noncoding RNA (lincRNA), a New Paradigm in Gene Expression Control." *Functional & Integrative Genomics* 1–9.

Denslow, S.A. & Wade, P.A. 2007. "The Human Mi-2/NuRD Complex and Gene Regulation." *Oncogene* **26**(37):5433–38.

Descostes, N., Heidemann, M., Spinelli, L., … Andrau, J.-C. 2014. "Tyrosine Phosphorylation of RNA Polymerase II CTD Is Associated with Antisense Promoter Transcription and Active Enhancers in Mammalian Cells." *eLife* **3**:e02105.

Devaiah, B.N., Case-Borden, C., Gegonne, A., … Singer, D.S. 2016. "BRD4 Is a Histone Acetyltransferase That Evicts Nucleosomes from Chromatin." *Nature Structural & Molecular Biology* **3**(August 2015):1–12.

Devaiah, B.N., Lewis, B. a, Cherman, N., … Singer, D.S. 2012. "BRD4 Is an Atypical Kinase That Phosphorylates serine2 of the RNA Polymerase II Carboxy-Terminal Domain." *Proceedings of the National Academy of Sciences of the United States of America* **109**(18):6927–32.

Dey, A., Chitsaz, F., Abbasi, A., … Ozato, K. 2003. "The Double Bromodomain Protein Brd4 Binds to Acetylated Chromatin during Interphase and Mitosis." *Proceedings of the National Academy of Sciences of the United States of America* **100**(15):8758–63.

Dhalluin, C., Carlson, J.E., Zeng, L., … Zhou, M.M. 1999. "Structure and Ligand of a Histone Acetyltransferase Bromodomain." *Nature* **399**(6735):491–96.

Dobin, A., Davis, C.A., Schlesinger, F., … Gingeras, T.R. 2013. "STAR: Ultrafast Universal RNA-Seq Aligner." *Bioinformatics (Oxford, England)* **29**(1):15–21.

Dölken, L., Ruzsics, Z., Rädle, B., … Koszinowski, U.H. 2008. "High-Resolution Gene Expression Profiling for Simultaneous Kinetic Parameter Analysis of RNA Synthesis and Decay." *RNA (New York, N.Y.)* **14**(9):1959–72.

Donato, E., Croci, O., Sabò, A., … Campaner, S. 2016. "Compensatory RNA Polymerase 2 Loading Determines the Efficacy and Transcriptional Selectivity of JQ1 in Myc-Driven Tumors." *Leukemia* (February):1–12.

Duan, Q., Xiao, Y., Zhu, L., … Yang, T. 2016. "BET Bromodomain Is a Novel Regulator of TAZ

and Its Activity." *Biochimica et Biophysica Acta* **1859**(12):1527–37.

Egloff, S., O'Reilly, D., Chapman, R.D., … Murphy, S. 2007. "Serine-7 of the RNA Polymerase II CTD Is Specifically Required for snRNA Gene Expression." *Science (New York, N.Y.)* **318**(5857):1777–79.

Egloff, S., Zaborowska, J., Laitem, C., … Murphy, S. 2012. "Ser7 Phosphorylation of the CTD Recruits the RPAP2 Ser5 Phosphatase to snRNA Genes." *Molecular Cell* **45**(1):111–22.

Ehrensberger, A.H., Kelly, G.P., & Svejstrup, J.Q. 2013. "Mechanistic Interpretation of Promoter-Proximal Peaks and RNAPII Density Maps." *Cell* **154**(4):713–15.

Eick, D. & Bornkamm, G.W. 1986. "Transcriptional Arrest within the First Exon Is a Fast Control Mechanism in c-Myc Gene Expression." *Nucleic Acids Research* **14**(21):8331–46.

Eick, D. & Geyer, M. 2013. "The RNA Polymerase II Carboxy-Terminal Domain Code." *Chemical Reviews*.

Filippakopoulos, P., Picaud, S., Mangos, M., … Knapp, S. 2012. "Histone Recognition and Large-Scale Structural Analysis of the Human Bromodomain Family." *Cell* **149**(1):214–31.

Filippakopoulos, P., Qi, J., Picaud, S., … Bradner, J.E. 2010. "Selective Inhibition of BET Bromodomains." *Nature* **468**(7327):1067–73.

Fowler, T., Ghatak, P., Price, D.H., … Roy, A.L. 2014. "Regulation of MYC Expression and Differential JQ1 Sensitivity in Cancer Cells." *PloS One* **9**(1):e87003.

French, C.A., Miyoshi, I., Kubonishi, I., … Fletcher, J.A. 2003. "BRD4-NUT Fusion Oncogene : A Novel Mechanism in Aggressive Carcinoma Advances in Brief BRD4-NUT Fusion Oncogene : A Novel Mechanism in Aggressive Carcinoma 1." *Cancer Research* **63**(2):304–7.

Fuchs, G., Voichek, Y., Benjamin, S., … Oren, M. 2014. "4sUDRB-Seq: Measuring Genomewide Transcriptional Elongation Rates and Initiation Frequencies within Cells." *Genome Biology* **15**(5):R69.

Fujinaga, K., Irwin, D., Huang, Y., … Peterlin, B.M. 2004. "Dynamics of Human Immunodeficiency Virus Transcription: P-TEFb Phosphorylates RD and Dissociates

Negative Effectors from the Transactivation Response Element." *Molecular and Cellular Biology* **24**(2):787–95.

Ghamari, A., van de Corput, M.P.C., Thongjuea, S., … Grosveld, F.G. 2013. "In Vivo Live Imaging of RNA Polymerase II Transcription Factories in Primary Cells." *Genes & Development* **27**(7):767–77.

Ghosh, A. & Lima, C.D. 2010. "Enzymology of RNA Cap Synthesis." *Wiley Interdisciplinary Reviews. RNA* **1**(1):152–72.

Ghosh, A., Shuman, S., & Lima, C.D. 2011. "Structural Insights to How Mammalian Capping Enzyme Reads the CTD Code." *Molecular Cell* **43**(2):299–310.

Gilchrist, D.A., Dos Santos, G., Fargo, D.C., … Adelman, K. 2010. "Pausing of RNA Polymerase II Disrupts DNA-Specified Nucleosome Organization to Enable Precise Gene Regulation." *Cell* **143**(4):540–51.

Glover-Cutter, K., Larochelle, S., Erickson, B., … Bentley, D.L. 2009. "TFIIH-Associated Cdk7 Kinase Functions in Phosphorylation of C-Terminal Domain Ser7 Residues, Promoter-Proximal Pausing, and Termination by RNA Polymerase II." *Molecular and Cellular Biology* **29**(20):5455–64.

Greenwald, R.J., Tumang, J.R., Sinha, A., … Denis, G. V. 2004. "E Mu-BRD2 Transgenic Mice Develop B-Cell Lymphoma and Leukemia." *Blood* **103**(4):1475–84.

Greifenberg, A.K., Hönig, D., Pilarova, K., … Geyer, M. 2016. "Structural and Functional Analysis of the Cdk13/Cyclin K Complex." *Cell Reports* **14**(2):320–31.

Gressel, S., Schwalb, B., Decker, T.M., … Cramer, P. 2017. "CDK9-Dependent RNA Polymerase II Pausing Controls Transcription Initiation." *eLife* **6**:1–24.

Gu, B., Eick, D., & Bensaude, O. 2013. "CTD Serine-2 Plays a Critical Role in Splicing and Termination Factor Recruitment to RNA Polymerase II in Vivo." *Nucleic Acids Research* **41**(3):1591–1603.

Gupta, K., Sari-Ak, D., Haffke, M., … Berger, I. 2016. "Zooming in on Transcription Preinitiation." *Journal of Molecular Biology* **428**(12):2581–91.

Hantsche, M. & Cramer, P. 2016. "The Structural Basis of Transcription: 10 Years After the Nobel Prize in Chemistry." *Angewandte Chemie (International Ed. in English)* **55**(52):15972–81.

Henriques, T., Gilchrist, D.A., Nechaev, S., … Adelman, K. 2013. "Stable Pausing by RNA Polymerase II Provides an Opportunity to Target and Integrate Regulatory Signals." *Molecular Cell* **52**(4):517–28.

Herkert, B. & Eilers, M. 2010. "Transcriptional Repression: The Dark Side of Myc." *Genes & Cancer* **1**(6):580–86.

Hintermair, C., Heidemann, M., Koch, F., … Eick, D. 2012. "Threonine-4 of Mammalian RNA Polymerase II CTD Is Targeted by Polo-like Kinase 3 and Required for Transcriptional Elongation." *The EMBO Journal* **31**(12):2784–97.

Hnisz, D., Abraham, B.J., Lee, T.I., … Young, R.A. 2013. "Super-Enhancers in the Control of Cell Identity and Disease." *Cell* **155**(4):934–47.

Hölzel, M., Rohrmoser, M., Orban, M., … Eick, D. 2007. "Rapid Conditional Knock-down-Knock-in System for Mammalian Cells." *Nucleic Acids Research* **35**(3):e17.

Itzen, F., Greifenberg, A.K., Bösken, C.A., & Geyer, M. 2014. "Brd4 Activates P-TEFb for RNA Polymerase II CTD Phosphorylation." *Nucleic Acids Research* **42**(12):7577–90.

Jang, M.K., Mochizuki, K., Zhou, M., … Ozato, K. 2005. "The Bromodomain Protein Brd4 Is a Positive Regulatory Component of P-TEFb and Stimulates RNA Polymerase II-Dependent Transcription." *Molecular Cell* **19**(4):523–34.

Jiang, Y.W., Veschambre, P., Erdjument-Bromage, H., … Kornberg, R.D. 1998. "Mammalian Mediator of Transcriptional Regulation and Its Possible Role as an End-Point of Signal Transduction Pathways." *Proceedings of the National Academy of Sciences of the United States of America* **95**(15):8538–43.

Jonkers, I., Kwak, H., & Lis, J.T. 2014. "Genome-Wide Dynamics of Pol II Elongation and Its Interplay with Promoter Proximal Pausing, Chromatin, and Exons." *eLife* **3**:e02407.

Jonkers, I. & Lis, J.T. 2015. "Getting up to Speed with Transcription Elongation by RNA Polymerase II." *Nat Rev Mol Cell Biol* **16**(3):167–77.

Kanno, T., Kanno, Y., LeRoy, G., … Ozato, K. 2014. "BRD4 Assists Elongation of Both Coding and Enhancer RNAs by Interacting with Acetylated Histones." *Nature Structural & Molecular Biology* **21**(12):1047–57.

Kazerouninia, A., Ngo, B., & Martinson, H.G. 2010. "Poly(A) Signal-Dependent Degradation of Unprocessed Nascent Transcripts Accompanies poly(A) Signal-Dependent Transcriptional Pausing in Vitro." *RNA (New York, N.Y.)* **16**(1):197–210.

Kharenko, O.A., Gesner, E.M., Patel, R.G., … Hansen, H.C. 2016. "RVX-297- a Novel BD2 Selective Inhibitor of BET Bromodomains." *Biochemical and Biophysical Research Communications* **477**(1):62–67.

Kim, J.B. & Sharp, P.A. 2001. "Positive Transcription Elongation Factor B Phosphorylates hSPT5 and RNA Polymerase II Carboxyl-Terminal Domain Independently of Cyclin-Dependent Kinase-Activating Kinase." *The Journal of Biological Chemistry* **276**(15):12317–23.

Kim, M., Suh, H., Cho, E.-J., & Buratowski, S. 2009. "Phosphorylation of the Yeast Rpb1 C-Terminal Domain at Serines 2, 5, and 7." *The Journal of Biological Chemistry* **284**(39):26421–26.

Kim, Y.H., Girard, L., Giacomini, C.P., … Pollack, J.R. 2006. "Combined Microarray Analysis of Small Cell Lung Cancer Reveals Altered Apoptotic Balance and Distinct Expression Signatures of MYC Family Gene Amplification." *Oncogene* **25**(1):130–38.

Kouzarides, T. 2007. "Chromatin Modifications and Their Function." *Cell* **128**(4):693–705.

Kraybill, B.C., Elkin, L.L., Blethrow, J.D., … Shokat, K.M. 2002. "Inhibitor Scaffolds as New Allele Specific Kinase Substrates." *Journal of the American Chemical Society* **124**(41):12118–28.

Krishnamurthy, S., He, X., Reyes-Reyes, M., … Hampsey, M. 2004. "Ssu72 Is an RNA Polymerase II CTD Phosphatase." *Molecular Cell* **14**(3):387–94.

Kwak, H. & Lis, J.T. 2013. "Control of Transcriptional Elongation." *Annual Review of Genetics* (September):501–26.

Laitem, C., Zaborowska, J., Isa, N.F., … Murphy, S. 2015. "CDK9 Inhibitors Define Elongation

Checkpoints at Both Ends of RNA Polymerase II-Transcribed Genes." *Nature Structural & Molecular Biology* **22**(5):396–403.

Larochelle, S., Amat, R., Glover-Cutter, K., … Fisher, R.P. 2012. "Cyclin-Dependent Kinase Control of the Initiation-to-Elongation Switch of RNA Polymerase II." *Nature Structural & Molecular Biology* **19**(11):1108–15.

Larochelle, S., Merrick, K.A., Terret, M.-E., … Fisher, R.P. 2007. "Requirements for Cdk7 in the Assembly of Cdk1/cyclin B and Activation of Cdk2 Revealed by Chemical Genetics in Human Cells." *Molecular Cell* **25**(6):839–50.

Lawrence, M., Daujat, S., & Schneider, R. 2017. "Lateral Thinking: How Histone Modifications Regulate Gene Expression." *Trends in Genetics* **32**(1):42–56.

Li, H., Handsaker, B., Wysoker, A., … 1000 Genome Project Data Processing Subgroup. 2009. "The Sequence Alignment/Map Format and SAMtools." *Bioinformatics (Oxford, England)* **25**(16):2078–79.

Liao, Y., Smyth, G.K., & Shi, W. 2014. "featureCounts: An Efficient General Purpose Program for Assigning Sequence Reads to Genomic Features." *Bioinformatics* **30**(7):923–30.

Liberzon, A., Subramanian, A., Pinchback, R., … Mesirov, J.P. 2011. "Molecular Signatures Database (MSigDB) 3.0." *Bioinformatics (Oxford, England)* **27**(12):1739–40.

Lin, C., Garrett, A.S., De Kumar, B., … Shilatifard, A. 2011. "Dynamic Transcriptional Events in Embryonic Stem Cells Mediated by the Super Elongation Complex (SEC)." *Genes & Development* **25**(14):1486–98.

Lin, C., Smith, E.R., Takahashi, H., … Shilatifard, A. 2010. "AFF4, a Component of the ELL/P-TEFb Elongation Complex and a Shared Subunit of MLL Chimeras, Can Link Transcription Elongation to Leukemia." *Molecular Cell* **37**(3):429–37.

Lin, P.S., Dubois, M.-F., & Dahmus, M.E. 2002. "TFIIF-Associating Carboxyl-Terminal Domain Phosphatase Dephosphorylates Phosphoserines 2 and 5 of RNA Polymerase II." *The Journal of Biological Chemistry* **277**(48):45949–56.

Linder, T., Zhu, X., Baraznenok, V., & Gustafsson, C.M. 2006. "The Classical srb4-138 Mutant Allele Causes Dissociation of Yeast Mediator." *Biochemical and Biophysical Research*

Communications **349**(3):948–53.

Liu, W., Ma, Q., Wong, K., … Rosenfeld, M.G. 2013. "Brd4 and JMJD6-Associated Anti-Pause Enhancers in Regulation of Transcriptional Pause Release." *Cell* **155**(7):1581–95.

Liu, X., Kraus, W.L., & Bai, X. 2015. "Ready, Pause, Go: Regulation of RNA Polymerase II Pausing and Release by Cellular Signaling Pathways." *Trends in Biochemical Sciences* **40**(9):516–25.

Lopez, M.S., Kliegman, J.I., & Shokat, K.M. 2014. "The Logic and Design of Analog-Sensitive Kinases and Their Small Molecule Inhibitors." *Methods in Enzymology* **548**:189–213.

Love, M.I., Huber, W., Anders, S., … Salzberg, S. 2014. "Moderated Estimation of Fold Change and Dispersion for RNA-Seq Data with DESeq2." *Genome Biology* **15**(12):550.

Lovén, J., Hoke, H. a, Lin, C.Y., … Young, R. a. 2013. "Selective Inhibition of Tumor Oncogenes by Disruption of Super-Enhancers." *Cell* **153**(2):320–34.

Lu, H., Flores, O., Weinmann, R., & Reinberg, D. 1991. "The Nonphosphorylated Form of RNA Polymerase II Preferentially Associates with the Preinitiation Complex." *Proceedings of the National Academy of Sciences of the United States of America* **88**(22):10004–8.

Lu, H., Xue, Y., Xue, Y., … Zhou, Q. 2015. "Compensatory Induction of MYC Expression by Sustained CDK9 Inhibition via a BRD4-Dependent Mechanism." *eLife* **4**(June):e06535.

Lu, H., Zawel, L., Fisher, L., … Reinberg, D. 1992. "Human General Transcription Factor IIH Phosphorylates the C-Terminal Domain of RNA Polymerase II." *Nature* **358**(6388):641–45.

Lu, X., Zhu, X., Li, Y., … Chen, R. 2016. "Multiple P-TEFbs Cooperatively Regulate the Release of Promoter-Proximally Paused RNA Polymerase II." *Nucleic Acids Research* **44**(14):6853–67.

Luger, K., Mäder, A.W., Richmond, R.K., … Richmond, T.J. 1997. "Crystal Structure of the Nucleosome Core Particle at 2.8 A Resolution." *Nature* **389**(6648):251–60.

Ma, W., Ay, F., Lee, C., … Duan, Z. 2015. "Fine-Scale Chromatin Interaction Maps Reveal the Cis-Regulatory Landscape of Human lincRNA Genes." *Nature Methods* **12**(1):71–78.

Marmorstein, R. & Zhou, M.-M. 2014. "Writers and Readers of Histone Acetylation: Structure, Mechanism, and Inhibition." *Cold Spring Harbor Perspectives in Biology* **6**(7):a018762.

Marshall, N.F., Peng, J., Xie, Z., & Price, D.H. 1996. "Control of RNA Polymerase II Elongation Potential by a Novel Carboxyl-Terminal Domain Kinase." *The Journal of Biological Chemistry* **271**(43):27176–83.

Martin, M. 2011. "Cutadapt Removes Adapter Sequences from High-Throughput Sequencing Reads." *EMBnet.journal* **17**(1):10–12.

McCracken, S., Fong, N., Rosonina, E., … Bentley, D.L. 1997. "5'-Capping Enzymes Are Targeted to Pre-mRNA by Binding to the Phosphorylated Carboxy-Terminal Domain of RNA Polymerase II." *Genes & Development* **11**(24):3306–18.

Medlin, J., Scurry, A., Taylor, A., … Murphy, S. 2005. "P-TEFb Is Not an Essential Elongation Factor for the Intronless Human U2 snRNA and Histone H2b Genes." *The EMBO Journal* **24**(23):4154–65.

Mertz, J. a, Conery, A.R., Bryant, B.M., … Sims, R.J. 2011. "Targeting MYC Dependence in Cancer by Inhibiting BET Bromodomains." *Proceedings of the National Academy of Sciences of the United States of America* **108**(40):16669–74.

Di Micco, R., Fontanals-Cirera, B., Low, V., … Hernando, E. 2014. "Control of Embryonic Stem Cell Identity by BRD4-Dependent Transcriptional Elongation of Super-Enhancer-Associated Pluripotency Genes." *Cell Reports* **9**(1):234–47.

Morales, F. & Giordano, A. 2016. "Overview of CDK9 as a Target in Cancer Research." *Cell Cycle (Georgetown, Tex.)* **15**(4):519–27.

Mulholland, C.B., Smets, M., Schmidtmann, E., … Bultmann, S. 2015. "A Modular Open Platform for Systematic Functional Studies under Physiological Conditions." *Nucleic Acids Research* **43**(17):e112.

Muse, G.W., Gilchrist, D.A., Nechaev, S., … Adelman, K. 2007. "RNA Polymerase Is Poised for Activation across the Genome." *Nature Genetics* **39**(12):1507–11.

Nicodeme, E., Jeffrey, K.L., Schaefer, U., … Tarakhovsky, A. 2010. "Suppression of Inflammation by a Synthetic Histone Mimic." *Nature* **468**(7327):1119–23.

Nishikura, K., Erikson, J., Ar-Rushdi, A., … Croce, C.M. 1985. "The Translocated c-Myc Oncogene of Raji Burkitt Lymphoma Cells Is Not Expressed in Human Lymphoblastoid Cells." *Proceedings of the National Academy of Sciences of the United States of America* **82**(9):2900–2904.

Nojima, T., Gomes, T., Grosso, A.R.F., … Proudfoot, N.J. 2015. "Mammalian NET-Seq Reveals Genome-Wide Nascent Transcription Coupled to RNA Processing." *Cell* **161**(3):526–40.

O'Donnell, K.A., Yu, D., Zeller, K.I., … Dang, C. V. 2006. "Activation of Transferrin Receptor 1 by c-Myc Enhances Cellular Proliferation and Tumorigenesis." *Molecular and Cellular Biology* **26**(6):2373–86.

Olins, A.L. & Olins, D.E. 1974. "Spheroid Chromatin Units (v Bodies)." *Science (New York, N.Y.)* **183**(4122):330–32.

Pak, V., Eifler, T.T., Jäger, S., … Peterlin, B.M. 2015. "CDK11 in TREX/THOC Regulates HIV mRNA 3' End Processing." *Cell Host & Microbe* **18**(5):560–70.

Paparidis, N.F.D.S., Durvale, M.C., & Canduri, F. 2017. "The Emerging Picture of CDK9/P-TEFb: More than 20 Years of Advances since PITALRE." *Molecular bioSystems* **13**(2):246–76.

Peng, J., Zhu, Y., Milton, J.T., & Price, D.H. 1998. "Identification of Multiple Cyclin Subunits of Human P-TEFb." *Genes & Development* **12**(5):755–62.

Pettersen, E.F., Goddard, T.D., Huang, C.C., … Ferrin, T.E. 2004. "UCSF Chimera--a Visualization System for Exploratory Research and Analysis." *Journal of Computational Chemistry* **25**(13):1605–12.

Plaschka, C., Nozawa, K., & Cramer, P. 2016. "Mediator Architecture and RNA Polymerase II Interaction." *Journal of Molecular Biology* **428**(12):2569–74.

Proudfoot, N.J. 2016. "Transcriptional Termination in Mammals: Stopping the RNA Polymerase II Juggernaut." *Science (New York, N.Y.)* **352**(6291):aad9926.

Pulvertaft, J. V. 1964. "Cytology of Burkitt's Tumour (African Lymphoma)." *Lancet* **1**(7327):238–40.

Rahman, S., Sowa, M.E., Ottinger, M., … Howley, P.M. 2011. "The Brd4 Extraterminal Domain Confers Transcription Activation Independent of pTEFb by Recruiting Multiple Proteins, Including NSD3." *Molecular and Cellular Biology* **31**(13):2641–52.

Ran, F.A., Hsu, P.D., Wright, J., … Zhang, F. 2013. "Genome Engineering Using the CRISPR-Cas9 System." *Nature Protocols* **8**(11):2281–2308.

Renner, D.B., Yamaguchi, Y., Wada, T., … Price, D.H. 2001. "A Highly Purified RNA Polymerase II Elongation Control System." *The Journal of Biological Chemistry* **276**(45):42601–9.

Robinson, M.D., McCarthy, D.J., & Smyth, G.K. 2010. "edgeR: A Bioconductor Package for Differential Expression Analysis of Digital Gene Expression Data." *Bioinformatics* **26**(1):139–40.

Rodriguez, C.R., Cho, E.J., Keogh, M.C., … Buratowski, S. 2000. "Kin28, the TFIIH-Associated Carboxy-Terminal Domain Kinase, Facilitates the Recruitment of mRNA Processing Machinery to RNA Polymerase II." *Molecular and Cellular Biology* **20**(1):104–12.

Roeder, R.G. & Rutter, W.J. 1969. "Multiple Forms of DNA-Dependent RNA Polymerase in Eukaryotic Organisms." *Nature* **224**(5216):234–37.

Rougvie, A.E. & Lis, J.T. 1988. "The RNA Polymerase II Molecule at the 5' End of the Uninduced hsp70 Gene of D. Melanogaster Is Transcriptionally Engaged." *Cell* **54**(6):795–804.

Saldi, T., Cortazar, M.A., Sheridan, R.M., & Bentley, D.L. 2016. "Coupling of RNA Polymerase II Transcription Elongation with Pre-mRNA Splicing." *Journal of Molecular Biology* **428**(12):2623–35.

Sansó, M., Levin, R.S., Lipp, J.J., … Fisher, R.P. 2016. "P-TEFb Regulation of Transcription Termination Factor Xrn2 Revealed by a Chemical Genetic Screen for Cdk9 Substrates." *Genes & Development* 117–31.

Sawadogo, M. & Roeder, R.G. 1985. "Interaction of a Gene-Specific Transcription Factor with the Adenovirus Major Late Promoter Upstream of the TATA Box Region." *Cell* **43**(1):165–75.

Schlosser, I., Hölzel, M., Hoffmann, R., … Eick, D. 2005. "Dissection of Transcriptional Programmes in Response to Serum and c-Myc in a Human B-Cell Line." *Oncogene* **24**(3):520–24.

Schröder, S., Cho, S., Zeng, L., … Ott, M. 2012. "Two-Pronged Binding with Bromodomain-Containing Protein 4 Liberates Positive Transcription Elongation Factor B from Inactive Ribonucleoprotein Complexes." *The Journal of Biological Chemistry* **287**(2):1090–99.

Schuhmacher, M., Kohlhuber, F., Hölzel, M., … Eick, D. 2001. "The Transcriptional Program of a Human B Cell Line in Response to Myc." *Nucleic Acids Research* **29**(2):397–406.

Schüller, R., Forné, I., Straub, T., … Eick, D. 2016. "Heptad-Specific Phosphorylation of RNA Polymerase II CTD." *Molecular Cell* **61**(2):305–14.

Schwalb, B., Michel, M., Zacher, B., … Cramer, P. 2016. "TT-Seq Maps the Human Transient Transcriptome." *Science (New York, N.Y.)* **352**(6290):1225–28.

Shandilya, J. & Roberts, S.G.E. 2012. "The Transcription Cycle in Eukaryotes: From Productive Initiation to RNA Polymerase II Recycling." *Biochimica et Biophysica Acta* **1819**(5):391–400.

Shu, S., Lin, C.Y., He, H.H., … Polyak, K. 2016. "Response and Resistance to BET Bromodomain Inhibitors in Triple-Negative Breast Cancer." *Nature* **529**(7586):1–24.

Sievers, F., Wilm, A., Dineen, D., … Higgins, D.G. 2011. "Fast, Scalable Generation of High-Quality Protein Multiple Sequence Alignments Using Clustal Omega." *Molecular Systems Biology* **7**:539.

Skourti-Stathaki, K. & Proudfoot, N.J. 2014. "A Double-Edged Sword: R Loops as Threats to Genome Integrity and Powerful Regulators of Gene Expression." *Genes & Development* **28**(13):1384–96.

Skourti-Stathaki, K., Proudfoot, N.J., & Gromak, N. 2011. "Human Senataxin Resolves RNA/DNA Hybrids Formed at Transcriptional Pause Sites to Promote Xrn2-Dependent Termination." *Molecular Cell* **42**(6):794–805.

Smyth, G.K. 2005. "Limma: Linear Models for Microarray Data." Pp. 397–420 in *Bioinformatics and Computational Biology Solutions Using R and Bioconductor*, edited by R. Gentleman,

V. J. Carey, W. Huber, R. A. Irizarry, and S. Dudoit. New York: Springer-Verlag.

Søgaard, T.M.M. & Svejstrup, J.Q. 2007. "Hyperphosphorylation of the C-Terminal Repeat Domain of RNA Polymerase II Facilitates Dissociation of Its Complex with Mediator." *Journal of Biological Chemistry* **282**(19):14113–20.

Stathis, A., Zucca, E., Bekradda, M., … French, C.A. 2016. "Clinical Response of Carcinomas Harboring the BRD4-NUT Oncoprotein to the Targeted Bromodomain Inhibitor OTX015/MK-8628." *Cancer Discovery* **6**(5):492–500.

Strahl, B.D. & Allis, C.D. 2000. "The Language of Covalent Histone Modifications." *Nature* **403**(6765):41–45.

Taniguchi, Y. 2016. "The Bromodomain and Extra-Terminal Domain (BET) Family: Functional Anatomy of BET Paralogous Proteins." *International Journal of Molecular Sciences* **17**(11):1849.

Taub, R., Moulding, C., Battey, J., … Leder, P. 1984. "Activation and Somatic Mutation of the Translocated c-Myc Gene in Burkitt Lymphoma Cells." *Cell* **36**(2):339–48.

Taunton, J., Hassig, C.A., & Schreiber, S.L. 1996. "A Mammalian Histone Deacetylase Related to the Yeast Transcriptional Regulator Rpd3p." *Science (New York, N.Y.)* **272**(5260):408–11.

The UniProt Consortium. 2017. "UniProt: The Universal Protein Knowledgebase." *Nucleic Acids Research* **45**(D1):D158–69.

Thomas, M.C. & Chiang, C.-M. 2006. "The General Transcription Machinery and General Cofactors." *Critical Reviews in Biochemistry and Molecular Biology* **41**(3):105–78.

Thompson, C.M., Koleske, A.J., Chao, D.M., & Young, R.A. 1993. "A Multisubunit Complex Associated with the RNA Polymerase II CTD and TATA-Binding Protein in Yeast." *Cell* **73**(7):1361–75.

Trembley, J.H., Hu, D., Slaughter, C.A., … Kidd, V.J. 2003. "Casein Kinase 2 Interacts with Cyclin-Dependent Kinase 11 (CDK11) in Vivo and Phosphorylates Both the RNA Polymerase II Carboxyl-Terminal Domain and CDK11 in Vitro." *The Journal of Biological Chemistry* **278**(4):2265–70.

Vannini, A. & Cramer, P. 2012. "Conservation between the RNA Polymerase I, II, and III Transcription Initiation Machineries." *Molecular Cell* **45**(4):439–46.

Vardabasso, C., Gaspar-Maia, A., Hasson, D., … Bernstein, E. 2015. "Histone Variant H2A.Z.2 Mediates Proliferation and Drug Sensitivity of Malignant Melanoma." *Molecular Cell* **59**(1):75–88.

Veloso, A., Kirkconnell, K.S., Magnuson, B., … Ljungman, M. 2014. "Rate of Elongation by RNA Polymerase II Is Associated with Specific Gene Features and Epigenetic Modifications." *Genome Research* **24**(6):896–905.

Venkatesh, S. & Workman, J.L. 2015. "Histone Exchange, Chromatin Structure and the Regulation of Transcription." *Nature Reviews. Molecular Cell Biology* **16**(3):178–89.

Verdin, E. & Ott, M. 2015. "50 Years of Protein Acetylation: From Gene Regulation to Epigenetics, Metabolism and Beyond." *Nature Reviews. Molecular Cell Biology* **16**(4):258–64.

Viktorovskaya, O. V. & Schneider, D.A. 2015. "Functional Divergence of Eukaryotic RNA Polymerases: Unique Properties of RNA Polymerase I Suit Its Cellular Role." *Gene* **556**(1):19–26.

Vollmuth, F., Blankenfeldt, W., & Geyer, M. 2009. "Structures of the Dual Bromodomains of the P-TEFb-Activating Protein Brd4 at Atomic Resolution." *The Journal of Biological Chemistry* **284**(52):36547–56.

Wang, R., Li, Q., Helfer, C.M., … You, J. 2012. "Bromodomain Protein Brd4 Associated with Acetylated Chromatin Is Important for Maintenance of Higher-Order Chromatin Structure." *The Journal of Biological Chemistry* **287**(14):10738–52.

Wang, S. & Fischer, P.M. 2008. "Cyclin-Dependent Kinase 9: A Key Transcriptional Regulator and Potential Drug Target in Oncology, Virology and Cardiology." *Trends in Pharmacological Sciences* **29**(6):302–13.

Wang, Y., Dow, E.C., Liang, Y.-Y., … Rice, A.P. 2008. "Phosphatase PPM1A Regulates Phosphorylation of Thr-186 in the Cdk9 T-Loop." *The Journal of Biological Chemistry* **283**(48):33578–84.

Wani, S., Yuda, M., Fujiwara, Y., … Hirose, Y. 2014. "Vertebrate Ssu72 Regulates and Coordinates 3'-end Formation of RNAs Transcribed by RNA Polymerase II." edited by A. Kanai. *PloS One* **9**(8):e106040.

Wood, A. & Shilatifard, A. 2006. "Bur1/Bur2 and the Ctk Complex in Yeast: The Split Personality of Mammalian P-TEFb." *Cell Cycle (Georgetown, Tex.)* **5**(10):1066–68.

Wu, C.-H., Yamaguchi, Y., Benjamin, L.R., … Gilmour, D. 2003. "NELF and DSIF Cause Promoter Proximal Pausing on the hsp70 Promoter in Drosophila." *Genes & Development* **17**(11):1402–14.

Wu, S.-Y.Y., Lee, A.-Y.Y., Lai, H.-T.T., … Chiang, C.-M.M. 2013. "Phospho Switch Triggers Brd4 Chromatin Binding and Activator Recruitment for Gene-Specific Targeting." *Molecular Cell* **49**(5):843–57.

Yamada, T., Yamaguchi, Y., Inukai, N., … Handa, H. 2006. "P-TEFb-Mediated Phosphorylation of hSpt5 C-Terminal Repeats Is Critical for Processive Transcription Elongation." *Molecular Cell* **21**(2):227–37.

Yamaguchi, Y., Takagi, T., Wada, T., … Handa, H. 1999. "NELF, a Multisubunit Complex Containing RD, Cooperates with DSIF to Repress RNA Polymerase II Elongation." *Cell* **97**(1):41–51.

Yan, J., Li, Q., Lievens, S., … You, J. 2010. "Abrogation of the Brd4-Positive Transcription Elongation Factor B Complex by Papillomavirus E2 Protein Contributes to Viral Oncogene Repression." *Journal of Virology* **84**(1):76–87.

Yang, Z., Yik, J.H.N., Chen, R., … Zhou, Q. 2005. "Recruitment of P-TEFb for Stimulation of Transcriptional Elongation by the Bromodomain Protein Brd4." *Molecular Cell* **19**(4):535–45.

Yap, K.L. & Zhou, M.-M. 2010. "Keeping It in the Family: Diverse Histone Recognition by Conserved Structural Folds." *Critical Reviews in Biochemistry and Molecular Biology* **45**(6):488–505.

Yu, D., Cozma, D., Park, A., & Thomas-Tikhonenko, A. 2005. "Functional Validation of Genes Implicated in Lymphomagenesis: An in Vivo Selection Assay Using a Myc-Induced B-Cell

Tumor." *Annals of the New York Academy of Sciences* **1059**:145–59.

Yudkovsky, N., Ranish, J.A., & Hahn, S. 2000. "A Transcription Reinitiation Intermediate That Is Stabilized by Activator." *Nature* **408**(6809):225–29.

Zaborowska, J., Egloff, S., & Murphy, S. 2016. "The Pol II CTD: New Twists in the Tail." *Nat Struct Mol Biol* **23**(9):771–77.

Zeitlinger, J., Stark, A., Kellis, M., … Young, R.A. 2007. "RNA Polymerase Stalling at Developmental Control Genes in the Drosophila Melanogaster Embryo." *Nature Genetics* **39**(12):1512–16.

Zeller, K.I., Jegga, A.G., Aronow, B.J., … Dang, C. V. 2003. "An Integrated Database of Genes Responsive to the Myc Oncogenic Transcription Factor: Identification of Direct Genomic Targets." *Genome Biology* **4**(10):R69.

Zhang, D.W., Mosley, A.L., Ramisetty, S.R., … Ansari, A.Z. 2012. "Ssu72 Phosphatase-Dependent Erasure of Phospho-Ser7 Marks on the RNA Polymerase II C-Terminal Domain Is Essential for Viability and Transcription Termination." *Journal of Biological Chemistry* **287**(11):8541–51.

Zhang, G., Smith, S.G., & Zhou, M.-M. 2015. "Discovery of Chemical Inhibitors of Human Bromodomains." *Chemical Reviews* **115**(21):11625–68.

Zhang, H., Rigo, F., & Martinson, H.G. 2015. "Poly(A) Signal-Dependent Transcription Termination Occurs through a Conformational Change Mechanism That Does Not Require Cleavage at the Poly(A) Site." *Molecular Cell* **59**(3):437–48.

Zhang, Q., Chakravarty, S., Ghersi, D., … Zhou, M.-M. 2010. "Biochemical Profiling of Histone Binding Selectivity of the Yeast Bromodomain Family." *PloS One* **5**(1):e8903.

Zhao, D.Y., Gish, G., Braunschweig, U., … Greenblatt, J.F. 2015. "SMN and Symmetric Arginine Dimethylation of RNA Polymerase II C-Terminal Domain Control Termination." *Nature.*

Zippo, A., Serafini, R., Rocchigiani, M., … Oliviero, S. 2009. "Histone Crosstalk between H3S10ph and H4K16ac Generates a Histone Code That Mediates Transcription Elongation." *Cell* **138**(6):1122–36.

Zuber, J., Rappaport, A.R., Luo, W., … Lowe, S.W. 2011. "An Integrated Approach to Dissecting Oncogene Addiction Implicates a Myb-Coordinated Self-Renewal Program as Essential for Leukemia Maintenance." *Genes & Development* **25**(15):1628–40.

Zuber, J., Shi, J., Wang, E., … Vakoc, C.R. 2011. "RNAi Screen Identifies Brd4 as a Therapeutic Target in Acute Myeloid Leukaemia." *Nature* **478**(7370):524–28.

VI Appendix

A Publications

Decker, TM., Kluge, M., Krebs, S., Shah, N., Blum, H., Friedel, CC., and Eick, D. 2017. "Transcriptome analysis of dominant-negative Brd4 mutants identifies Brd4-specific target genes of small molecule inhibitor JQ1." *Scientific Reports* **7**(1):1684

Gressel, S., Schwalb, B., **Decker, TM.**, Qin, W., Leonhardt, H., Eick, D. and Cramer, P. 2017. " CDK9-dependent RNA polymerase II pausing controls transcription initiation." *eLife* **6**:1-24

Shah, N., Maqpool, MA., Yahia, Y., Forné, I., El Aabidine, AZ., **Decker, TM.**, Martin, D., Schüller, R., Krebs, S., Blum, H., Imhof, A., Eick, D., and Andrau, JC. 2017. "Tyrosine-1 of RNA Polymerase II CTD controls global termination of gene transcription in mammals." *Molecular Cell* (in print)

Schüller, R., Forné, I., Straub, T., Schreieck, A., Texier, Y., Shah, N., **Decker, TM.**, Cramer, P., Imhof, A. and Eick, D. 2016. "Heptad-Specific Phosphorylation of RNA Polymerase II CTD." *Molecular Cell* **61**(2):305–14.

Acknowledgements

Completing my doctoral thesis I would like to highlight that this process was not only achieved by me alone but by many others who have contributed to this result. Hereby, I would like to thank all of them.

I thank my supervisor Prof. Dr. Dirk Eick for giving me the opportunity to completing my doctoral thesis in his laboratory. Dirk's advice and encouragement in times of struggles was priceless. I thank all current laboratory members Anita-Gruber Eber, Dr. Corinna Hintermair, Dr. Michaela Rohrmoser, Nilay Shah, and Yousra Yahia for advice whenever I needed some, fruitful discussions, and a fantastic work environment. I especially thank Nilay, who not only made me familiar with the fascinating Indian culture but became a dear friend along my path as a doctoral student. I thank my colleagues who have recently left the laboratory, Dr. Kirsten Voß, Dr. Roland Schüller, Dr. Markus Kellner, and Dr. Kaspar Burger. I particularly thank Roland who introduced me to the lab and became a dear friend.

I very much appreciate having supervised the students within the recent years, Kerstin Dörner, Umut Erdogdu, Ramya Nair, and Heyoung Oh. All of them are highly talented scientists and helped me a lot to push my projects up to the next level. My students were the ones making me discover my passion for teaching.

Without sharing ideas and collaborating on projects science would be far less exciting, not to mention successful. Thus, I thank my collaborators, Sylvia Mallok and Dr. Stefan Krebs from the group of Dr. Helmut Blum (Gene Center, LMU) for helping me preparing RNA-seq libraries and carrying out sequencing of the Brd4 mutant cell lines. Many thanks to Michal Kluge and his supervisor Prof. Dr. Caroline Friedel (Institute for Bioinformatics, LMU) for putting so much effort into analyzing Brd4 RNA-seq data. I thank Dr. Weihua Qin from the group of Prof. Dr. Heinrich Leonhardt (Biocenter, LMU) for constructing and sharing analog-sensitive Cdk9 cell lines. I thank Saskia Gressel and Dr. Björn Schwalb from the group of Prof. Dr. Patrick Cramer (MPI, Gröttin-

gen) for helping me with TT-seq library preparation and carrying out bioinformatics analysis of the Cdk9as cell line. Their expertise substantially advanced the entire project.

I thank the members of my thesis advisory committee (TAC), Prof. Dr. Dirk Eick, Prof. Dr. Irmela Jeremias, and PD Dr. Ursula Zimber-Strobl. Their guidance showed me which paths to take and which to abandon. I thank my graduate schools HELENA (Helmholtz) and the IRTG of SFB 1064 for financially supporting visits to workshops and conferences. The seminars and workshops organized by both schools were of great value, both professionally and personally. I especially thank Dr. Elizabeth Schroeder-Reiter who coordinates the IRTG 1064. Her passion and commitment for the doctoral students and their needs are invaluable.

Life would be much harder without friends, especially the life of a doctoral student. I thank my friends who have accompanied me in the past three and a half years. They taught me when to be focused and when to just have a beer (or two).

Finally, I thank my beloved family, my parents for supporting me in every step I have taken. They have taught me what is important in life and how to achieve my dreams. I thank my sister for always being there when I needed her. Certainly, without her I would not be the man I am today. I thank my, for all the love they gave me. They taught me modesty and that my efforts will pay off.